Electronic technology

principal contents

Modified N.T.S.C. Colour T.V. Signal

Linear Frequency Discriminator

Silicon P-N-P-N Switch — I

Transient Response of F.M. Signals

FIVE SHILLINGS

NOVEMBER 1961 VOLUME 38 NUMBER 11

BICC

polypole couplers for Pye microwave TV links

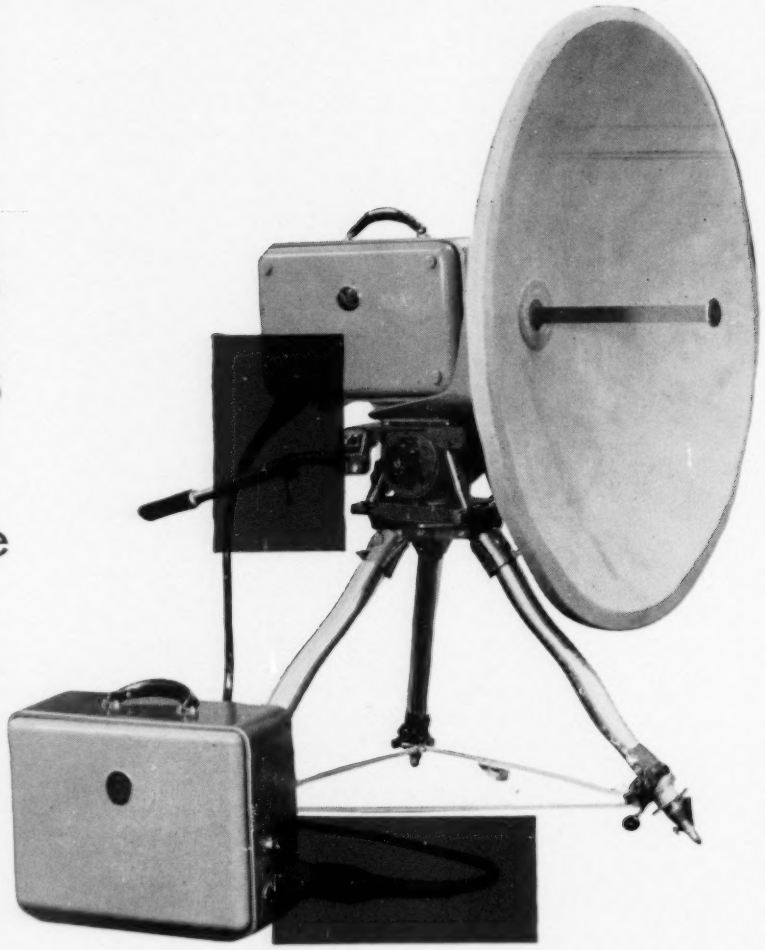

Robust, reliable and lightweight BICC Polypole Couplers and Multicore Cables are used exclusively by PYE as part of the standard equipment for their transportable long range television links.

BICC design and manufacture Polypole Coupler Systems to meet special requirements. These systems cover a wide variety of types and sizes of cable, terminated with moulded-on couplers.

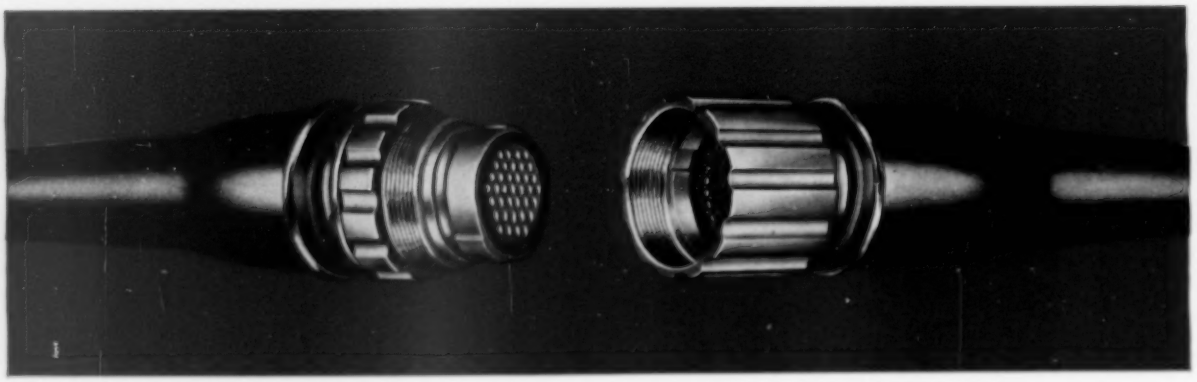

Further information is in Publication TD WG CD 6—available on request

BRITISH INSULATED CALLENDER'S CABLES LIMITED 21 BLOOMSBURY STREET LONDON WC1

Second Class Postage Paid at New York, N.Y.

Mallory not only build unique
'Sound Power' into their batteries—
they've solved the problem of keeping it there.
Mallory battery cell cases play no part
in the electro-chemical process:
they resist corrosion, protect cell materials.
Double seals, specially moulded gaskets,
new sealing techniques also help to make
Mallory batteries leakproof. These and other
original features help to underwrite the claim—
Mallory batteries are the greatest dry cell development
for more than eighty years. They are fadeproof
not only on the shelf but on the job.
They offer a constant voltage discharge
over a very long life to all manufacturers
who wish to miniaturise their products
and retain full 'Sound Power'.

Mallory batteries do not leak

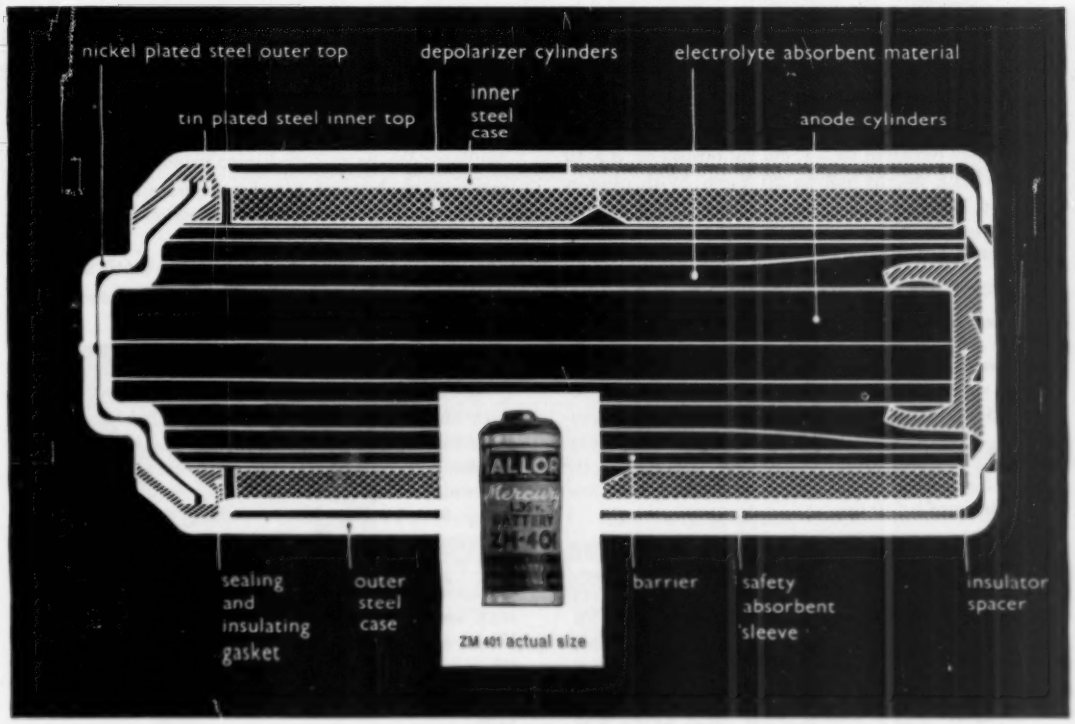

Manufacturers are advised to consult Mallory at
the design stage so that full benefit can be gained from
the world's most space-saving source of power.

Please write for literature to **Mallory Batteries Limited,**
33 Duke Street, London W1

MALLORY

miniature batteries for powerful applications

Cossorscope model 1076

SPECIFICATION

CATHODE-RAY TUBE: 5 in. (12.7 cm) diameter screen, single-beam, operating at 10 kV. Green fluorescence—phosphor P1. Phosphors P7 and P11 available to special order. Display area 10 cm (horizontal) by 6 cm (vertical).

Y AMPLIFIER: Basic Model 1076; d.c. to 80 Mc/s (30% down); rise-time 5 mμsec; sensitivity 200 mV/cm. With plug-in unit Model 1078; rise-time 6 mμsec to 7 mμsec; 50 mV/cm to 50 V/cm calibrated. With plug-in unit Model 1080; d.c. to 1 Mc/s (30% down); 1 mV/cm to 50 V/cm calibrated (*differential inputs*). With plug-in unit Model 1081; 3 c/s to 40 Mc/s (30% down); rise-time 10 mμsec; 5mV/cm to 2 V/cm calibrated or, d.c. to 60 Mc/s, 50 mV/cm to 20 V/cm. With plug-in unit Model 1085; d.c. to 40 Mc/s (30% down), dual-channel beam switch; rise-time 10 mμsec; 50 mV/cm to 20 V/cm calibrated.

SIGNAL DELAY: 150 mμ sec.

TIME-BASE: 24 calibrated ranges from 0.1 μsec/cm to 5 sec/cm in a 1, 2, 5 series. Continuously variable un-calibrated ranges from 0.1 μsec/cm to 12 sec/cm. Calibrated sweep expansion of x 1 or x 5 on all ranges from 0.1 μsec/cm to 12 sec/cm. D.C. coupled bright-up pulse to CRT grid gives uniform brightness along the trace length and complete fly-back suppression on all ranges. Scan length: 10 cm.

TRIGGER: with plug-in unit Model 1079—five modes of operation, H.F. Sync, Auto, A.C. Fast, A.C. Slow, and D.C. With plug-in unit model 1083—as given above for model 1079 and also with calibrated delayed sweep ranges: 100μsec, 1 msec, 10 msec, 50 msec. With plug-in unit Model 1082—calibrated sweep delay from 2 μsec to 10 sec. Separate trigger selection for main sweep and delaying sweep. Trace may be displayed on delaying sweep. "Lock-out" delay for jitter-free operation.

X AMPLIFIER: with plug-in unit Model 1079—d.c. to 2 Mc/s. 1V/cm to 100 V/cm calibrated. With plug-in unit Model 1083 as given above for Model 1079.

CALIBRATION: Amplitude. A 1 kc/s square-wave calibration source provides eighteen fixed voltage levels from 0.2 mV to 100 V peak-to-peak in a 1, 2, 5 series. Accuracy is within 2 per cent. Time. Basic calibration ranges are within ± 3 per cent. In addition, a gated 500 (± 2%) Mc/s oscillator can be switched in to provide 2 mμsec intensity modulation dots for accurate measurement of pulse rise-times. Time marker pips are also available at 50 (± 2%) Mc/s.

OUTPUT WAVEFORMS: time-base saw-tooth and gate; vertical-amplifier output; 1 kc/s calibrator square wave.

GENERAL: small neon indicators show the direction in which the CRT beam lies when deflected off the screen. An illuminated rotatable graticle with anti-parallax ruling in centimetre squares with 2 mm base, line divisions and green filter is provided. Fittings for camera attachment.

POWER SUPPLY: Mains. 100 V to 130 V and 200 V to 250 V. Frequency. 50 c/s to 100 c/s. Consumption. 650 W (approximate). Stabilized E.H.T., H.T. and transistor-stabilized d.c. heater supply to drift and hum-sensitive circuits.

SIZE AND WEIGHT: Height 18½ in. (47.0 cm). Width 13 in. (33.0 cm). Depth 29½ in. (74.3 cm). Weight with two plug-in units 104 lb (47.3 kg).

ACCESSORIES: Probe Model 1077. Camera Model 1458.

Full details of plug-in units will be supplied on application.

COSSOR INSTRUMENTS LIMITED, COSSOR HOUSE,

HIGH WRITING *SPEED*

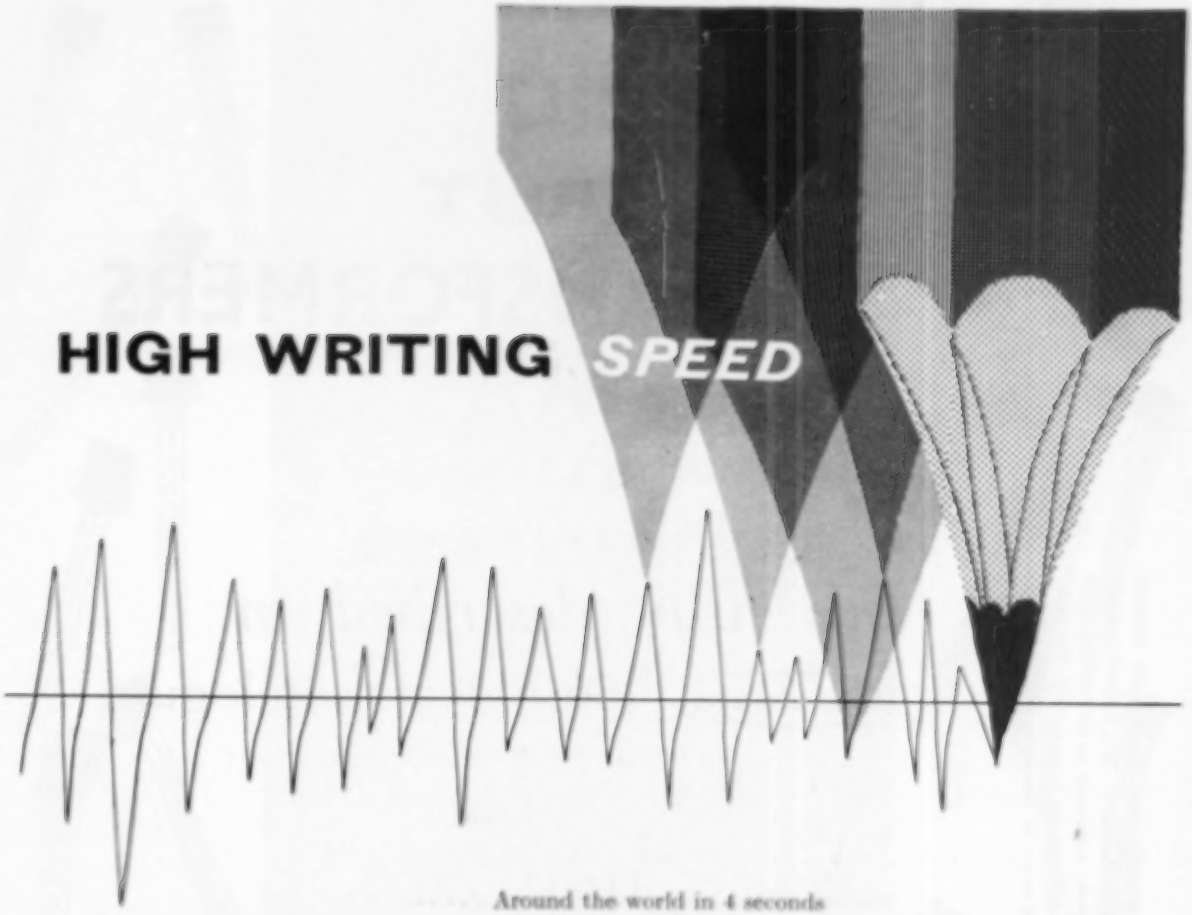

Around the world in 4 seconds —or 1500 years—these extremes of velocity are attainable by the recording spot of the Cossorscope Model 1076. This high writing speed is one of the many advantages which has earned it acclaim as the most advanced oscilloscope available commercially. The 1076 is yet another significant contribution to research and industry made possible by the imagination and experience of Cossor developmental laboratories.

Cossor manufacture the most extensive range of measuring oscilloscopes available commercially. Please write for details of instrumentation comprising over 50 different aids to industry.

COSSOR
INSTRUMENTS LIMITED

HIGHBURY GROVE, LONDON, N.5, ENGLAND, TELEPHONE: CANONBURY 1234

24 AUDIO OUTPUT TRANSFORMERS

are fully described in
Gardners loose leaf catalogue

AMONGST THESE ARE TRANSFORMERS SUITABLE FOR

Mullard 510

Osram 912

GEC 88-50

Baxandall Inexpensive Amplifier and

Mullard 3-3 Amplifiers

Every copy of this catalogue, which has been prepared specially for industrial and research establishments, is numbered and registered in the name of the holder. It is regularly brought up to date by the supply of amendment sheets covering every addition to Gardners' standard ranges. Please apply on the Company's or the Establishment's official letterheading. For other users a catalogue covering the full Solent and Miniford series is available on request.

Please write for catalogue to:
GARDNERS RADIO LTD · SOMERFORD · CHRISTCHURCH *Tel: 1734*

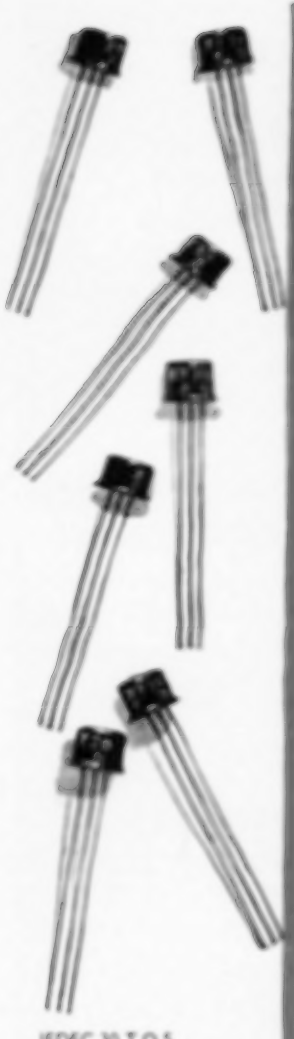

JEDEC 30 T.O.5.
SHOWN ACTUAL SIZE

FERRANTI
silicon
MESA TRANSISTORS

Temperature stabilised
High frequency cut-off
Rugged construction
Low saturation voltage
Small spread in current gain
Very low leakage currents

APPLICATION REPORTS
will be supplied on request

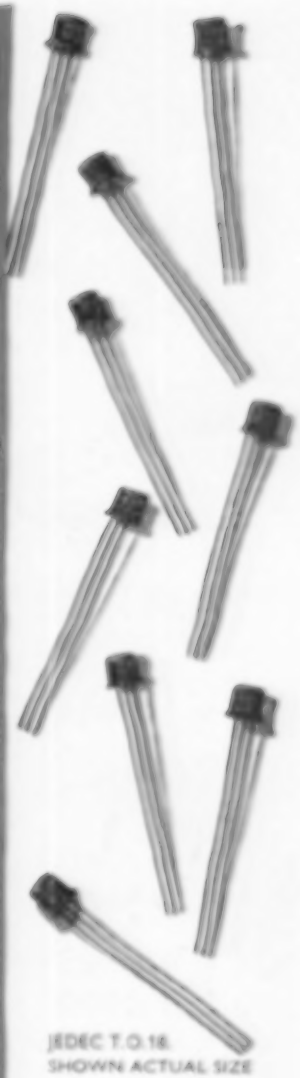

JEDEC T.O.18.
SHOWN ACTUAL SIZE

MAXIMUM RATINGS AT 25° C AMBIENT						
	ZT20	ZT21	ZT22	ZT23	ZT42	ZT43
Collector Base Voltage	20	20	45	45	45	45 volts
Collector Emitter Voltage	20	20	45	45	45	45 volts
Emitter Base Voltage	6	6	6	6	6	6 volts
Collector Current	50	50	50	50	50	50 mA
Total Dissipation	350	350	350	350	350	300 m/W
Temp. Range operating and storage	−55 to +150°C					

CHARACTERISTICS							
	ZT20	ZT21	ZT22	ZT23	ZT42	ZT43	Test Conditions
Common Emitter D.C. Current gain h_{FE}	18—42	38—83	18—42	38—83	18—42	38—83	V_{CE} = 6V, I_C = 10mA
Common Emitter A.C. Current gain h_{fe}	30•	60•	30•	45•	30•	45•	V_{CE} = 6V, I_C = 1mA
Collector Saturation Voltage Max. $V_{CE\,sat.}$	0·5V	0·5V	1·0V	1·0V	1·0V	1·0V	I_C = 10mA, I_B = 2mA
Gain Bandwidth Product. Min. f_T	60mc/s	60mc/s	60mc/s	60mc/s	70mc/s	70mc/s	V_{CE} = 6V, I_C = 10mA

• Typical Values

FERRANTI
First into the Future

offer a wide range of SILICON SEMICONDUCTOR DEVICES

FERRANTI LTD · GEM MILL · CHADDERTON · OLDHAM · LANCS Telephone: MAin 6661
London Office: Telephone TEMple Bar 6666

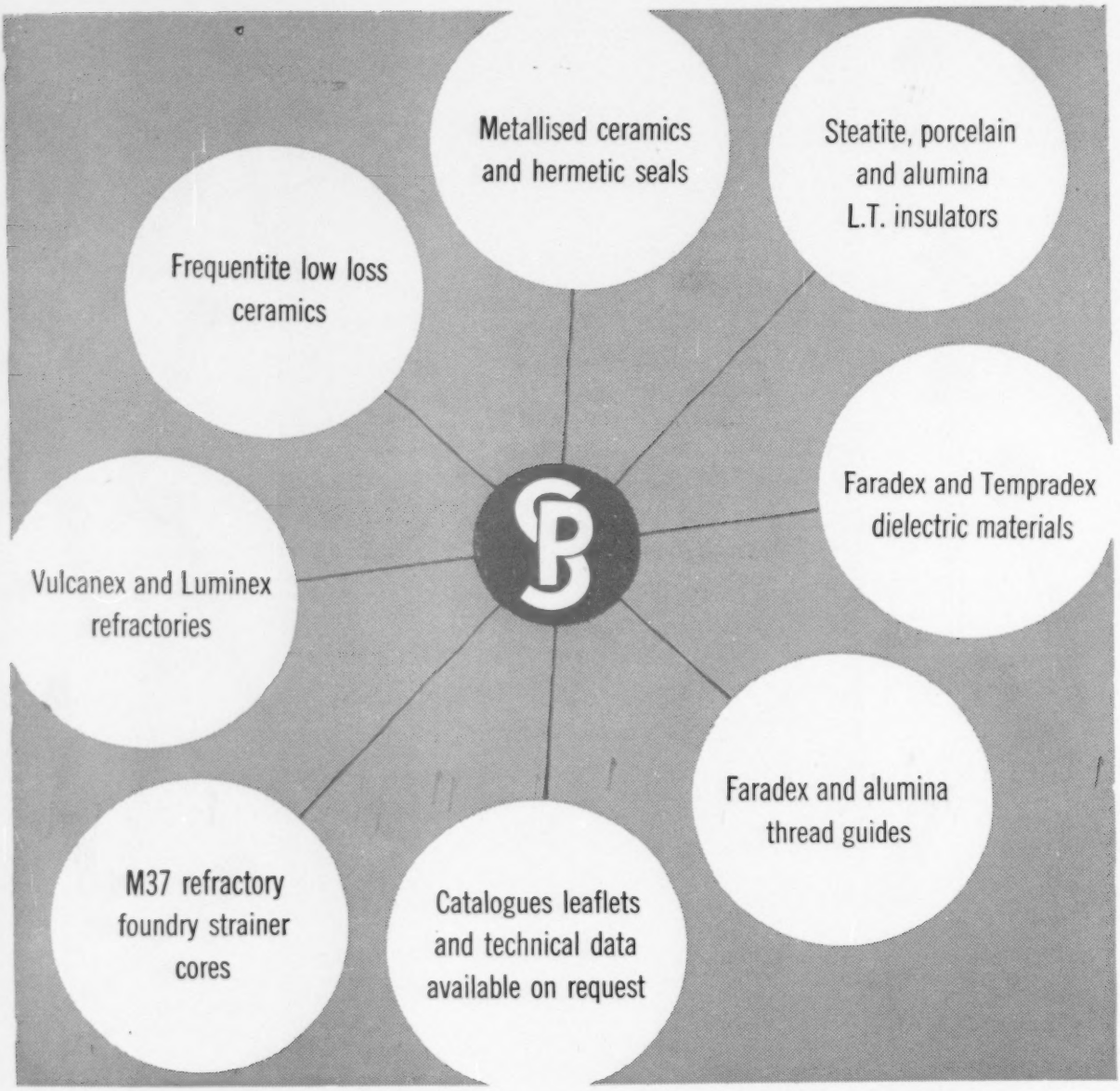
Metallised ceramics and hermetic seals
Steatite, porcelain and alumina L.T. insulators
Frequentite low loss ceramics
Faradex and Tempradex dielectric materials
Vulcanex and Luminex refractories
Faradex and alumina thread guides
M37 refractory foundry strainer cores
Catalogues leaflets and technical data available on request

FOR ALL RADIO, ELECTRONIC AND DOMESTIC ELECTRICAL CERAMICS CONSULT:

STEATITE & PORCELAIN PRODUCTS LTD.

STOURPORT ON SEVERN, WORCS. Telephone: Stourport 2271 Telegrams: Steatain, Stourport

SP110

SERVOMEX PRICE LIST

This list is effective September 18th, 1961

	U.K. price (delivered)	F.O.B. Charge	Export price (F.O.B. or at Airport)
MISCELLANEOUS EQUIPMENT	£	£	£
ES.1B Instructional servo system (designed by Feedback Ltd.)	330	22	352
TFA.46 Transfer function Analyser	2300	40	2340
LF.51 Low frequency waveform generator (*with wooden ends*)	395	10	405
RG.77 Random signal generator (*with wooden ends*)	180	10	190
FP.92 Field Plotter	33	Nil	33
Resistance Paper 33/– for roll 50′ × 22″ (*width may be increased to 29″ during* 1961, *but no price change*)			
Silver conducting paint 49/– for a ¼ lb. pot			
Decade Capacitor, type B	21	Nil	21
A.C. VOLTAGE STABILISERS			
AC.2 Mk. IIA 2 KVA, rackmounting	87	10	97
AC.2 Mk. IIB 2 KVA, rackmounting	99	10	109
AC.7 7 KVA, rackmounting	143	10	153
STABILISED D.C. POWER SUPPLIES			
DC.56 3—30V 0—40A	445	25	470
DC.58 6—60V 0—20A	445	25	470
DC.59 12—120V 0—10A	445	25	470
DC.60 24—240V 0—5A	445	25	470
DC.65 6—14V 0—1A	39	5	44
DC.68 250—350V 0—150mA	40	5	45
DC.84 0—72V 0—1.5A (*with wooden ends*)	183	10	193
DC.105 Twin Supply, plus and minus 300V 0—50mA	57	5	62
DC.112 300V 0–250mA	59	5	64
HIGH PRECISION SERVO SPEED CONTROLLERS			
MC.43 95 watt, rackmounting (*less motor*)	150	10	160
MC.47 350 watt, rackmounting (*less motor*)	192	10	202
Motor for MC.43, with lead and plug	35	4	39
Motor for MC.47, with lead and plug	95	10	105
SERVO SUB ASSEMBLIES			
SA.61 Servo-amplifier	17	Nil	17
AS.69 Armature supply 0.5 Amps.	22	5	27
CHEMICAL INSTRUMENTS DIVISION			
D.C.L.83 Servomex-DCL Oxygen Analyser (*less recorder and sampling equipment*)	800	25	825
G.S.96 Gas Sampling Panel	98	10	108
D.C.L.101 Portable Oxygen Analyser	216	5	221
D.C.L.104 Infra-red analyser (*provisonal price*)	1400	25	1425

NOTES

(1) *WOODEN ENDS. The instruments specified as rackmounting fit the standard 19″ rack. When not used in a rack they need the SERVOMEX wooden ends to provide carrying handles and protection, the price of which is £4 per pair, home and export.*

(2) *U.K. PRICE. Routine delivery is included, but if special "express" service, e.g., passenger train is demanded, it will be charged at cost. Customers in U.K. who retain the packing case will be charged half the "F.O.B. Charge" shown in the list.*

(3) *EXPORT PRICE. This price applies to all countries except U.K. (And North America in certain cases). Our agents abroad are authorised to add the cost of freight, duty, etc., but no other "profit" or "mark-up."*

(4) *VARIATIONS from standard colour or design add greatly to the cost of production and will be charged accordingly.*

(5) *DISCOUNTS. These are the lowest profitable prices and there are no trade or educational discounts. Deduct 1½% for cash fifteen days from despatch of goods. Bulk DELIVERY may lower costs and qualify for special discount.*

SERVOMEX CONTROLS LIMITED

CROWBOROUGH · SUSSEX · TELEPHONE CROWBOROUGH 1247

Printed in U.K., Sept., 1961

AEI STABILISED POWER UNITS

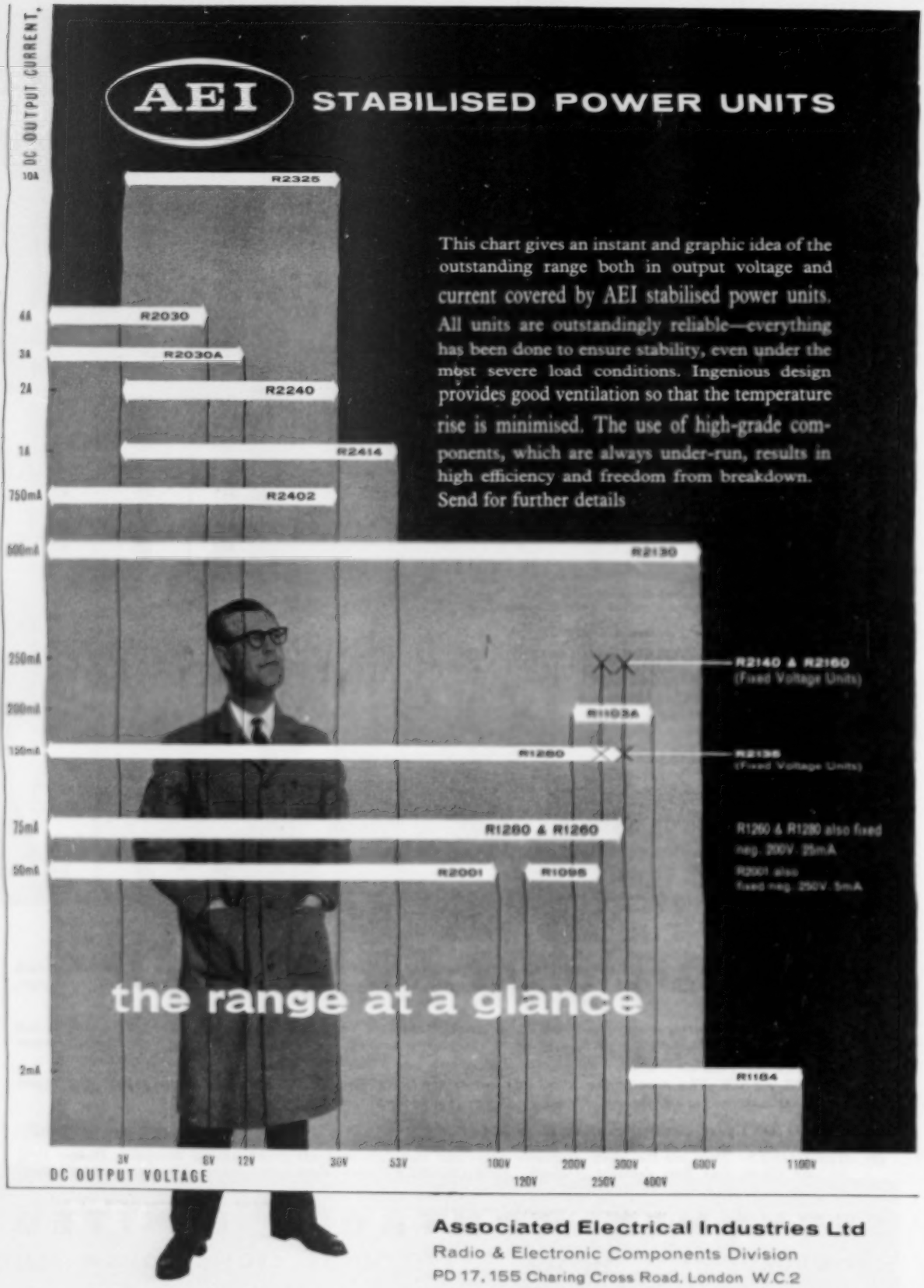

This chart gives an instant and graphic idea of the outstanding range both in output voltage and current covered by AEI stabilised power units. All units are outstandingly reliable—everything has been done to ensure stability, even under the most severe load conditions. Ingenious design provides good ventilation so that the temperature rise is minimised. The use of high-grade components, which are always under-run, results in high efficiency and freedom from breakdown. Send for further details

Associated Electrical Industries Ltd
Radio & Electronic Components Division
PD 17, 155 Charing Cross Road, London W.C.2
Telephone: GERrard 9797 Telegrams: Sieswan Westcent London

17/163

Electronic technology

incorporating WIRELESS ENGINEER
ELECTRONIC & RADIO ENGINEER

HUGH S. POCOCK M.I.E.E. *Managing Editor*
W. T. COCKING M.I.E.E. *Editor*

Editorial Advisory Board

H. E. M. BARLOW F.R.S., M.I.E.E., M.I.Mech.E. (*Fender Professor of Electrical Engineering, University College, London*); M. R. GAVIN M.B.E., M.A., D.Sc., F.Inst.P., M.I.E.E., M.Brit.I.R.E. (*Professor of Electronic Engineering, University College of North Wales*); A. H. MUMFORD O.B.E., B.Sc.(Eng.), M.I.E.E. (*Engineer-in-Chief, G.P.O.*); A. E. A. RENDALL O.B.E., Ph.D., D.Sc., M.I.E.E. (*British Broadcasting Corporation*); J. A. SAXTON D.Sc., Ph.D., M.I.E.E. (*Deputy Director, Radio Research Station, Department of Scientific and Industrial Research*); R. L. SMITH-ROSE C.B.E., D.Sc., Ph.D., M.I.E.E.

CONTENTS

VOLUME 38 NUMBER 11 NOVEMBER 1961

25 Years of Television	387	Editorial
Modified N.T.S.C. Colour T.V. Signal	388	*by J. Davidse*
Shielded Dielectric Waveguide	393	*by K. W. H. Foulds, Ph.D., and P. Sampaio, M.Sc.*
The Fringe of the Field	398	*by Quantum*
Linear Frequency Discriminator	401	*by U. S. Ganguly*
Silicon P-N-P-N Switch—1	406	*by A. Bardsley, B.Sc., and J. Walker*
Mathematical Tools	411	*by Computer*
Transient Response of F.M. Signals	414	*by S. J. Cotton, B.Sc.*
Correspondence	419	
New Books	421	
Standard Frequency Transmissions	423	
New Products	424	
Abstracts and References	A173–A190	

Established 1923

Published on the fifth of each month

ANNUAL SUBSCRIPTION
(including Annual Index to Abstracts and References)
Home and Overseas £3 7s 0d, Canada and U.S.A. $9.50
Second-class mail privileges authorized at New York, N.Y.

© **Iliffe Electrical Publications Ltd. 1961**

Permission in writing from the Editor must first be obtained before letterpress or illustrations are reproduced from this journal. Brief abstracts or comments are allowed provided acknowledgement to the journal is given.

Published by

ILIFFE ELECTRICAL PUBLICATIONS LTD. *Managing Director:* H. S. Pocock M.I.E.E., Dorset House, Stamford Street, London S.E.1
Telephone · Waterloo 3333 Telegrams · Wirenger, London · S.E.1

Branch Offices

COVENTRY · *8-10 Corporation Street–Telephone · Coventry 25210*: BIRMINGHAM · *King Edward House, New Street, 2–Telephone · Midlands 7191*
MANCHESTER · *260 Deansgate, 3–Telephone · Blackfriars 4412 and Deansgate 3595*: GLASGOW · *62 Buchanan Street, C.1–Telephone · Central 1265/6*

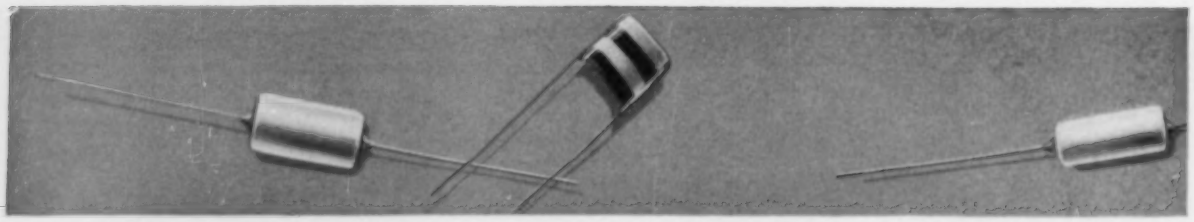

Mullard POLYESTER CAPACITORS...

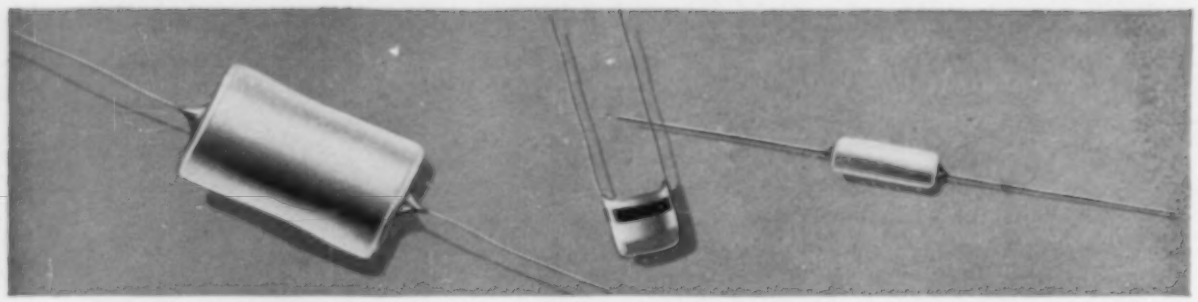

designed for peak performance with economy...

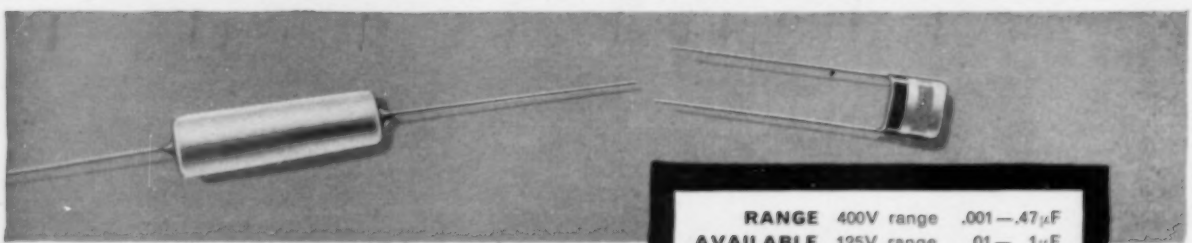

SMALL PHYSICAL SIZE

HIGH WORKING TEMPERATURES

CLOSE CAPACITANCE TOLERANCE

HIGH INSULATION RESISTANCE

FULLY TROPICALISED

COST SAVING

RANGE AVAILABLE	400V range	.001—.47μF
	125V range	.01— 1μF
	30V range	.01— .1μF

Write to Mullard House for leaflets giving full technical details

MULLARD LTD · COMPONENT DIVISION · MULLARD HOUSE · TORRINGTON PLACE · LONDON W.C.1

NOVEMBER 1961
VOLUME 38 NUMBER 11

Electronic technology

incorporating WIRELESS ENGINEER
ELECTRONIC & RADIO ENGINEER

25 Years of Television

NOVEMBER marks the 25th anniversary of television as a public service, for on 2nd November 1936 the B.B.C. started the first regular high-definition service in the world with transmissions on 45 Mc/s from Alexandra Palace in North London. At first, two different standards were used in alternate weeks in order that their respective merits might become fully evident under service conditions. One was the Baird system with 240 lines sequentially scanned; the other was the Marconi-E.M.I. system having 405 lines with interlaced scanning. Receivers were fitted with a switch so that the repetition frequency of the line timebase could be either 6,000 c/s or 10,125 c/s.

These alternative standard transmissions continued only for a short time and on 8th February 1937 the 405-line standard was adopted for all transmissions and with minor modifications is the one still in use.

The war temporarily stopped television, of course, from 1st September 1939 until 6th June 1946. This 25th anniversary of the start of television thus marks just over 18 years of operation in which it has expanded from a single transmitter to two country-wide networks.

Many people now say that it was a mistake in 1946 to start television again on 405 lines and that a change should have been made then to a higher standard. They argue that it could then have been done very easily for there was only one transmitter and comparatively few receivers existed. In 1939 there were only about 23,000 sets in the hands of the public and probably many were no longer serviceable in 1946.

What the critics forget is that if the standards had been changed television would not have re-started in 1946 at all. It would have been delayed for several years while a new system was being developed. They forget the technical advances which have been made in the last 15 years and that what is now easy to accomplish was then difficult or impossible.

We think that it was right to re-start on 405 lines and no one can deny that the system has provided a television service which has been, and still is, perfectly acceptable to the public. And that is the function of a television service.

There is, however, little room for further improvement, apart from the introduction of colour. This is one reason why some people think that we should change to 625 lines. However, it is often forgotten that this is itself a highly developed system and offers no more scope for further development than does the 405-line standard. If we are now at a standstill with 405 lines, we make one small step forward in improving picture quality by changing to 625 lines but are then once again in a stationary condition.

Modified N.T.S.C. Colour T.V. Signal

FOR SINGLE-GUN DISPLAY SYSTEMS

By J. Davidse*

SUMMARY. *This paper discusses the possibility of modifying the standard N.T.S.C. signal in order to obtain a better adaptation to the needs of single-gun display systems. A practical proposal is made, and its consequences for the transmission of the signal are investigated. It appears that the proposed modification does not essentially affect the outstanding transmission characteristics of the system.*

In the N.T.S.C. system of colour television the choice of most system parameters is based upon considerations of transmission quality. In designing the system attention was paid, first and foremost, to the properties of electrical transmission systems as such and to the properties of the human eye. Simplicity of receiver design, however, was not considered as unessential, as is clear from the method of gamma-correction adopted. Here a design was deliberately accepted which is next best from the transmission point of view in order to gain important advantages in receiver construction. In this way a well-balanced colour television system was developed capable of meeting high standards of transmission quality as well as practical requirements of receiver design[6].

At the time when the N.T.S.C. standards were finally fixed there was no evidence as to what type of display system would in future prove to be the best practical solution, so no attempt was made to adapt the transmission system more or less to the preferences of a certain special type of display.

At present, the situation is not much changed. It is still rather generally doubted that the three-gun shadow-mask tube is the final answer. Some progress has been achieved in the field of one-gun display tubes[9,11,15], although no one-gun tubes are yet commercially available. There is a trend to find a solution for a one-gun display operating with continuous colour sequence (C.C.S.); that is, the sequence of sampling the primary colour signals is constant, in general red blue green red blue green, etc. It is certain that this type of tube shows marked advantages, in particular the absence of registration errors; and in connection with that the good quality of black and white pictures should be mentioned. In addition, stability of operation and simplicity of decoding techniques are important features.

In view of this development, and in view of the fact that in the near future a decision has to be taken as to the standardization of a European colour television system, it seems logical to investigate the possibilities of modifying the N.T.S.C. system in such a way as to simplify the demodulation techniques in one-gun receivers without losing the outstanding transmission characteristics of the system.

* *Philips Research Laboratories, N.V. Philips' Gloeilampenfabrieken, Eindhoven, Netherlands.*

Motivation of the Choice of the System Parameters in the N.T.S.C. System

The N.T.S.C. colour television signal consists of a wide-band luminance signal and a narrow-band subcarrier signal containing mainly the chrominance information. The choice of the luminance signal is primarily based on the consideration that, as a first approximation, the constant luminance principle should be valid[3]. Such a choice has moreover the important advantage that good compatibility is obtained with the existing black-and-white television transmissions.

As is well known the N.T.S.C. system does not fully accord with the constant luminance principle because of its method of gamma correction. For saturated colours, therefore, part of the luminance information is passed by the narrow-band chrominance channel, thus causing certain defects in the picture (commonly known as 'luminance notches'). These defects are normally hardly visible, as very saturated colours occur only rarely in normal scenes[13].

The composition of the chrominance signal is dictated by the following considerations:

(a) In view of the fact that the 'mixed highs' of the luminance signal have to be added to the primary colour signals E_R, E_G and E_B in the receiver, it is necessary to modulate the subcarrier by linear combinations of E_R–E_Y and E_B–E_Y. A further advantage is that in this way the subcarrier signal vanishes for colourless parts of the scene.

(b) The maximum 'overswing' of the subcarrier signal should not exceed a certain value. The value commonly chosen is 33% of the peak white to black range.

(c) The effect of improper phase of the subcarrier signal on the hue of the displayed picture should

be such that the noticeability of phase errors depends as little as possible on the hue to be rendered. In evaluating this point one has to take into account the differential sensitivity of the human eye to colour[1,11].

(d) The signal-to-noise ratio as well as the ratio of wanted-to-unwanted signal for the chrominance channel should be as good as possible. This means that the amplitude of the subcarrier signal must be taken as large as is possible, of course taking into account points (a), (b) and (c).

Further, a decision has to be made on the choice of the broadband I-axis.

In practice it is not possible to fulfil at the same time all requirements listed above; the actual transmission system is a reasonable compromise. The final formulation of the N.T.S.C. signal, based on these considerations, is well known and will not be repeated here[6].

Signal Requirements of Display Devices

Having thus summarized the considerations underlying the choice of the design parameters of the N.T.S.C. system we shall examine the signal requirements of display devices.

There are two large classes of such devices, those containing three electron guns and those containing one electron gun. Displays of the first type can reproduce any primary colour at any moment. They can therefore be said to be simultaneous displays. The best known example is the three-gun shadow mask tube. To this type of tube three separate primary colour signals have to be fed or, alternatively, three colour-difference signals and the luminance signal. In either case the composite signal, which is available from the detector, has to be fully demodulated; that is, the chrominance signal has to be separated from the composite signal and subsequently demodulated by means of synchronous detectors. Obviously, from the point of view of receiver simplicity there is no preference for a certain composition of the chrominance signal except for the requirement that linear combinations of E_B–E_Y and E_R–E_Y should be obtained by demodulation of the subcarrier signal.

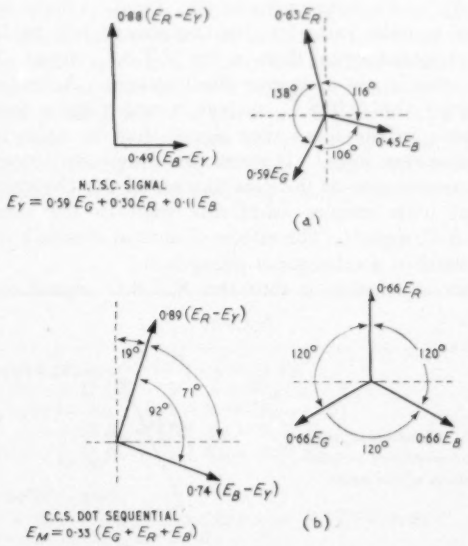

Fig. 1. *Comparison of N.T.S.C. signal and C.C.S. dot sequential signal*

Displays of the one-gun type can reproduce only one primary colour at a certain moment. They can therefore be said to operate sequentially. This means that in a certain given sequence, depending on the type of tube, samples of the primary colour signals have to be fed to the gun. For every type of tube, therefore, a composite driving signal can be given. The simplest type of signal is obtained when the sampling is of the continuous colour sequence (C.C.S.) type. It can be shown that it is not necessary to drive the tube with narrow pulses of primary colour signals. In general no essential information contained in the transmitted signal needs to be lost when only the d.c. component and the first harmonic component of the sampled signal are fed to the gun. Provided the picture tube is designed in such a manner that the beam hits the red, green and blue phosphors during equal times, and provided the phosphor efficiencies are balanced, it can be shown that the driving signal needed for this type of operation is given by

$$E_C = E_M + E_S \quad .. \quad .. \quad .. \quad .. \quad (1)$$

where

$$E_M = 0{\cdot}33\,(E_R + E_G + E_B) \quad .. \quad .. \quad .. \quad (1a)$$

$$E_S = 0{\cdot}66\,\{(E_R \cos \omega t) + E_B \cos(\omega t - 120^\circ) + E_G \cos(\omega t - 240^\circ)\} \quad .. \quad .. \quad (1b)$$

and ω denotes the angular frequency of the colour sampling[4,5,7,10].

The validity of Equ. (1) is easily verified by substituting subsequently $\omega t = 2k\pi$, $\omega t = 2k\pi + 120^\circ$ and $\omega t = 2k\pi + 240^\circ$. One finds respectively: $E_C = E_R$, $E_C = E_B$ and $E_C = E_G$, as should be the case.

For the signal E_S, which according to Equ. (1b), is the sum of three sinusoids, a vector representation can be given. It is shown in Fig. 1 (b).

As is well known, an analogous formulation can be given for the standard N.T.S.C. signal. For ease of comparison Fig. 1 (a) gives the vector representation of this signal. Both types of signal can be expressed also as the sum of two components, denoting so-called colour difference signals. For the C.C.S. signal we have

$$E_S = 0{\cdot}89\ (E_R - E_Y)\ \cos\ (\omega t - 19^\circ) + 0{\cdot}74\ (E_B - E_Y) \sin\ (\omega t - 21^\circ) \quad .. \quad .. \quad .. \quad (2)$$

while the standard N.T.S.C. chrominance signal is given by

$$E_S' = 0{\cdot}88\,(E_R - E_Y) \cos \omega t + 0{\cdot}49\,(E_B - E_Y) \sin \omega t \quad .. \quad .. \quad .. \quad .. \quad .. \quad (3)$$

The corresponding vector representations are also shown in Fig. 1.

Comparison of both figures shows that the C.C.S. dot sequential signal resembles the N.T.S.C. signal. The C.C.S. display can be said to work as a decoder for the C.C.S. signal. Where a C.C.S. display is to be used in a practical receiver for the N.T.S.C. signal, two operations on the composite signal have to be performed. First, the signal composition has to be changed in the manner indicated above, and second, the sampling frequency has to be changed from the subcarrier frequency to the

colour switching frequency of the display tube. In cases where the colour switching frequency equals the subcarrier frequency the last step can of course be omitted (e.g., one-gun focus-mask tubes). The first step requires special circuits known as 'signal translators'. Two things have to be done: the luminance signal has to be changed to the M-signal (Y-to-M conversion) and the N.T.S.C. chrominance signal has to be converted into the symmetrical signal of Fig. 1(b). Conversion of the luminance signal is accomplished by adding a signal $E_M - E_Y$ to E_Y. The signal $E_M - E_Y$ can be obtained simply from the subcarrier signal by synchronous detection.

Conversion of the chrominance signal can be effected by the use of an 'elliptical gain amplifier'[4,5,7]. Such an amplifier requires an auxiliary signal at the second harmonic of the subcarrier frequency. Experiments show that, although such circuits can operate properly, they rather complicate the receiver. In most practical receivers they have, therefore, hitherto been omitted at the cost of proper colour rendering. It seems consequently worth while to investigate the possibilities of modifying the transmitted signal.

Adaptation of the N.T.S.C. Signal to C.C.S. Display Requirements

If the N.T.S.C. signal composition should be changed care has to be taken that the outstanding transmission features of the signal are not lost. Any proposition impairing the essential properties of the system should therefore be discarded.

Among the essential features of the N.T.S.C. system is certainly its adherence to the constant-luminance principle. To preserve this feature we have to maintain the composition of the luminance signal Y. This means that the N.T.S.C. signal cannot be altered in such a manner as to avoid the Y-to-M conversion in the C.C.S. receiver. Fortunately enough this part of the signal translator does not complicate the receiver too much.

As to the chrominance signal, it would obviously be of great advantage if the translation of the chrominance signal could be entirely omitted. This can be done by transmitting the C.C.S. symmetrical chrominance signal instead of the N.T.S.C. chrominance signal. It is therefore interesting to inquire into the consequences of thus altering the transmitted chrominance signal. We have seen that the composition of the chrominance signal depends on four considerations.

To these we now add a fifth desideratum, namely that the chrominance signal be symmetrical. Together with the second, this determines fully the composition of the chrominance signal. It is easily calculated that if this signal is transmitted together with the standard N.T.S.C. luminance signal the amplitude of the subcarrier signal for saturated primary and complementary colours should equal 0·44 if the maximum overswing (occurring for blue and yellow) is not to exceed 33% of peak white. The amplitude and phase for saturated colours is depicted in Fig. 2, together with an equivalent representation with colour-difference vectors.

Turning now to the remaining requirements for the chrominance signal [points (a), (c) and (d) listed earlier] we note that the proposed signal can indeed

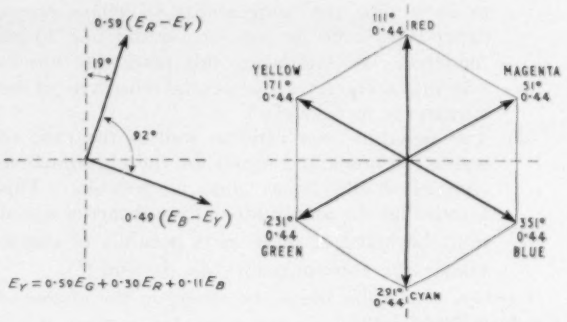

Fig. 2. *Proposed signal composition*

be written in linear combinations of $E_R - E_Y$ and $E_B - E_Y$, so adherence to point (a) is assured.

As to point (c), de Vrijer has investigated what the composition of the chrominance signal should be if the effect of phase errors on the hue should as much as possible be independent of the actual phase of the chrominance signal[12]. His investigation takes into account the differential sensitivity of the human eye to colour and the requirements that the transmitted signal be composed of linear combinations of $E_R - E_Y$ and $E_B - E_Y$ and should introduce no overswing larger than 33% of peak white. The signal composition optimally meeting the requirements is given in Fig. 3.

Comparison of Fig. 3 with Figs. 1 and 2 shows that the modified signal is even closer to the 'flat-hue-error' signal than the standard N.T.S.C. signal. From this point of view, therefore, we need have no objections to modifying the signal in the proposed way.

The only point remaining at this stage concerns the signal-to-noise ratio for the chrominance signal and the crosstalk of the luminance signal into the chrominance channel. Comparison of the proposed signal with the N.T.S.C. chrominance signal shows that the modification mainly consists in a reduction of the amplitude of the $E_R - E_Y$ component in the signal. Obviously the signal-to-noise ratio for this component will be less in the proposed signal than in the N.T.S.C. signal. However, this is not a serious disadvantage. According to Burgett[2] the N.T.S.C. system is much more sensitive to noise in the luminance signal than to noise in the chrominance signal. It seems therefore fully permissible to transmit one of the components of the chrominance signal with smaller amplitude than in the standard N.T.S.C. signal. (The effects of mutual crosstalk will be discussed in a subsequent paragraph.)

Our conclusion is that the N.T.S.C. signal can be

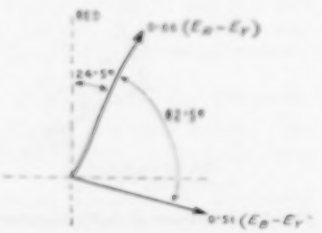

Fig. 3. *Chrominance signal for best adaptation to noticeability of hue errors*

modified in such a way that it better suits the requirements of a dot-sequential display device, without losing essential transmission properties. To this purpose it should consist of the unchanged luminance signal and a symmetrical subcarrier signal. Except for gain and phase alignment of the synchronous detectors, decoders for three-gun tubes with the new signal do not differ essentially from those employed with the normal N.T.S.C. signal.

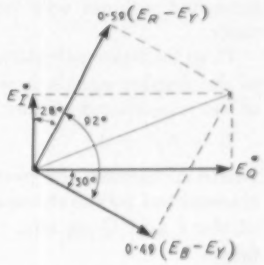

Fig. 4. *Choice of I- and Q-axes*

Choice of *I*- and *Q*-signals

Having justified the proposed modification of the N.T.S.C. signal we have now to ascertain what the best choice is for the broadband *I*-axis in the new subcarrier signal.

In the N.T.S.C. signal the *I*- and *Q*-axes are selected such that their loci cover certain colours in the C.I.E. colour diagram. The choice of these colours is commonly motivated by considerations on the properties of the human eye for colour vision of small objects. In the opinion of the author a better explanation of the experimental facts on bandwidth reduction of the chrominance signals can be deduced if the statistical properties of these signals are taken into account. However, either method leads to about the same choice of the broadband axis, so we need not to discuss here the various arguments leading to the different viewpoints. To select the broadband and the narrow-band axis for the proposed subcarrier signal we will here base our considerations on data concerning the statistical properties of the signal.

To start with we note that it is not possible to maintain the locus of both the *I*-axis and the *Q*-axis of the N.T.S.C. signal in the C.I.E. diagram. When one of these axes has been chosen the other is determined by the already fixed composition of the chrominance signal. Since the latter differs from the composition of the N.T.S.C. chrominance signal it is obvious that no more than one of the axes can be made to coincide with the corresponding axis in the N.T.S.C. system. If one chooses to maintain the locus of the *I*-axis in the C.I.E. diagram, it appears that the *Q*-axis turns towards a line connecting points quite near to green and magenta. If, on the other hand, one chooses to maintain the locus of the *Q*-axis, the *I*-axis turns to near the line red–cyan.

We have now to decide whether we shall choose one of these possibilities or a third one differing from both. In a series of experiments on the adaptation of the N.T.S.C. system to the 625-line television standard the author has carried out many measurements on the statistical properties of the N.T.S.C. chrominance signal[13]. Among these was a measurement of the average signal content in the demodulated N.T.S.C. chrominance signal as a function of demodulation axis. In this way axes of maximum and minimum signal content were determined. These appeared to be surprisingly near to the normalized *I*- and *Q*-axes. Thus, in the N.T.S.C. system the broadband *I*-signal carries much more information than the narrow-band *Q*-signal.

It should be noted that, if the probability of occurrence were equal for all colours, the described statistical measurement would nevertheless show an unequal probability of signal content values owing to the unsymmetrical nature of the N.T.S.C. chrominance signal. However, it is possible to correct for this known effect. In this way the measuring results can be used to select appropriate modulation axes for the proposed chrominance signal. Since the measured maximum appeared to be rather flat, this choice is not very critical.

Working on the lines indicated above the author has found that a good choice of axes is one in which the *Q*-axis is 30° from the $(B–Y)$-axis. The *I*-axis will then be located 28° from the $(R–Y)$-axis (Fig. 4). The composition of the *I* and *Q* signals for this case can now easily be calculated.

The results are listed in Table 1 below; for ease of comparison the formulae for the N.T.S.C. system have been included.

Rendering of Luminance and Crosstalk Phenomena

The modified signal employs the same luminance signal as the N.T.S.C. system. This means that the portion of the luminance information that is carried by the subcarrier signal is the same for both systems. However, due to the different composition of the broadband and the narrow-band components in the chrominance signal the luminance errors in transitions between

TABLE 1

N.T.S.C.	Modified signal
$E_Y = 0{\cdot}59\,E_G + 0{\cdot}30\,E_R + 0{\cdot}11\,E_B$ .. .. .. (4a)	$E_Y = 0{\cdot}59\,E_G + 0{\cdot}30\,E_R + 0{\cdot}11\,E_B$ .. .. (4b)
$E_I = -0{\cdot}27\,(E_B - E_Y) + 0{\cdot}74\,(E_R - E_Y)$ .. .. (5a)	$E_I^* = -0{\cdot}25\,(E_B - E_Y) + 0{\cdot}52\,(E_R - E_Y)$ .. (5b)
$E_Q = 0{\cdot}41\,(E_B - E_Y) + 0{\cdot}48\,(E_R - E_Y)$ .. .. (6a)	$E_Q^* = 0{\cdot}42\,(E_B - E_Y) + 0{\cdot}28\,(E_R - E_Y)$ .. .. (6b)
$E_I = -0{\cdot}28\,E_G + 0{\cdot}60\,E_R - 0{\cdot}32\,E_B$ .. .. (7a)	$E_I^* = -0{\cdot}16\,E_G + 0{\cdot}44\,E_R - 0{\cdot}28\,E_B$ .. .. (7b)
$E_Q = -0{\cdot}52\,E_G + 0{\cdot}21\,E_R + 0{\cdot}31\,E_B$ .. .. (8a)	$E_Q^* = -0{\cdot}42\,E_G + 0{\cdot}07\,E_R + 0{\cdot}35\,E_B$ .. .. (8b)
Composite signal: $E_Y + E_Q \sin(\omega t + 33°) + E_I \cos(\omega t + 33°)$ if phase 0° represents the phase of $(E_B - E_Y)$ .. .. .. (9a)	Composite signal: $E_Y + E_Q^* \sin(\omega t + 30°) + E_I^* \cos(\omega t + 30°)$ if phase 0° represents the phase of $(E_B - E_Y)$ .. (9b)

D

saturated colours will be somewhat different in both cases.

If, to facilitate calculation, we assume that the gamma of the display equals 2, we find for the total luminance of the reproduced picture

$$L = E_y^2 + \Delta^2 \quad .. \quad .. \quad .. \quad .. \quad .. \quad (10)$$

where Δ^2 denotes the portion of the luminance which is transmitted by the chrominance signal. Δ^2 is a function of the I and Q signals. For the N.T.S.C. system one finds[8]

$$\Delta^2 = 0{\cdot}46\, E_I^2 + 0{\cdot}45\, E_I E_Q + 0{\cdot}67\, E_Q^2 \quad .. \quad (11)$$

The loci of constant Δ^2 in the I-Q plane are ellipses. The ratio of the lengths of the major and minor axes is 1·27. The angle between the major axis and the I axis is 17°.

In the same manner Δ^2 can be expressed in the I and Q signals of the proposed system. One finds

$$\Delta^2 = 0{\cdot}94\, E_I^{*2} + 0{\cdot}93\, E_Q^{*2} + 0{\cdot}88\, E_I^* E_Q^* \quad (12)$$

The ratio of the lengths of the major and minor axes is 1·68. The angle between the major axis and the I axis is 45°.

It should be emphasized that the magnitude of Δ^2 in Equs (11) and (12) is exactly the same since both systems employ the same luminance signal. Only the manner in which the constant-luminance error depends on the I and Q signals differs for both cases.

Comparing these data we see that the ellipticity of the proposed signal is larger than that of the N.T.S.C. signal. This is a slight disadvantage for two reasons. First, compensation of the luminance errors in a colour receiver, if wanted, is less efficient if the compensation should be accomplished by a signal representing the envelope of the subcarrier signal alone. Second, in the compatible black-and-white picture the luminance contribution of the chrominance signal, caused by rectification of this signal in the picture tube, depends only on the amplitude of the subcarrier signal. However, the luminance errors due to the lack of constant luminance depend also on the phase of the subcarrier signal owing to its ellipticity. This means that theoretically both effects cannot compensate for each other as well as in the N.T.S.C. system. In practice, the compensation will be very poor in both cases as the frequency response of the receiver is normally so much down at subcarrier frequency that the effect of subcarrier rectification is much less than theoretically could be expected.

It will occur to the reader that the two effects mentioned above are of so theoretical a nature that they can hardly be looked upon as serious disadvantages. For the sake of completeness they should however be mentioned.

Finally, some remarks on the mutual crosstalk between the luminance and the chrominance signal. Since in the modified system the average amplitude of the subcarrier signal is smaller than in the N.T.S.C. system, the crosstalk of the chrominance signal into the luminance channel will also be smaller. As is well known, this type of crosstalk manifests itself by desaturation effects and visibility of the dot structure. To reduce it a notch filter is commonly inserted into the receiver luminance channel.

On the other hand, the crosstalk of the 'mixed highs' into the chrominance channel (cross-colour) will be somewhat larger in the modified system. Moreover, the effect will be slightly enhanced by the fact that, according to Equ. (12), the luminance contribution in the modified system is about equal for spurious signals in the I-channel and in the Q-channel. In the N.T.S.C. system advantage is taken of the fact that the I signal contributes less to the luminance than does the Q signal. Because of its larger bandwidth, spurious signals occurring in the I-channel will have a larger amplitude than those in the Q-channel. As the crosstalk effects are visible mainly because of their luminance contribution, the relatively small coefficient of I in Equ. (11) is advantageous[14].

However, it is very unlikely that these minor effects, which are normally hardly visible, would deteriorate the picture to any extent. If necessary, a notch filter might be inserted into the luminance channel at the camera end.

In conclusion it may be said that the crosstalk effects on the average will be of the same magnitude in both systems, and therefore from this point of view, too, no objections need be made against the proposed modification of the transmission system.

REFERENCES

[1] F. J. Bingley, "Transfer characteristics in N.T.S.C. color television, Part I", *Proc. Inst. Radio Engrs*, 1953, Vol. 41, p. 838.
[2] M. J. Burgett, "A subjective study of color synchronization performance", *Proc. Inst. Radio Engrs*, 1953, Vol. 41, p. 979.
[3] W. F. Bailey, "The constant luminance principle in N.T.S.C. color television", *Proc. Inst. Radio Engrs*, 1954, Vol. 42, p. 60.
[4] B. D. Loughlin, "Processing of the N.T.S.C. color signal for one-gun sequential color displays," *Proc. Inst. Radio Engrs.*, 1954, Vol. 42, p. 299.
[5] S. K. Alfes and A. P. Stern, "Single-gun picture tubes in N.T.S.C. color television", Conv. Rec. Inst. Radio Engrs, 1954, Vol. 2, Part 7, p. 46.
[6] D. G. Fink, "Color television standards", McGraw-Hill, 1955.
[7] K. McIlwain and C. E. Dean, "Principles of color television", Chapter 16. Wiley 1956.
[8] D. Richman, "Directions of improvements in N.T.S.C. color television systems", *Proc. Inst. Radio Engrs*, 1956, Vol. 44, p. 1125.
[9] R. G. Clapp a.o., "A new beam-indexing color television display system", *Proc. Inst. Radio Engrs* 1956, Vol. 44, p. 1108, and Conv. Rec. Inst. Radio Engrs, 1956, Vol. 4, Part 3, p. 94.
[10] J. B. Chatten and R. A. Gardner, "Accuracy of color reproduction in the 'Apple' system", Conv. Rec. Inst. Radio Engrs, 1957, Vol. 5, Part 3, p. 230.
[11] R. A. Bloomsburgh a.o., "An advanced color television receiver using a beam indexing picture tube", Conv. Rec. Inst. Radio Engrs, 1957, Vol. 5, Part 3, p. 243.
[12] F. W. de Vrijer, "The choice of chrominance signals in the N.T.S.C. system with a view to the differential sensitivity of the human eye to colour", *Acta Electronica*, 1957–1958, Vol. 2, p. 103.
[13] J. Davidse, "N.T.S.C. Colour television signals", *Electronic Radio Engr*, 1958, Vol. 36, p. 370 and p. 416.
[14] J. Davidse, "Transmission of colour television signals", *Tijdschr. Ned. Radiogenootschap*, 1959, Vol. 24, p. 255 and *Trans. Inst. Radio Engrs*, 1960, Vol. BC-6, p. 31.
[15] R. N. Jackson, "Single-gun versus three-gun tubes", *J. Telev. Soc.*, 1960, Vol. 9, p. 207.

MASS-PRODUCED SUPERCONDUCTIVE MAGNETS

The Radio Corporation of America have announced the development of a new process for the mass production of a superconductive material which will retain its properties in magnetic fields up to 94,000 gauss and, it is claimed, at somewhat higher temperatures than other known superconductors. Technical details of the development have not been given except that it is a chemical method for the rapid and continuous growth of crystalline niobium-tin.

It has been known for some time that niobium-tin has many advantages as a superconductor but, until now, no satisfactory method has been devised to produce the material in the desired crystal form in large quantities, largely because of the extreme brittleness of the crystalline substance and the consequent difficulty of working with it.

Laboratory apparatus which is capable of producing a uniform crystal coating of niobium-tin on fine wire, at a rate of up to 30 ft/hr, has been constructed by R.C.A. and it is expected that this rate will be increased when production machines are produced. The finished wire has been used successfully to wind coils of up to 90 turns on a $\frac{1}{4}$ in. former. The same basic process has been used to produce hollow tubes and thin films of crystalline niobium-tin.

Shielded Dielectric Waveguide

MEASUREMENT OF THE PROPAGATION CHARACTERISTICS

By K. W. H. Foulds, Ph.D., A.M.I.E.E.* and P. Sampain, M.Sc.

SUMMARY. *The term 'shielded dielectric waveguide' is the name given to the transmission system formed by a narrow rectangular slab of dielectric placed between the plates of a wide parallel-plate transmission line. The electric field distribution has been measured in both the air and the dielectric regions of this shielded dielectric waveguide, and the results verify that the fields decay exponentially outside the dielectric slab. The experimental values of this decay, and of the guide wavelength, agree very closely with the theoretical values.*

Recently Clarricoats[1,2] has published a comprehensive theoretical analysis of the propagation of electromagnetic waves along circular dielectric rods. He considers two cases, a dielectric rod in an unbounded medium, and a dielectric rod placed along the axis of a bounding circular metallic waveguide.

This paper deals with measurements of the characteristics of propagation along a bounded dielectric rod of rectangular cross section. A narrow strip of low-loss dielectric material is placed between the plates of a very wide parallel-plate transmission line, fitted with absorbing loads along the edges. This transmission system is referred to subsequently as the shielded dielectric waveguide. If the plate separation is small the shielded dielectric waveguide supports a simple TE_0 mode. The field components of this mode are similar to those of the dominant mode in rectangular waveguide except that the field amplitudes decrease exponentially away from the dielectric-air boundaries.

The transverse and longitudinal variations of the electric field are measured by conventional standing wave probe techniques. The experimental results for the transverse distribution of the electric field show an anomalous rapid variation in the apparent electric field strength at the interfaces. This is the same phenomenon as reported by Strauss[3]. A full explanation of this behaviour, which is due to the method of measurement, is given in a later section ('Variations of Electric Field at an Air-Dielectric Interface').

Description of the Field Patterns

The theoretical analysis of the propagation of an electromagnetic wave along the shielded dielectric waveguide shown in Fig. 1 (a) is outlined in the Appendix, but it is worthwhile describing here the more important features.

The dominant mode is a TE_0 and this has three field components, E_x the transverse electric field normal to the parallel plates, H_y a transverse magnetic field, and H_z a longitudinal magnetic field. There is no variation of any field with x and consequently these resemble somewhat the fields of the normal TE_{01} mode in a rectangular waveguide. The amplitude dependence upon y is shown in Figs. 1 (b) and (c), which show that each component decreases exponentially with distance away from the dielectric-air interfaces.

One of the characteristic properties of metallic waveguide propagation is the closed-loop configuration of the magnetic field lines. It is interesting to plot the corresponding magnetic field patterns for the shielded dielectric waveguide and to examine how these depend upon the thickness of the slab. The total magnetic field at any point is determined by the amplitudes of two field components, and the direction in which the magnetic

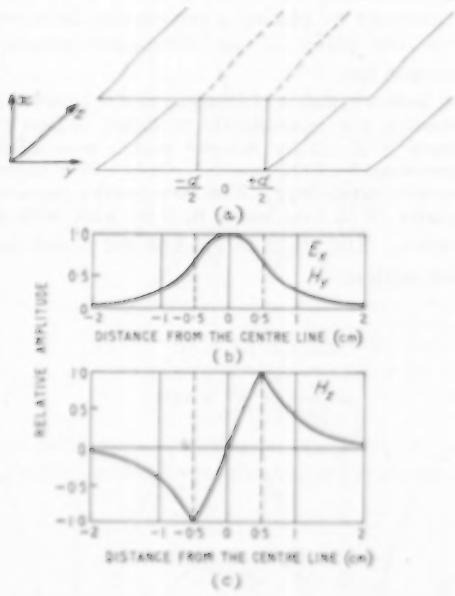

Fig. 1. *Shielded dielectric waveguide (a) Schematic arrangement of dielectric slab and parallel plate transmission line; (b) Transverse distribution of E_x and H_y; (c) Transverse distribution of H_z. $d = 1$ cm. $\lambda_0 = 3{\cdot}2$ cm.*

* Battersea College of Technology, Dept. of Physics.

field acts depends upon their relative amplitudes. The magnetic field patterns have been deduced following the technique of Barlow[4] and are plotted in Fig. 2. Although there is no sharp cut-off associated with this shielded dielectric waveguide TE_0 mode, Fig. 2 shows very clearly that as the ratio (dielectric width)/λ becomes small the wave pattern corresponds more and more nearly to an ordinary plane T.E.M. wave.

It is interesting to point out that, at a quarter of a cycle before these loops represent the magnetic field lines, the same loops correspond to points of a given electric field strength. In this case the value of the constant C expresses the electric field strength relative to the maximum value existing at the centre of the dielectric.

Apparatus and Experimental Procedure

General Description of Apparatus

The experiments were designed to measure both the transverse and longitudinal characteristics of wave propagation along the simple shielded dielectric waveguide obtained by placing a rectangular dielectric slab between the plates of an air-spaced parallel-plate transmission line.

The dielectric slab is of Distrene and the parallel-plate transmission line is a slightly modified version of that described in detail by Adey[5,6] and is very similar to that described by El Kharadly[7]. Only a brief description is therefore given here. The line consists essentially of two plates 16 ft. long and 2 ft. 6 in. wide with a $\frac{1}{2}$ in. separation. The edges of the line are closed by lossy wooden wedges.

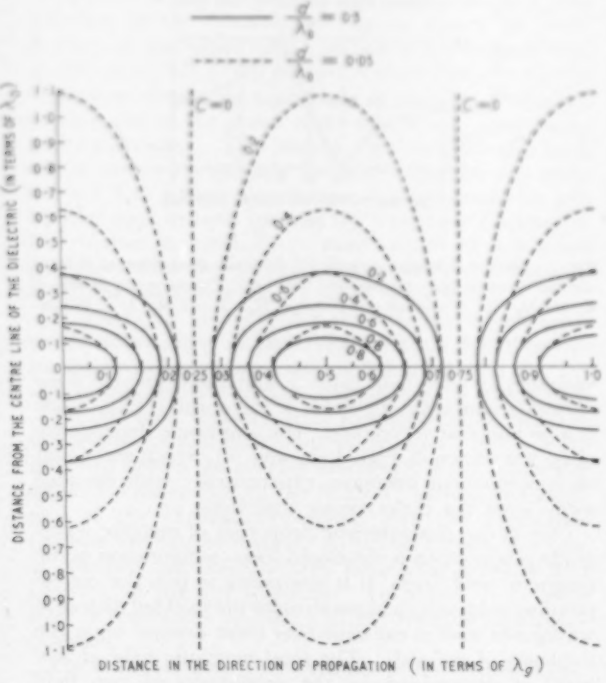
$\frac{d}{\lambda_0} = 0.5$
$\frac{d}{\lambda_0} = 0.05$
C=0
C=0
DISTANCE FROM THE CENTRE LINE OF THE DIELECTRIC (IN TERMS OF λ_0)
DISTANCE IN THE DIRECTION OF PROPAGATION (IN TERMS OF λ_g)

Fig. 2. *Magnetic field patterns in the shielded dielectric waveguide*

LIST OF SYMBOLS

In general the symbols are explained in the text where they are first introduced, but for convenience the more important symbols are listed below.

d = width of the dielectric slab.
E = total electric field.
E_y' = the transverse electric field in region 1.
E_y'' = the transverse electric field in region 2.
E_y''' = the transverse electric field in region 3.
K_1 = field decay factor in the regions 1 and 3.
k_2 = field variation factor in region 2.
β = $2\pi/\lambda_g$, propagation constant in the shielded dielectric waveguide.
λ_g = wavelength in the shielded dielectric waveguide.
λ_0 = wavelength of a plane wave in free space.
$\mu_1\epsilon_1$ = permeability and permittivity of region 1.
$\mu_2\epsilon_2$ = permeability and permittivity of region 2.
ω = $2\pi \times$ frequency.

The measuring section, which has not been modified, consists of a section of the upper plate 2 ft. 6 in. × 2 ft. 6 in. This square plate is slotted along a centre line and carries a conventional standing-wave indicator carriage and probe located in the slot by a tongue. This section can be removed from the rest of the top plate and can be turned through 90°, enabling field amplitude measurements to be made either along or at right angles to the axis of the line. The dielectric slab was placed approximately along the centre line of the parallel-plate line and parallel to the slot in the square measuring section. Apart from the region immediately beneath this slotted section the upper and lower surfaces of the dielectric slab were coated with thin aluminium foil to ensure good contact with the plates.

In previous applications of the parallel-plate line the power has been fed into the line by a microwave horn, but this arrangement has been modified for these guided wave experiments. For the X-band measurements the dielectric slab was fed directly from an open-ended waveguide. For the S-band measurements power was coupled into the dielectric slab by a coaxial probe placed about $\lambda_g/4$ from the end of the slab.

Two dielectric slabs were used, the widths being 1 cm and 2·54 cm. Each slab was at least 9-ft. long and consisted of 20-in. lengths of Distrene cemented together. In each case the end of the slab was made flush with the end of the parallel plates so that this composite line could be properly short circuited.

Measurements

The Guide Wavelength

The measurement of the wavelength in the shielded dielectric waveguide was straightforward. The dielectric slab was placed parallel to the slot in the measuring section and the composite line short-circuited. The standing-wave pattern was then traced out in detail and the guide wavelength deduced from the average separation of adjacent zeros.

The Transverse Distribution

The transverse distribution of the electric field can be obtained by setting up the measuring section with its slot perpendicular to the dielectric slab. It is worthwhile to point out that since the probe must traverse the

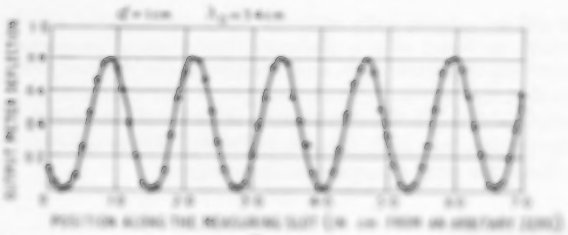

Fig. 3. *Longitudinal standing-wave pattern in the shielded dielectric waveguide with short-circuit termination*

dielectric slab the maximum probe penetration in the region of the slab is zero. It was decided to measure the transverse field distribution over as much of the cross section as possible with this zero probe penetration, although it was realized that any surface irregularities would become important.

The relative field amplitudes were measured using a calibrated attenuator in the input waveguide.

Results

Measurements were made on a dielectric slab 1-cm wide at a free space wavelength of 3·0 cm, 3·2 cm, 3·4 cm, and 9·14 cm, and on a slab 2·54-cm wide at a free space wavelength of 9·02 cm. Figs. 3 and 4 show typical results for the longitudinal standing-wave pattern and the transverse field distribution. These figures have been given primarily to show the regularity of the standing-wave pattern and the sudden discontinuity in the apparent electric field at the air-dielectric interfaces. Fig. 4 shows that apart from the rapid increase at the interfaces, the sinusoidal variation over the dielectric region, and the exponential decay in the air region agree very well with the theoretical curves.

The important factors of the propagation along the shielded dielectric waveguide are the wavelength λ_g and the exponential decay factor of the field in the air, K_1. It is shown in the Appendix that the quantities λ_g/λ_0 and $K_1\lambda_0$ do not depend directly upon the frequency but depend only upon the ratio d/λ_0. (The quantity $K_1\lambda_0$ is the decrease, in nepers, of the field amplitudes as one moves perpendicularly away from the dielectric slab through a distance λ_0.)

Thus all the experimental results, for different frequencies and different slab widths, can be plotted on a single diagram, as shown in Fig. 5 and compared with the theoretical values. The agreement between predicted and measured values is good but it must be remembered that the existence of the rapid change at the interfaces is not shown in the generalized Fig. 5.

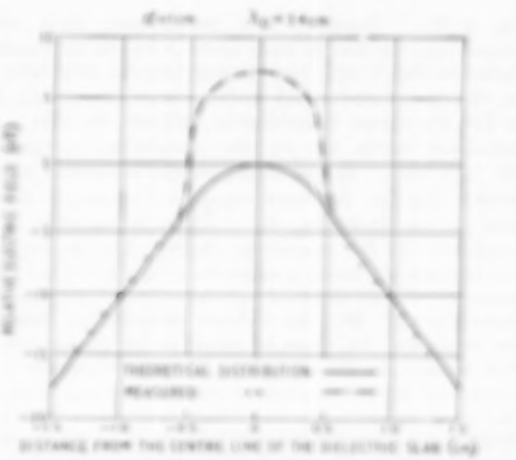

Fig. 4. *Transverse distribution of the electric field in the shielded dielectric waveguide*

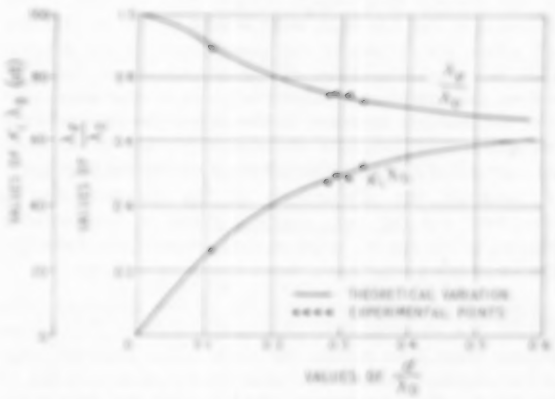

Fig. 5. *Theoretical and experimental results shown as a function only of d/λ_0*

Variations of Electric Field at an Air-Dielectric Interface

Explanation of the step

The sudden change in the apparent electric field at the air-dielectric boundaries is best explained with the aid of Fig. 6, in which for simplicity the carriage tongue and probe have been omitted. For this set-up the electric field in the slot is the fringing field shown in

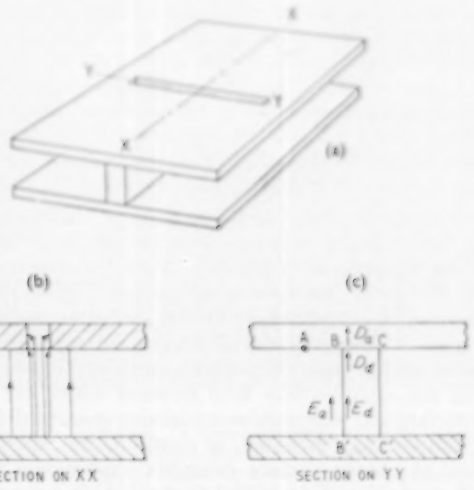

Fig. 6. *Fringing of the electric field into the measuring slot*

Fig. 6 (b). Consider now the electric field which fringes into the slot at some point A in the air region as shown in Fig. 6 (c). The fringing electric field here will be directly proportional to the transverse electric field in the air region immediately beneath the slot. This argument holds up to the air-dielectric interfaces BB′ and CC′. At the interface the transverse electric field in the air, E_a, must equal the transverse electric field in the dielectric, E_d. There is therefore a discontinuity in the transverse electric flux density, that in the dielectric being greater than that in the air by the factor ϵ_r. At the dielectric-air interface at the top of the dielectric slab, BC, the normal electric flux density in the dielectric, D_d, must be equal to the normal electric flux density in the air, D_a. There is therefore a discontinuity in the associated normal electric fields, i.e., the electric field in the air, which determines the electric field fringing into the slot, is greater than the transverse electric field in the dielectric immediately beneath it by the factor ϵ_r.

In use, the probe output depends upon the electric field in the vicinity of the probe and this is determined by the electric field which fringes into the slot. The presence of the carriage tongue and probe in the slot will affect the details of the distribution of the electric field, but the principles of the argument of the preceding paragraph are unaltered. It is therefore seen that the sudden increase in the apparent electric field strength at the edges of the dielectric slab arises from the method of measurement and has no other significance. In practice the abruptness of the discontinuity is smoothed out by two factors, there is considerable fringing of the electric fields at the corners of the dielectric slab, and the probe has a finite coupling volume.

Since the relative permittivity of the dielectric slab is 2·57 the electric field above the slab is 2·57 times greater than that within the slab. The observed step in the relative electric field distribution shown in Fig. 4 should therefore be $20 \log_{10} 2{\cdot}57$, or 8·2 dB. However, the measured value is 7 dB and the corresponding values from the measurements at $\lambda_0 = 3{\cdot}2$ cm and $\lambda_0 = 3{\cdot}0$ cm are 7·2 dB and 7·4 dB respectively. The magnitude of the step in the S-band measurements, using a different standing-wave detector carriage and probe assembly, were 9·0 dB at 9·14 cm and 8·5 dB at 9·02 cm. It is seen that the measured values of the step are all of the same order as the predicted value. There is little doubt that the principle explained above is the basis of the explanation of the rapid change at the boundary.

The scatter in the individual values and particularly the fact that the average value for the 3-cm measurements is appreciably different from the average value for the 9-cm measurements indicates that the true situation is not as simple as the preceding explanation suggests. The problem of measuring transverse field distributions is quite important, especially in connection with the asymmetrical field patterns which are set up in rectangular waveguides containing polarized ferrites. It was decided, therefore, to continue the experimental work to obtain a more complete explanation for the step at the interface. The results, which have already been published in a brief form[8], showed that the step could be substantially reduced by using a probe which could be fitted with a dielectric sleeve when measuring over the dielectric slab, thus removing the discontinuity in E at the interface. It was suggested that the remaining step (about $2\frac{1}{2}$ dB) would be eliminated by using a probe that was fully tunable instead of the usual design which has only a single tuning plunger.

Conclusion

The results of the experiments made on the shielded dielectric waveguide have verified that the fields decay exponentially outside the dielectric slab. The experimental values of the decay and of the guide wavelength have agreed very closely with the theoretical values.

The experiments revealed a rapid variation in the apparent electric field strength at the air-dielectric interface. This phenomenon is more apparent than real, and is caused by the method of measurement.

Acknowledgements

The authors would like to thank Professor Tustin for the facilities offered in the laboratory. The experimental results on the shielded dielectric waveguide were obtained by one of the authors doing postgraduate work and thanks are due to the Commissao de Estudos da Energia Nuclear and Institute de Alta Cultura of Lisbon for the provision of a maintenance grant making this possible.

REFERENCES

[1] P. J. B. Clarricoats, I.E.E. Monograph No. 409E.
[2] P. J. B. Clarricoats, I.E.E. Monograph No. 410E.
[3] T. M. Strauss, Inst. Radio Engrs Wescon Convention Record, Part 1, 1958, p. 135.
[4] H. M. Barlow, "Microwaves and Waveguides", Constable, 1947, p. 62.
[5] A. W. Adey, Ph.D. Thesis of Electrical Engineering, University of London, 1954.
[6] A. W. Adey, *Canad. J. Phys.*, 1955, Vol. 33, No. 8, p. 407.
[7] El-Kharadly, *Proc. Instn elect. Engrs*, 1955, Vol. 102B, p. 17.
[8] K. W. H. Foulds and P. Sampaio, Proc. Inst Radio Engrs, 1959, Vol. 47, No. 9, p. 1663.

APPENDIX

Determination of the Propagation Constants of the TE_0 Modes in the Shielded Dielectric Waveguide

The propagation constants in the various TE_0 modes which can propagate along the shielded dielectric waveguide are determined by a characteristic transcendental equation which is derived in the following manner. We shall restrict our attention to dielectrics of zero conductivity.

Since the separation of the parallel plates is small, we can put $\partial/\partial x = 0$, and $E_z = 0$, into Maxwell's equations and this shows that the only non-zero field components are E_x, H_y and H_z. The simplified Maxwell's equations lead to the wave equation which must be satisfied by the transverse electric field inside and outside the dielectric slab. Solutions of these equations are chosen which make the fields zero at infinite distance from the sides of the dielectric slab.

The expressions for the transverse electric field are

$$E_x'(y, z, t) = A_1 e^{K_1 y} e^{j(\omega t - \beta z)} \text{ in the region } -\infty < y < -\frac{d}{2} \quad (1)$$

$$E_x''(y, z, t) = (A_2 \cos k_2 y + B_2 \sin k_2 y)\, e^{j(\omega t - \beta z)} \text{ in the region } -\frac{d}{2} < y < +\frac{d}{2} \quad (2)$$

$$E_x'''(y, z, t) = B_3 e^{-K_3 y} e^{j(\omega t - \beta z)} \text{ in the region } \frac{d}{2} < y < \infty \quad (3)$$

$$\text{where } K_1^2 = \beta^2 - \omega^2 \mu_1 \epsilon_1 \text{ and } k_2^2 = \omega^2 \mu_2 \epsilon_2 - \beta^2 \quad (4)$$

In these equations β is the propagation constant, μ_1, ϵ_1 and μ_2, ϵ_2 are the permeability and permittivity of air and the dielectric

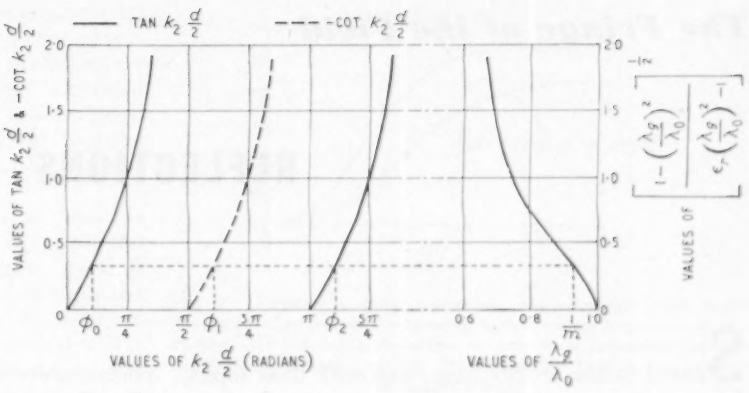

Fig. 7. *Curves illustrating the graphical solution of Equs.* (5) *and* (6)

——————— $\tan k_2 \frac{d}{2}$ *v* $k_2 \frac{d}{2}$

— — — — — $\cot k_2 \frac{d}{2}$ *v* $k_2 \frac{d}{2}$

respectively and A_1, A_2, B_2 and B_3 are constants to be determined. We shall assume that $\mu_1 = \mu_3$.

The boundary conditions which have to be satisfied are that the tangential field components in the two media must be equal at the dielectric interfaces, i.e., E_x and H_z must be continuous at $y = \pm d/2$. This leads to the condition that either $A_2 = 0$, or $B_2 = 0$. Equs (1), (2) and (3), then show that if $A_2 = 0$, $A_1 = -B_3$ and the field has odd symmetry about the centre of the slab. If $B_2 = 0$, however, it follows that $A_1 = B_3$ and the field has even symmetry about the centre of the slab. Eliminating the remaining constants A_1 and B_2, or A_1 and A_2 leads to the equations

$$\tan k_2 \frac{d}{2} = \frac{K_1}{k_2} = \sqrt{\frac{\beta^2 - \omega^2 \mu \epsilon_1}{\omega^2 \mu \epsilon_2 - \beta^2}} \text{ for even symmetry}$$

$$\text{and } \cot k_2 \frac{d}{2} = -\frac{K_1}{k_2} = -\sqrt{\frac{\beta^2 - \omega^2 \mu \epsilon_1}{\omega^2 \mu \epsilon_2 - \beta^2}} \text{ for odd symmetry.}$$

Expressing these equations in terms of λ_g, the wavelength in the shielded dielectric waveguide, λ_0 the free space, or air, plane wavelength and ϵ_r the relative permittivity of the dielectric, we have:

$$\tan k_2 \frac{d}{2} = \tan\left[\pi \sqrt{\epsilon_r - \left(\frac{\lambda_g}{\lambda_0}\right)^2} \frac{d}{\lambda_0}\right] = \sqrt{\frac{1 - \left(\frac{\lambda_g}{\lambda_0}\right)^2}{\epsilon_r \left(\frac{\lambda_g}{\lambda_0}\right)^2 - 1}} \quad \ldots \ldots \quad (5)$$

$$\text{and } \cot k_2 \frac{d}{2} = \cot\left[\pi \sqrt{\epsilon_r - \left(\frac{\lambda_g}{\lambda_0}\right)^2} \frac{d}{\lambda_0}\right] = -\sqrt{\frac{1 - \left(\frac{\lambda_g}{\lambda_0}\right)^2}{\epsilon_r \left(\frac{\lambda_g}{\lambda_0}\right)^2 - 1}} \quad (6)$$

Since the relative permittivity of the dielectric slab is known, these equations give λ_g/λ_0 as a function of d/λ_0, although rather indirectly. The method of solving the equations is indicated in Fig. 7. For a chosen value of $\lambda_g/\lambda_0 = 1/m$, say, the value of $k_2 d$ can take a series of values ϕ_0, ϕ_1, ϕ_2 . . . etc.,

Where

$0 < \phi_0 < \pi/2$	determines the necessary value of d/λ_0 to give the chosen value of λ_g/λ_0 for propagation in the lowest order mode.
$\pi/2 < \phi_1 < \pi$	determines the corresponding value of d/λ_0 for propagation in the first asymmetrical mode.
$\pi < \phi_2 < 3\pi/2$	determines the corresponding value of d/λ_0 for propagation in the second symmetrical mode.

It is clear that all modes except the lowest order symmetrical mode exhibit a cut-off phenomenon, e.g. the first order asymmetrical mode cuts off for $\phi_1 = \pi/2$. This cut-off is characterized by $\lambda_g/\lambda_0 = 1$. The cut-off wavelength λ_c for the nth mode is found from Equ. (4) and is simply

$$\lambda_c = \frac{2d}{n} \sqrt{\epsilon_r - 1}$$

The experiments were restricted to propagation in the lowest order mode which as can be seen exhibits no cut-off behaviour.

Equ. (5) shows that if one deals with the ratios λ_g/λ_0 and d/λ_0 rather than merely λ_g and d, the relation between λ_g/λ_0 and d/λ_0 is independent of the frequency.

Another important factor associated with the propagation of the wave is K_1 the rate at which the fields decay in the air space; i.e., the relation between K_1 and d. From Equ. (4) it follows that

$$K_1 \lambda_0 = 2\pi \sqrt{\left(\frac{\lambda_0}{\lambda_g}\right)^2 - 1}$$

Using the already derived relation between λ_g/λ_0 and d/λ_0 enables a graph to be drawn of $K_1 \lambda_0$, the transverse decay over a distance of one free space wavelength, as a function of d/λ_0. This relation is again independent of the actual frequency.

Curves of λ_g/λ_0 and $K_1 \lambda_0$ for the dominant mode are shown in Fig. 5 as a function of d/λ_0 corresponding to $\epsilon_r = 2 \cdot 57$.

ALUMINIUM HONEYCOMB PANELS

An interesting application of metal honeycomb panel construction has been demonstrated in the Leo III computer. The doors and end covers of the tape machines are all constructed with Ciba aluminium honeycomb bonded in a sandwich fashion between 0·036 in. aluminium-alloy skins. The edges of the honeycomb are surrounded

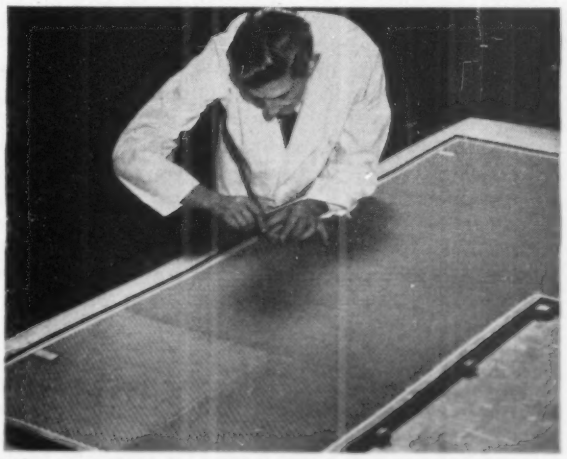

by a standard extrusion. A completed door or panel gives the appearance of solid aluminium and combines extreme rigidity with low weight. The picture shows the honeycomb being cut away and an aluminium block inserted where the panel will eventually be bolted to the main frame.

REFLECTIONS

Several earlier articles have dealt with these topics, I know. The sun as a source of energy, and the direct conversion of heat into electrical energy have both been in the syllabus fairly often. But this is not mere recapitulation; in any case, I cannot remember capitulating at all—on the contrary I am perpetually in hot pursuit, and sometimes fail to keep the quarry within sight. For, you see, the nicely balanced equilibrium in which it is possible to digest sufficient new material in 30 days to provide an article every month seems to have been displaced by the exponential expansion of physics on every front. And what catches the eye as an interesting topic for an elementary treatment turns out quite often to have reached the stature of material for a major international conference by the time one has got down to business. In this instance, the depressing sequence is reversed. When I visited the *Four Solaire* at Montlouis a couple of years ago as an innocent tourist I had already been hopelessly outstripped by events; they had had the conference the year before!

The present article is occasioned by the publication by the Centre National de la Recherche Scientifique of a full-scale report of a colloquium held at Montlouis in 1958, and entitled "Applications Thermiques de L'Energie Solaire dans la Domaine de la Recherche et de l'Industrie". (My aunt, on seeing this, took penumbrage. She even suggested that I should call this article "On All Fours".) Much of the work described in this report is, of course, rather technical and deals with the problems of focusing, absorbing, and reflecting the sun's radiation, with the spectral distribution of the energy, and with the practical details of harnessing it for specific purposes such as, for example, cooking and refrigeration. Well, it is all there for you to read. Here I only propose, if rough arithmetic doesn't let me down, to deal with two points from a very elementary viewpoint—the high temperatures that ought to be available by optical focusing, and the sort of energy concentration that is possible without any critical effort at this.

Focusing Solar Radiation

Well, this is familiar enough. As a relief from the recurrent determination of g in your elementary physics you doubtless spent many hours engaged in $1/v + 1/u = 1/f$, and know as much as it is good for anyone to know about the behaviour of concave mirrors under textbook conditions. The paraboloidal reflector, of course, gives a point image at the focus of an infinitely distant object point, greatly to the satisfaction of the astronomer who is simply interested in getting sufficient *energy* on his photosensitive device to be able to locate the point at all. But geometrical optics leads to instantaneous nonsense when we start dealing with the energy and power radiated. For any radiating *point* would have to be infinitely bright and so at an infinitely high temperature; and any *point* image would receive an infinitely great concentration of power. The wave-nature (or wave-behaviour) of radiation itself protects us from such inconveniences, for no optical system can form point images. Elementary photometry (which, alas, seems at some stage to bring in point sources, which we won't worry too much about for the moment) suggests that the maximum temperature, or at least the maximum power density, that could ever be attained at the focus under ideal conditions should be that of the source in practice, the radiation from the sun, effectively acting as a disc at about 6 000 °K under favourable conditions.

If we imagine the sun to be presenting a series of elements of area δS_1 each emitting uniformly in all directions, and W_1 the power emitted per unit area (again in all directions) then the fraction collected by a mirror of projected area A at distance u will be $A/4\pi u^2$, and the actual power received from this element is $W_1\delta S_1 A/4\pi u^2$ (Fig. 1). If this is cast on to an image of the element of area δS_2, then the power received per unit area is $(W_1 A/4\pi u^2)\ (\delta S_1/\delta S_2)$; and as $\delta S_1/\delta S_2 = u^2/f^2$ since the image is formed in the focal plane at distance f from the pole, the power per unit area is $W_1 A/4\pi f^2$. Now, if D is the diameter of the mirror aperture, $A = \pi D^2/4$. So the expression for the power per unit area becomes $W_1 D^2/16f^2$.

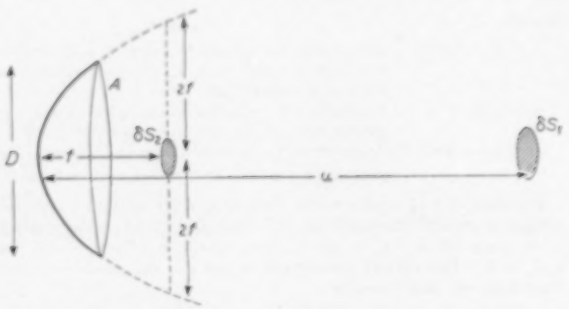

Fig. 1. *The element δS_1 of the sun's surface, at distance u from the parabolic reflector, is supposed to be "radiating uniformly in all directions". The reflector forms an image of area δS_2 at its focus. The power concentrated on δS_2, with the assumptions made, is $A/4\pi u^2$ that emitted from δS_1*

The power received per unit area is thus proportional to the square of the relative aperture. Every photographer of course knows this obvious piece of elementary optics. There has, however, been some concealed fiddling with the inverse-square law and uniform point sources (of finite area) to get the factor 1/16; and the best we can do about that is to show that it does not lead us into nonsense.

With a paraboloid there is no geometrical limit (as there is with a sphere) to the value of D/f; but the usable limit is in fact in each case the same, for if D exceeds $4f$ then energy will fall on the *back* of the supposed receiving surface. The maximum value for D^2/f^2 is thus 16, and the maximum power concentration is W_1, the same as the power per unit area from the source. For many of the 30 or so mirror systems in use in various parts of the world, D/f is a little over 2, giving a power concentration about a quarter of that of the solar surface. Using Stefan's law, this concentration corresponds to a black-body temperature $\sqrt[4]{1/4}$ times that of the sun's surface, say 4 250 °K; the 3 000 °K or so actually attained seems consistent with this, when we think of the reflection and absorption factors involved.

Incidentally, simply as a means of reaching very high temperatures the solar furnace is perhaps not so spectacular after all (Fig. 2). The positive crater of the carbon arc is at about the 3 000 °K mark, and indeed one of the papers in this colloquium describes a two-paraboloid system, and also an ellipsoidal mirror, in both cases with an arc at one focus and a specimen to be heated at the other, which would do the same kind of job. But on a much smaller scale. The chief interest is in getting the power itself, which is of course available on a huge scale.

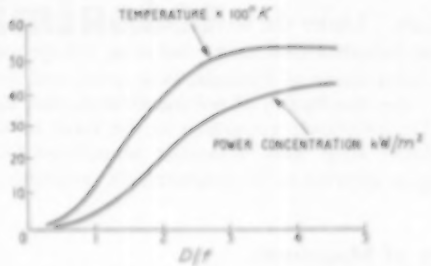

Fig. 2. Variation of power concentration and calculated "black body temperature" (not the actual temperature reached, but the temperature of an emitting black body which would have the same power concentration as the image) for various values of D/f. These curves are based on a table given in the CRNS Report

Power and the Solar Constant

The figure usually quoted for the mean rate of reception of solar energy per unit area at the earth's surface is about 1·3 kW/sq. m. This is called the "solar constant", and is anything but. Noon sunshine, when the altitude of the sun is 55°? Above or below the earth's atmosphere? Nobody seems to be very precise about this, but the round figure taken in several of the discussions in this volume is 1 kW/sq. m.

The main object for most applications is to use this power without necessarily concentrating it more than is needed either to get it in the right place, or to produce thermodynamically desirable temperatures. It must first of all be absorbed; and if R is the reflection coefficient of the surface on which it is directed, the usable fraction is $(1 - R)$. Next, the energy must be retained. Quite apart from losses by conduction and convection, we are up against the unpleasant fact that a good absorber is also a good radiator; and the emissive power ϵ of the receiver ought to be *low*. The full calculation of the equilibrium temperature attained by a surface that is receiving $(1 - R)$ kW/sq. m. by radiation and losing the same power by various methods is quite complicated. But we might look at what is to be expected of a perfectly black body.

First, suppose that we have a perfectly black surface $(R = 0)$ completely insulated and losing heat to the surroundings (at 300 °K) by radiation only. Stefan's constant is $5{\cdot}67 \times 10^{-11}$ kW/sq. m./deg^4, so the equilibrium temperature T °K at which it loses 1 kW/sq. m. is given by $1 = 5{\cdot}67 \times 10^{-11}\,(T^4 - 300^4)$, which means $T = 400$ °K = 127 °C.

If the receiver *is* a thin perfectly conducting plate, perfectly black on both sides, so that it receives radiation on one face and radiates from both, then $1 = 2 \times 5{\cdot}67 \times 10^{-11}\,(T^4 - 300^4)$, giving $T = 360$ °K = 87 °C.

But for practical purposes, the "radiation valve" principle of the greenhouse (which is so inaccurately described in the elementary textbooks) is invoked. A surface which has a reflection coefficient R for the incident radiation and emissive power ϵ *at the temperature the surface eventually attains* will be $(1 - R)/\epsilon$ times as effective as an ideal black body as a receiver of radiation. Thus, aluminium ($R = 0{\cdot}03$, $\epsilon = 0{\cdot}14$) is seven times better than a black body. One of the contributions in this volume describes experiments using an arc giving 5 kW/sq. m. in place of sunshine, irradiating various surfaces in air, with conduction and convection operating, and also in a high vacuum where radiation alone was involved. A blackened plate reached 120 °C in air and 200 °C in a vacuum; an aluminium surface reached only 75 °C in air, but 450 °C in a vacuum.

The power made available, then, depends (given the radiation in the first place) only on the area of the collecting mirror and the efficiency of absorption. If, for example, you can concentrate the power falling on 2 sq. m. of mirror on to an area of 1 sq. m. you have effectively multiplied the solar constant by 2. The 90 sq. m. Montlouis mirror concentrates 75 kW; and that of the 2 000 sq. m. one at Odeillo-Font Romeu is rated at 1 000 kW.

Applications

As the title of this volume indicates, most of the applications are directed to pure research or to industry. Under the first heading come projects like that to obtain temperatures of the order 10^5–10^6 °K by the exploding-wire method, after first preheating the wire to 3 000 °K in a solar furnace; experiments on the production of refractories of greater purity and at far less cost than by using an electric furnace; and the development of suitable materials for the extraction of power either by cyclic engines or by direct thermoelectric

generators. Under the second, since the modern home is almost industrialized, come the solar refrigerator, the famous solar house at Phoenix, Wisconsin, and the solar cooker; the distillation of sea water is another application. Do-it-yourself apparatus in the form of aluminized plastic strip and inflatable aluminium-foil heat exchangers appears to be commercially available.

Orders of Magnitude

How does the power available from the sun compare with the power actually used, and likely to be used, by civilized life in the near or foreseeable future? According to one of Putnam's famous predictions, it is conceivable that by A.D. 2050 the world's demands for power may approach 1 per cent of that reaching us from the sun. This forecast is discussed in the opening chapter of "Plasmas and Controlled Fusion", by David J. Rose and Melville Clark, Jr. (John Wiley, Massachusetts Institute of Technology, 1961). The authors are respectively Professor and Associate Professor of Nuclear Engineering at M.I.T., and the book deals mainly with recent technical progress in this field at a postgraduate level. Its comments on the future, based on Putnam, are interesting. Working in terms of a unit called "Q", which is approximately 10^{21} joules and is roughly rather more than the quantity of energy that would raise Lake Ontario from 0 °C to 100 °C, the consumption has risen from 0·017 Q per year in 1860 to an estimated probable 0·74 Q per year by 1975. The solar constant is some 1 500 Q per year; and in 100–130 years from now, human consumption may reach 15 Q per year! Well, one might feel, why not? Our descendants will never have had it so much better. But there is an attendant risk; 1 per cent of the solar constant derived by combustion of fuels is reaching the stage at which there is the possibility of competing with the sun itself and interfering with the climate everywhere. Unless a good deal of the 15 Q comes itself from the direct utilization of solar energy; when, say these authors, a considerable fraction of the earth's surface would have to be covered with energy conversion elements—for example, thermocouples. Such a solution, they say, is not appealing. But perhaps, after all, it may merely continue as at present, to be paved with good intentions; while the effective utilization of solar energy remains still in the province of those highly skilled artists who hold the mirror up to Nature.

DIRECT PLOTTER FOR RADAR DISPLAY

An optical attachment which permits direct plotting on the face of a marine radar display, enabling future positions of other vessels to be predicted, has been produced by A.E.I.

This is the Reflection Plotter and in effect it is a clear plastic disc assembly which fits on to the face of a marine radar display c.r.t. and provides a plotting surface without the gross parallax errors which would normally be introduced by the thickness of the glass and the distance of the plotting surface above the c.r.t.

Fig. 1 illustrates how parallax is eliminated, by showing that a mark made on the plotting surface produces a reflection which appears to be on the c.r.t. screen perpendicularly below the mark, irrespective of the position of the observer's eyes. A half-silvered mirror is placed half-way between the c.r.t. screen and the plotting surface, the latter having a curvature equal and opposite to that of the c.r.t. face. Hence the height above the mirror of any point on the plotting surface is equal to the distance between the mirror and the point perpendicularly below on the c.r.t. screen.

When the eye of the observer is at P_1 and the pencil point is at A_1, the light rays from A_1 will reach P_1 via the route $A_1B_1P_1$, since the angle of incidence (CB_1A_1) is equal to the angle of reflection (DB_1P_1). Because the plotting surface and the c.r.t. screen are equi-distant from the mirror point A_1 will appear to lie on the c.r.t. screen at point A_2. If the observer moves to P_2 the position of the reflection of A_1, which appears at A_2, will not change.

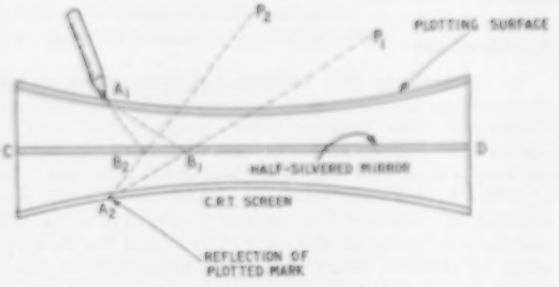

Fig. 1. *A cross-sectional drawing of the Reflection Plotter*

When fitted to the A.E.I. Escort and RMS-2 radar equipments edge-illumination of the plotting screen is provided which makes the reflections of the wax pencil marks clearly visible; when the illumination is switched off the reflections of the plotted marks cannot be seen.

Fig. 2. *The Reflection Plotter fitted on to a radar display c.r.t.*

Linear Frequency Discriminator

FOR LOW-FREQUENCY F.M. SIGNALS OF LARGE DEVIATION

By U. S. Ganguly*

SUMMARY. *In this article a simple method is presented for distortionless demodulation of low-frequency f.m. signals with large deviations, as used in multichannel communication systems utilizing the so called f.m.–f.m. method of frequency multiplexing. The design of a practical discriminator circuit, based on this method, is discussed and its performance is analysed theoretically to determine the conditions for maximum linearity. The theoretical results are confirmed experimentally.*

In modern multichannel communication systems using the f.m.–f.m. method of frequency-multiplexing, each of the information signals is made to modulate the frequency of a separate low-frequency sub-carrier, lying in the range 400 c/s to 75 kc/s, with comparatively large deviation (amounting to 7·5% to 15%). The modulated sub-carriers, operating at different frequencies, are then added together and the resulting composite-signal is used to frequency modulate the main r.f. carrier. At the receiving end, after preliminary demodulation, the sub-carriers are sorted out by bandpass channel filters and are finally demodulated. For recovery of the transmitted information with sufficient fidelity, it is mandatory that the characteristics of the final demodulator be accurately linear over the required bandwidth. This is difficult to achieve in practice because of the low centre frequency and large deviation characterizing the sub-carrier signals. For instance, the well-known Foster-Seeley or Travis[1] types of discriminators, which depend for their operation on the phase shift and impedance characteristics of tuned LC circuits, cannot be readily adopted for satisfactory operation at sub-carrier frequencies because of the impractically large values of inductance required. These large inductors are temperature sensitive, are prone to generate harmonics because of their inherent non-linearity and are susceptible to stray pickups. Bulk and cost apart, their incorporation in a circuit often entails shielding and shunt-feeding problems. Moreover, the output of these discriminators can be shown to be proportional to the logarithm of the input frequency. While this causes little distortion in the detection of ordinary f.m. signals, for which the frequency swing is only a small percentage of the carrier frequency, it does necessitate additional modifications in the circuit, if sub-carrier signals, with the aforementioned wideband characteristics, have to be detected with sufficiently small distortion. The design of a suitable demodulator for sub-carrier signals is thus substantially different from that of its counterpart in the conventional, narrowband, radio frequency, f.m. system.

One satisfactory solution[2] of this problem consists essentially in shaping the incoming signal to a pulse train, the recurrence frequency of which is then measured by a suitable digital-to-analog converter. In a similar method[3], the mark-space ratio of an internally-generated pulse train is controlled by two sets of timing pulses derived from the input signal; the instantaneous average of the resulting pulse train indicates the signal frequency. The circuitry of both these methods is rather involved and critical adjustments are required to ensure accuracy, stability and linearity. A simpler solution proposed by Tillman[4] and Stine[5] consists in passing the signal through two parallel-T, RC null networks with suitably-staggered centre frequencies. The two outputs are then differentially rectified. The discriminator output is proportional to the logarithm of the input frequency and linearizing networks have to be used with attendant loss in overall sensitivity. These circuits have the merit of being without inductors but suffer from a lack of tunability on account of the inherently complicated structure of the twin-T network. The same factor has a detrimental influence on the zero stability of the discriminator as the twelve elements of the two twin-T circuits have to be maintained in accurate alignment against the perturbing influence of temperature variations. Another simple method[6] consists in delaying the signal by an amount proportional to the input frequency and then measuring this frequency-dependent delay or phase shift by mixing, multiplicatively, the original and the phase-shifted signals in a heptode; the change in the d.c. component of the anode current of the mixer then indicates the phase shift and hence the frequency. The heptode, however, in common with other multi-electrode valves, has a small dynamic range. With strong signals, the higher order terms in the Taylor series expansion of the transfer characteristics about the quiescent point contribute significant amounts of d.c. and tend to vitiate results expected on the assumption of a square-law operation. The discriminator described in this paper is largely free from the above mentioned shortcomings of the existing circuits. It is simple, without inductors and can be readily adjusted to provide stable, wideband, linear characteristics about low centre frequencies.

* *Department of Tele-Communication Engineering, Jadavpur University, Calcutta, India.*

Principle of Operation

The working principle of the discriminator is presented with reference to the block schematic diagram in Fig. 1. The input signal, after transmission through the usual preamplifier, limiter and sinewave-forming circuits is passed through two parallel channels marked 1 and 2. The two outputs e_1 and e_2 from channel 1 are equal in amplitude and 180° out-of-phase. The output e_3 from channel 2, which contains an active all-pass phase-shifting circuit, remains constant in amplitude but is shifted in phase from 0 to 180° as the frequency is varied from zero to infinity. The gains of the two channels are adjusted to be equal and the three voltages e_1, e_2 and e_3 are applied to a pair of shunt diode detectors as shown in Fig. 2 (a). If the time constants C_1R_1 and C_2R_2 of the detectors are made large compared to the time period of the lowest frequency likely to be encountered, then the d.c. voltages developed at P & Q are proportional to the peak values of the vector sums $e_1 + e_3$ and $e_2 + e_3$. From the sinor diagram in Fig. 2 (b), it can be seen that at the frequency ($f = f_0$ say) for which e_3 is in phase quadrature with e_1 or e_2, the vector sums are equal in magnitude and the d.c. differential voltage across PQ will be zero. At a lower frequency the phase shift is smaller than 90° and P is more positive than Q; for a higher frequency the reverse is true. Thus a balanced output is obtained about $f = f_0$ and it is shown in the following section that the differential-detected output V_{PQ} varies with frequency according to

$$V_{PQ} = 2\,e\,\frac{1-u}{(1+u^2)^{\frac{1}{2}}}$$

where $u = f/f_0$, f = frequency of the input signal, e = equalized amplitude of the signals e_1, e_2 and e_3, f_0 = frequency for which e_3 is in phase quadrature with e_1 or e_2.

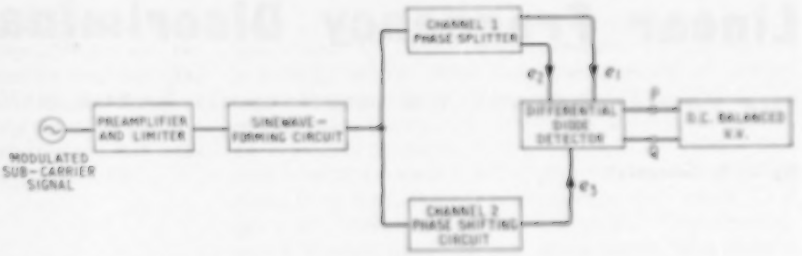

Fig. 1. *Block schematic diagram illustrating the operating principle of the discriminator*

Theoretical Analysis

A properly terminated LC lattice structure is well known as an all-pass phase-shifting circuit but, in view of the aforementioned practical difficulties associated with the use of large inductors at low frequencies, a more readily realizable circuit configuration shown in Fig. 3 was used in channel 2. The output of the circuit is easily shown to be

$$e_3 = e\,\frac{j\omega CR - 1}{j\omega CR + 1}$$

and it is obvious that the magnitude of e_3 equals e and is independent of frequency, while the phase angle of e_3 with respect to e is $2\tan^{-1}\omega CR$.

Since the amplitudes of the output voltages e_1, e_2 and e_3 of the two channels in Fig. 1 are each adjusted to be equal to e, the inputs to the diodes D_1 and D_2 in Fig. 2(a) are respectively

$$\left.\begin{aligned} e_1 + e_3 &= -e + e\,\frac{j\omega CR-1}{j\omega CR+1} = \frac{-2\,e}{j\omega CR+1} = \frac{-2\,e}{1+ju} \\ e_2 + e_3 &= \quad e + e\,\frac{j\omega CR+1}{j\omega CR+1} = \frac{2j\omega CRe}{j\omega CR+1} = \frac{2jue}{1+ju} \end{aligned}\right\} \quad (1)$$

where $u = \omega CR = \omega/\omega_0$ and $\omega_0 = 1/CR$.

The rectified outputs V_P and V_Q are given by

$$\left.\begin{aligned} V_P &= |e_1 + e_3| = \frac{2\,e}{(1+u^2)^{\frac{1}{2}}} \\ V_Q &= |e_2 + e_3| = \frac{2\,e\,u}{(1+u^2)^{\frac{1}{2}}} \end{aligned}\right\} \quad .. \quad .. \quad .. \quad (2)$$

The differential output V_{PQ} is therefore equal to

$$V_{PQ} = V_P - V_Q = 2\,e\,\frac{1-u}{(1+u^2)^{\frac{1}{2}}} \quad .. \quad .. \quad (3)$$

which shows that a balanced response is obtained about $u = 1$ or $\omega = 1/CR$. The range over which the discriminator output varies linearly with frequency obviously

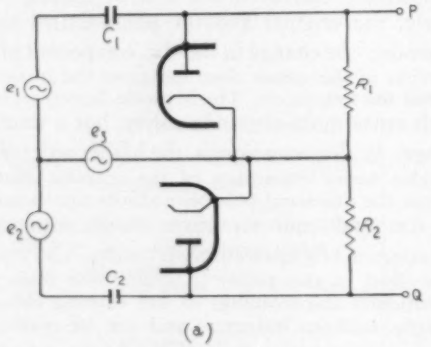

(a)

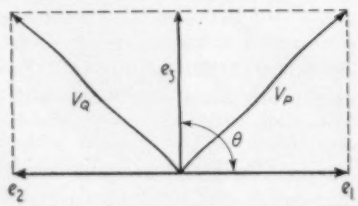

(b)

Fig. 2. *(a) Differential diode detector; (b) Sinor diagram showing phase relations between the voltages shown in (a)*

depends on the location of the operating point. The optimum location of the quiescent operating point is determined in the following section.

Linearity of the Discriminator

It can be seen from Equ. (3) that although the discriminator output is balanced about $u = 1$, it varies linearly with frequency over a rather limited range. For securing the desired wideband linear characteristics, the quiescent operating point should be shifted from $u = 1$ to the point of inflexion of the normalized response curve. Symmetrical operation about this point can then be obtained by balancing out the output of the discriminator at the corresponding frequency.

From Equ. (3) the normalized output is given by

$$y = \frac{V_{eq}}{2e} = \frac{1-u}{(1+u^2)^{\frac{1}{2}}} \quad .. \quad .. \quad .. \quad .. \quad (4)$$

The slope m at any point of the response curve is

$$m = \frac{dy}{du} = -\frac{(1+u)}{(1+u^2)^{3/2}} \quad .. \quad .. \quad .. \quad (5)$$

From Equ. (5)

$$\frac{d^2y}{du^2} = -\frac{(1+u^2)^{3/2} - 3u\,(1+u)\,(1+u^2)^{\frac{1}{2}}}{(1+u^2)^3} \quad .. (6)$$

At the point of inflexion, $d^2y/du^2 = 0$. Therefore, from Equ. (6)

$$(1+u^2)^{3/2} - 3u\,(1+u)\,(1+u^2)^{\frac{1}{2}} = 0$$

which simplifies to

$$2u^2 + 3u - 1 = 0$$

from which $u = 0{\cdot}282 = u_1$ (say) .. .. .. (7)

Thus if the unmodulated radial frequency of the signal is ω_c, the time constant CR of the phase-shifting circuit is to be adjusted to $CR = 0{\cdot}282/\omega_c$ in order to obtain

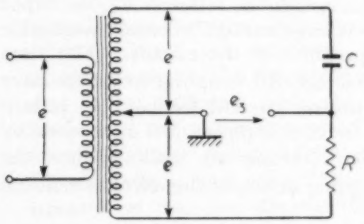

Fig. 3. *The all-pass RC phase-shifting circuit*

linear variation of output voltage with frequency of input signal, over a wide range. If a straight line is now drawn tangential to the response characteristics at the chosen operating point, the degree of non-linearity at any frequency can be assessed quantitatively from the extent of departure of the actual response from this line. The assessment is made for operating points located at $u = 0{\cdot}3$ and $u = 0{\cdot}4$ rather than exactly at point of inflexion ($u = 0{\cdot}282$) because of the resulting simplification in practical adjustments.

(a) Linearity about $u = 0{\cdot}3$ or $\omega_c = 0{\cdot}3/CR$

The equation of a straight line drawn tangential to the discriminator characteristics at $u = 0{\cdot}3$ is given by

$$y - y_1 = m_1\,(u - 0{\cdot}3) \quad .. \quad .. \quad .. \quad .. \quad (8)$$

TABLE 1

Normalized frequency $u_1 = \omega/\omega_c$	Corresponding value of $u = \omega/\omega_0$	Values of y Computed from Equ. (4)	Values of y Computed from Equ. (9)	Percentage Non-linearity from Equ. (10)
0·6	0·18	0·8071	0·80754	+0·05475
0·7	0·21	0·7731	0·77328	+0·02328
0·8	0·24	0·7392	0·73902	−0·02435
0·9	0·27	0·7047	0·70476	−0·06815
1·0	0·30	0·6705	0·67050	0·0000
1·1	0·33	0·6363	0·63624	−0·09830
1·2	0·36	0·6023	0·60198	−0·05313
1·3	0·39	0·5683	0·56772	−0·1021
1·4	0·42	0·5346	0·53346	−0·2123

where y_1 = value of the normalized response at $u = 0{\cdot}3$ and m_1 = slope of the response characteristics at $u = 0{\cdot}3$. From Equs (4) and (5) $y_1 = 0{\cdot}6705$ and $m_1 = -1{\cdot}142$, thus Equ. (8) becomes

$$y = 0{\cdot}6705 - 1{\cdot}42\,(u - 0{\cdot}3) \quad .. \quad .. \quad .. \quad (9)$$

From Equs (4) and (9) the percentage non-linearity may be expressed as

$$N\% = 100\,\frac{[0{\cdot}6705 - 1{\cdot}14\,(u - 0{\cdot}3)] - \left[\frac{1-u}{(1+u^2)^{\frac{1}{2}}}\right]}{(1-u)/(1+u^2)^{\frac{1}{2}}} \quad (10)$$

In Table 1 the computed values of N for different values of percentage deviations about $\omega_c = 0{\cdot}3/CR$ are tabulated.

(b) Linearity about $u = 0{\cdot}4$ or $\omega_c = 0{\cdot}4/CR$.

The equation of straight line drawn tangential to the discriminator characteristics at $u = 0{\cdot}4$ is

$$y - y_2 = m_2\,(u - 0{\cdot}4) \quad .. \quad .. \quad .. \quad .. \quad (11)$$

where y_2 = value of the normalized response at $u = 0{\cdot}4$ and m_2 = slope of the response characteristics at $u = 0{\cdot}4$. From Equs (4) and (5) $y_2 = 0{\cdot}5577$ and $m_2 = -1{\cdot}12$, thus Equ. (11) becomes

$$y_2 = 0{\cdot}5577 - 1{\cdot}12\,(u - 0{\cdot}4) \quad .. \quad .. \quad .. \quad (12)$$

The percentage non-linearity is given by

$$N\% = \frac{[0{\cdot}5577 - 1{\cdot}12\,(u - 0{\cdot}4)] - \left[\frac{(1-u)}{(1+u^2)^{\frac{1}{2}}}\right]}{(1-u)/(1+u^2)^{\frac{1}{2}}} \quad (13)$$

Computed values of N for different values of percentage deviations around $\omega_c = 0{\cdot}4/CR$ are tabulated in Table 2.

TABLE 2

Normalized Frequency $u_1 = \omega/\omega_c$	Corresponding value of $u = \omega/\omega_0$	Values of y Computed from Equ. (4)	Values of y Computed from Equ. (12)	Percentage Non-linearity from Equ. (13)
0·6	0·24	0·7392	0·7369	−0·3120
0·7	0·28	0·6936	0·6921	−0·2170
0·8	0·32	0·6475	0·6473	−0·0390
0·9	0·36	0·6027	0·6025	−0·0332
1·0	0·40	0·5577	0·5577	0·0000
1·1	0·44	0·5124	0·5129	+0·0980
1·2	0·48	0·4689	0·4681	−0·1745
1·3	0·52	0·4259	0·4233	−0·6150
1·4	0·56	0·3836	0·3785	−1·2880

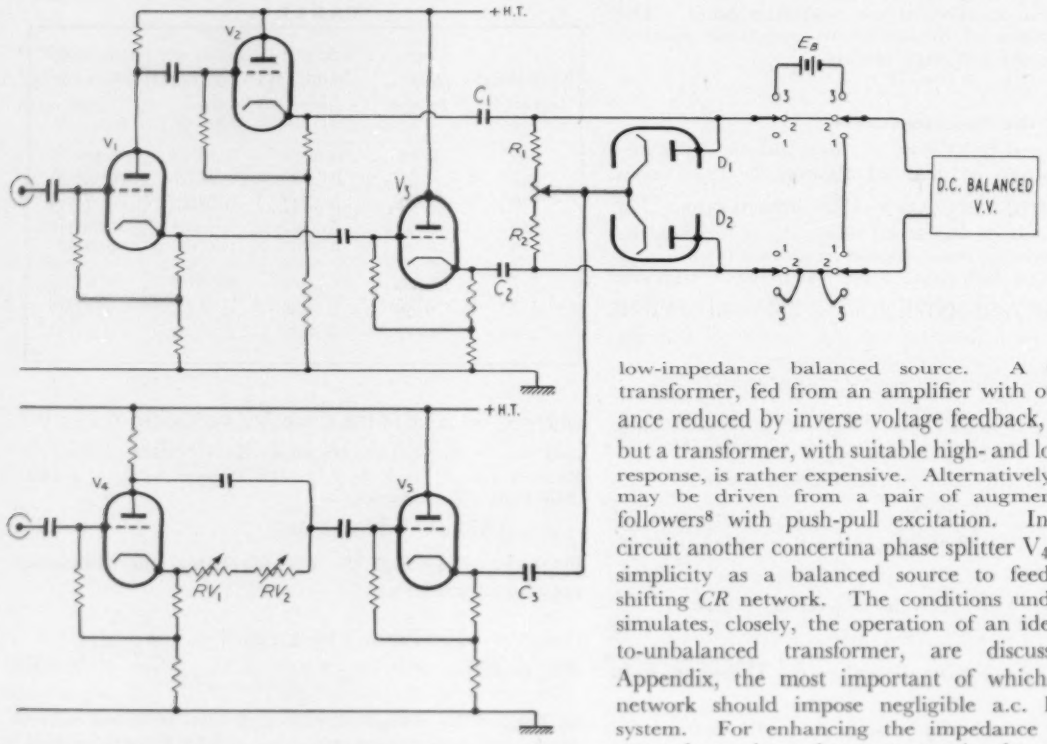

Fig. 4. *Circuit diagram of the Discriminator*

Details of Experimental Circuit

An experimental circuit, based on the conceptual scheme suggested in the block-diagram of Fig. 1, is shown in its essentials in Fig. 4. The two equal and antiphase outputs e_1 and e_2 of channel 1 are obtained from a 'concertina' phase splitter, the design considerations for which have been published[7]. The values of the anode and cathode loads for this circuit are dictated by the requirement of nearly unity gain. A high-mu triode ($\mu = 60, r_a = 15\,k\Omega$) was used with anode and cathode loads of 15 kΩ each, the proper operating grid bias having been obtained from a 270 Ω resistor in the cathode circuit. An 1 kΩ variable resistance was used in the anode circuit for amplitude equalization. For greater precision however, it is advisable to use a ring-of-three, unity-gain inverse-feedback amplifier with a see-saw imaging circuit. The circuit normally produces no unbalance when two equal loads are fed from its two outputs, although the output impedance viewed from the anode is much higher than that from the cathode; the reason being that for a symmetrical load, the ratio of the anode to cathode impedances remains equal to unity and the same anode current flows through them in series. In the present instance however, it may do so, since the two diodes, which may not be simultaneously conductive because of the phase difference between the diode inputs, may thus constitute effectively an asymmetrical load. This difficulty is obviated by the use of buffering cathode followers V_2 and V_3. In Fig. 3 the series *RC* network of the phase-shifting circuit is shown to be driven from a low-impedance balanced source. A well-designed transformer, fed from an amplifier with output impedance reduced by inverse voltage feedback, may be used but a transformer, with suitable high- and low-frequency response, is rather expensive. Alternatively the network may be driven from a pair of augmented cathode followers[8] with push-pull excitation. In the present circuit another concertina phase splitter V_4 was used for simplicity as a balanced source to feed the phase-shifting *CR* network. The conditions under which V_4 simulates, closely, the operation of an ideal balanced-to-unbalanced transformer, are discussed in the Appendix, the most important of which is that the network should impose negligible a.c. load on the system. For enhancing the impedance level of the network, a given time constant in the phase-shifting circuit (determined by the desired centre frequency) should be realized with high value of R and low value of C. Since precision components have to be used, the value of the variable resistor R cannot be increased beyond 100 kΩ and convenient values of the phase-shifting components, for sub-carrier frequencies lying in the range 1 kc/s to 5 kc/s, are $R = 100\,k\Omega$ and $C = 0{\cdot}001\,\mu F$. The output of the phase-shifting circuit is fed through an isolating cathode follower V_5, the input impedance of which is large enough to ensure negligible influence on the operation of the circuit. The time constants of the interstage *RC* coupling networks have been increased by inverse current feedback to reduce the undesirable and inevitable phase-shift introduced by them. Since the two channels are made to have the same number of coupling networks the effect of residual

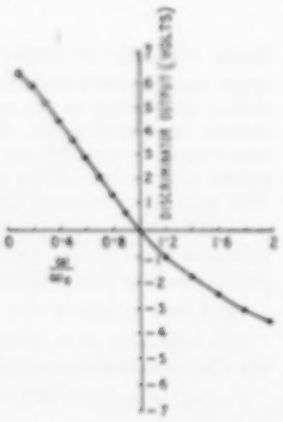

Fig. 5. *Measured general response characteristics of the discriminator*

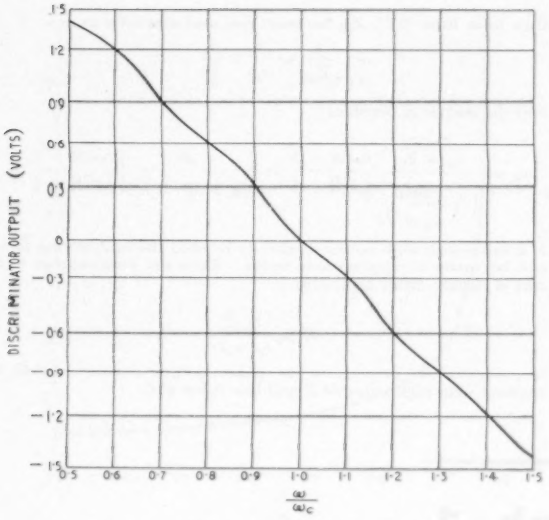

Fig. 6. *Measured operating characteristics of the discriminator*

phase-shift is practically negligible. The design of the d.c. differential V.V. is conventional. The circuit was supplied from a stabilized d.c. source.

Adjustment and Operation

Let the sub-carrier signal, which the discriminator will be expected to demodulate, have a nominal frequency of 2 kc/s. If it is decided to locate the operating point of the discriminator at $u = 0{\cdot}4$, the setting-up procedure [c.f. Fig. 4] is as follows. Allowing warm-up time for the circuit and test oscillator to stabilize (a) the switch is set in position 1 and the differential V.V. is set to zero; (b) An unmodulated signal of 5 kc/s ($f_0 = f_c 0{\cdot}4$) is applied to the input. The switch is set to position 2. The coarse and fine-control potentiometers, RV_1 and RV_2, in the phase-shifting circuit are adjusted to reduce the V.V. reading to zero. The frequency of the test oscillator is next set at different multiples and sub-multiples of 5 kc/s, and the response curve of Fig. 5 is plotted, the signal amplitude being maintained constant. (c) The test oscillator is next set at 2 kc/s and its amplitude is adjusted so that the discriminator output equals the value of the balancing battery E_b. Prior to this adjustment and to the subsequent choice of E_b, the waveforms at various parts of the circuit are monitored to determine the maximum input signal level that can be handled without overloading. E_b is then brought into the circuit with the switch in position 3. The discriminator now provides a balanced output about 2 kc/s. In Fig. 6 is shown the measured response characteristics about 2 kc/s for deviations up to 40% of this centre frequency.

Conclusions

Results of a theoretical analysis of the discriminator circuit (c.f. Tables 1 and 2) show it to be remarkably linear over frequency deviations as large as 40% of the mean carrier frequency and the experimental data confirm the theoretical expectations. Considerable amount of inverse feedback present in the circuit contributes to stability and enhances the signal handling capacity with attendant increase in sensitivity. The zero drift in the discriminator, taking into account the drift characteristics of the *RC* test oscillator, was found to be insignificant for short intervals; long-term drifts, if any, are readily corrected by a simple and single adjustment. Simplicity, reliability and ease of alignment suggest its use as a suitable demodulator for low-frequency f.m. signals with large deviation, as used in f.m.–f.m. telemetry and telephony.

Acknowledgements

The author is deeply indebted to Dr. J. S. Chatterjee for help and guidance during preparation of the paper.

REFERENCES

1 G. G. Johnstone, "Limiters and Discriminators for F.M. Receivers", *Wireless World*, 1957, Vol. 63, pp. 8–14 & 70–74.
2 Vallarino, Snow & Greenwald, "Counter Circuit Multiplexer Receiver", *Electronics*, 1953, Vol. 26, pp. 178–181.
3 M. Tepper, "Radio Telemetry", 1959, J. F. Rider, New York, pp. 50–51.
4 J. R. Tillman, "Linear Frequency Discriminator", *Wireless Engr*, 1946, Vol. 23, pp. 281–286.
5 Paul T. Stine, "Parallel-T Discriminator Design Technique", Proc. Nat. Elec. Conference, 1950, Vol. IX, pp. 26–39.
6 P. Kundu, "Linear Frequency Discriminator for Subcarrier Frequencies", *Electronic Radio Engr*, 1958, Vol. 35, pp. 309–313.
7 Anon., "Concertina Phase Splitter", *Electronic Radio Engr*, 1959, Vol. 36, pp. 271–274.
8 O. Billington, "A direct Coupled Phase Splitter", *Electronic Engng*, 1958, Vol. 30, pp. 480–482.
9 S. J. Mason, "Feedback Theory—Some properties of Signal Flow Graphs", *Proc. Inst. Radio Engrs*, Sept. 1953, pp. 1144–1156.
10 S. J. Mason, "Feedback Theory—Some Properties of Signal Flow Graphs", *Proc. Inst. Radio Engrs*, July 1956, pp. 920–926.

APPENDIX

The *RC* all-pass phase-shifting circuit is shown in Fig. 7(a) and its a.c. equivalent at (b). If E is the a.c. voltage from anode to cathode then the output e_0 can be written as

$$e_0 = E\frac{R}{R+x} - \frac{E}{2} = \frac{E}{2}\frac{R-x}{R+x} \quad \ldots\ \ldots\ \ldots\ \ldots\ (14)$$

where $x = 1/j\omega C$

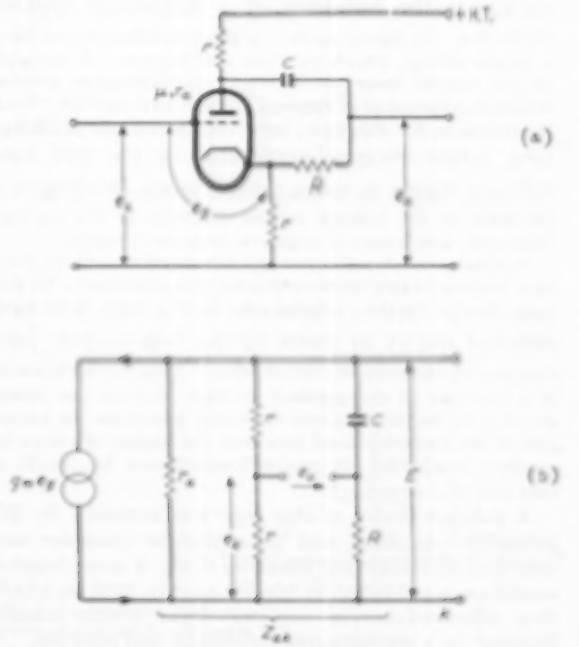

Fig. 7. *(a) The RC all-pass phase-shifting circuit; (b) A.C. equivalent circuit of (a)*

Now $E = g_m e_g Z_{ak}$ where $\frac{1}{Z_{ak}} = \frac{1}{r_a} + \frac{1}{2r} + \frac{1}{R + s}$ .. (15)

and $e_g = e_i + \frac{E}{2} = e_i - \frac{g_m e_g Z_{ak}}{2}$ .. .. .. (16)

From Equs (14), (15) and (16)

$$e_o = \left[\frac{\frac{1}{2} g_m Z_{ak}}{1 + \frac{1}{2} g_m Z_{ak}}\right] \frac{j\omega CR - 1}{j\omega CR + 1} \quad .. \quad .. \quad .. \quad (17)$$

The frequency dependance of Z_{ak} in the multiplying factor within the brackets causes the actual phase shift to be different from the ideal, assumed value $2 \tan^{-1}\omega CR$ and also some amplitude variation with frequency. If however, $\frac{1}{2} g_m Z_{ak}$ is large compared to unity the effect is not serious, as the numerator and the denominator tends to cancel each other out. Even if this is not true, proper operation of the phase shifter is realizable if the impedance level of the CR network is made high. That is if

$$\frac{1}{R} \ll \frac{1}{r_a} + \frac{1}{2r} \quad .. \quad .. \quad .. \quad .. \quad .. \quad .. \quad (18)$$

then from Equ. (15), Z_{ak} becomes real and simplifies to

$$\frac{1}{Z_{ak}} = \frac{1}{r_a} + \frac{1}{2r}$$

and the output e_o becomes

$$e_o = \frac{\frac{g_m r^2}{r_a + 2r}}{1 + \frac{g_m r^2}{r_a + 2r}} \frac{j\omega CR - 1}{j\omega CR + 1} = \left[\frac{\mu r}{r_a + (\mu + 2)r}\right] \frac{j\omega CR - 1}{j\omega CR + 1} e_i$$

If a valve with high power sensitivity be used the multiplying factor can be made to approximate unity. Thus the requirement to be met is clearly, from Equ. (18)

$$R \gg \frac{r_a 2r}{r_a + 2r}$$

i.e., a given RC product in the phase shifting network should be realized with high value of R and low value of C.

Silicon P-N-P-N Switch—1

DEVELOPMENT OF TWO-TERMINAL DEVICES

By A. Bardsley, B.Sc.,* and J. Walker*

The use of amplifying elements, such as valves and transistors in a suitable circuit, to give a bistable output is by now well known. The inherent feature of these circuits is the formation of a differential negative resistance. In many cases it is more satisfactory to have a single device which exhibits this feature. A suitable device would have an internal multiplication process which is a function of applied voltage and current. Such a process is, for example, involved in the gas discharge tube, where electrons accelerated by the field have sufficient energy to ionize the gas atoms, resulting in a decrease in the voltage across the tube as the current increases, and hence a negative resistance region.

A similar avalanche process has been shown to exist in a reverse biased semiconductor p-n junction[1]. In this case charge carriers accelerated by the high field have sufficient energy to create further hole-electron pairs causing an increase in current flow. This multiplication is a function of the applied voltage, and by the introduction of forward-biased emitting junctions on either side of the reverse-biased junction, the supply of minority carriers available for multiplication can be made a function of current.

A p-n-p-n device of this type was proposed by W. Schockley[2] in 1950 and an avalanche transistor was described by Miller and Ebers[3] in 1955. A more detailed analysis was published by Moll et alia[4] in 1956, in which they discussed results obtained from devices manufactured by a combination of diffusion and alloying.

We will give a brief resumé of the theory of operation before discussing the parameters important to a circuit designer and the manner in which these parameters influence the manufacture of such a device.

* *Ferranti Ltd., Electronics Dept., Manchester.*

Theory of Operation

Let us first consider the two important processes involved separately; i.e., the voltage-dependent charge-carrier multiplication process and the current-dependent supply of minority charge carriers available for multiplication.

The charge carrier multiplication factor is the ratio of the number of carriers which arrive in a region to the number of carriers which leave that region.

It is shown by Miller[3] that the multiplication factor, M, at a reverse-biased junction, is given empirically by

$$M = \frac{1}{1 - \left(\frac{V}{V_B}\right)^n} \quad .. \quad .. \quad .. \quad .. \quad (1)$$

where V_B is the avalanche breakdown voltage of the junction, V is the applied voltage and n is a function of the type of carrier and usually lies between 2 and 9 for silicon. M is shown plotted in Fig. (1) for $n = 3$. M is slightly different for holes and electrons, but for simplicity we will assume a single value. It can be seen that $M \simeq 1$ for voltages well below the breakdown voltage, V_B.

Consider now the forward biased p-n junction illustrated in Fig. (2). If the p-region is heavily doped with impurity compared with the n-region, at high current levels the main fraction of the current, I, across the junction is carried by holes flowing from left to right

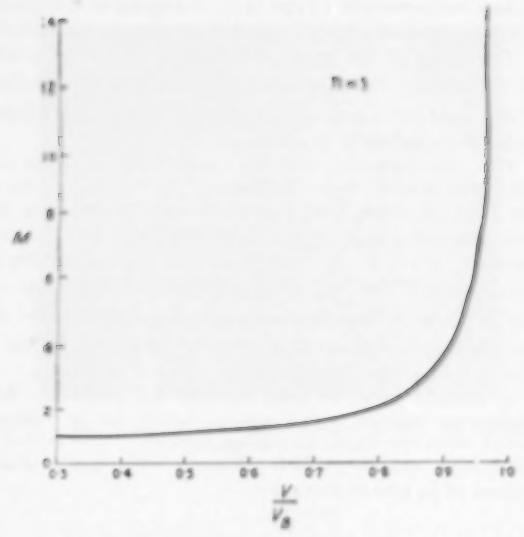

Fig. 1. *Variation of multiplication factor, M, with applied voltage, for n = 3*

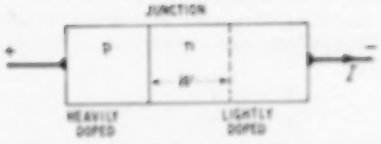

Fig. 2. *Schematic diagram of forward biased p-n junction*

and being injected as minority carriers into the n-region. This fraction is termed the injection efficiency of the junction. The injected minority carriers progress into the n-region for a distance dependent on their lifetime, the current thereafter being carried by majority carriers (in this case electrons) travelling in the opposite direction. Thus at a distance, W, from the junction the number of minority carriers depends on the injection efficiency at the junction, the lifetime in the base and the base width, W. The actual fraction of the current that is carried by minority carriers at this point is the α peculiar to that junction and base width. Now both injection efficiency and lifetime are a function of current density, so that the supply of minority carriers is current dependent. This is illustrated in Fig. 3 for two different structures.

Consider the structure illustrated in Fig. 4 (a) with the bias voltage as shown, such that the centre junction, J_2, is reversed biased and the outer junctions, J_1 and J_3, are forward biased. The schematic voltage–current characteristic of this device is shown in Fig. 4 (b).

Equal currents I, flow across all the junctions, and in particular the current across J_2 is given by

$$I = MI_0 + MI\alpha_1 + MI\alpha_2 \quad \ldots \quad \ldots \quad \ldots \quad (2)$$

This current comprises three terms: first, the basic leakage current, I_0, associated with J_2 alone, increased by the multiplication factor; secondly, the fraction of minority carriers injected at J_1 which arrive at J_2 ($\alpha_1 I$) increased again by the multiplication factor at J_2 and similarly a third term for injected minority carriers from J_3. It is assumed here that all the current, I, across J_1 and J_3 is carried by minority carriers injected into the inner n- and p-regions.

From Equ. (2)

$$I = \frac{MI_0}{1 - M(\alpha_1 + \alpha_2)} \quad \ldots \quad \ldots \quad \ldots \quad \ldots \quad (3)$$

The characteristic can be considered as consisting of four regions; three of these are regions of positive resistance and one of negative resistance. Regions 1 and 2 occur at small currents, when $(\alpha_1 + \alpha_2)$ is negligibly small, and correspond to $I = MI_0$, the normal reverse characteristic and breakdown region of junction J_2. It will be shown later that region 2 does not always occur. The negative resistance region 3 occurs as $(\alpha_1 + \alpha_2)$ rises with current and is the locus of $M(\alpha_1 + \alpha_2) \to 1$. The multiplication factor (hence the voltage across the device) falls to maintain equilibrium. In region 4 where M is unity and due to the high currents $(\alpha_1 + \alpha_2) \geq 1$, it has been suggested that to maintain equilibrium the centre junction becomes forward biased[4] such as to

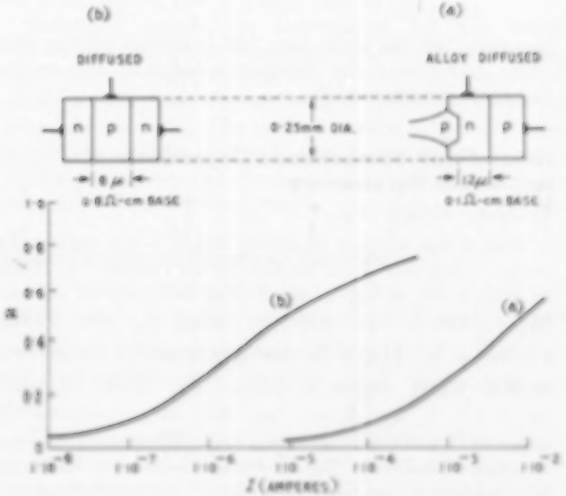

Fig. 3. *Variation of α with current in the structures shown*

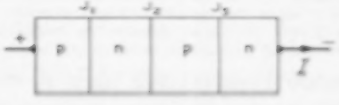

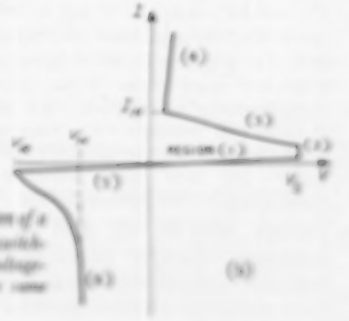

Fig. 4. *(a) Schematic diagram of a p-n-p-n switch biased in the switching direction; (b) Schematic voltage-current characteristic of the same device*

inject holes and electrons back into the n and p base regions respectively, giving region 4 a net positive resistance equivalent to a single forward biased diode.

When biased in the reverse direction, junctions J_1 and J_3 are reversed biased and J_2 is forward biased. In this case region 5 is a high impedance mode similar to region 1. We then have a similar argument with a voltage dependent multiplication at J_1 and J_3 and a current dependent α_1' and α_2', for the fraction of the current arriving at J_1 and J_3 which are injected minority carrier holes and electrons respectively from J_2.

If we make the assumptions that the leakage currents of J_1 and J_3 are similar, I_0', and the multiplication factors are equal, M', then we obtain for the characteristic:

$$I = \frac{M' I_0'}{1 - \frac{M'}{2}\{\gamma(\alpha_1' - \alpha_2') + \alpha_2'\}} \qquad \ldots \quad \ldots \quad (4)$$

where α_1' and α_2' are the reverse αs in the respective base regions, and γ is the injection efficiency of J_2 for holes into the n-base region. The locus of region 6 is

$$\frac{M'}{2}\{\gamma(\alpha_1' - \alpha_2') + \alpha_2'\} \to 1$$

However, for this to be true, M' is always greater than unity and hence the holding voltage in the reverse direction is always high.

Control and Temperature Dependence of Important Parameters

Switching Voltage, V_S

This is the voltage at which $M(\alpha_1 + \alpha_2)$ approaches unity. This will occur in two distinct cases. (a) Those in which $(\alpha_1 + \alpha_2)$ is small (say 0·1) up to currents approximately one hundred times I_0, the leakage current of J_2. This is the case mentioned in the previous section where region 2 exists. (b) Those in which $(\alpha_1 + \alpha_2)$ is significant (say 0·5) at currents of the order of I_0. These two types are analogous to the two examples shown in Fig. 3 for a three layer structure. The negative resistance regions of the equivalent four layer structures are shown in Fig. 5. Type (a) clearly has regions 2 and 3, whereas Type (b) passes directly from region 1 to region 3. It can be noted here that Type (a) will require high currents at high voltage to switch on, whereas Type (b) will switch on with low currents.

At room temperature Type (a) will have $V_S \triangleq V_b$ and Type (b) will have V_S less than V_b; typically $V_S = 0{\cdot}8V_b$ for $(\alpha_1 + \alpha_2) = 0{\cdot}5$ and $M = 2$. With increasing temperature the leakage current, I_0, increases and, for a given current density, α increases. Hence a structure may show Type (a) characteristics at low temperatures and Type (b) at higher temperatures. Breakdown voltage, V_b, has a positive temperature coefficient and consequently switching voltage, V_S, for Type (a) will also have a positive temperature coefficient. In general, for Type (b) increases in leakage current, I_0, and α with temperature will dominate changes in breakdown voltage giving a negative temperature coefficient. Thus it is possible for a structure to show positive temperature coefficient at low temperatures [Type (a)], changing to a negative temperature coefficient [Type (b)] at higher temperatures.

The value of the avalanche voltage, V_b, is controlled by the resistivity of the base material and the gradient of the impurity forming the junction, both these being under the control of the designer.

The variations of α with current density are not fully understood, being influenced by the resistivity of the base material, lifetimes of minority carriers in the base material and emitter efficiency of the emitting junction, which is itself dependent on the resistivities on either side of the emitting junction. Resistivities are under control but lifetimes less so, particularly the variation of lifetime with current density; hence in practice an empirical control is used for varying α.

A further point to note here is the possibility of a fast-rising voltage switching-on the device at voltages lower than the static switching voltage. This is due to capacitive current which flows to the space charge region of J_2 and is given by

$$I = C(V)\frac{dV}{dt} \quad \text{where } C(V) \text{ is}$$

the capacitance of the junction and is a function of the voltage across it. Near the static switching voltage in the devices to be considered $C(V)$ is about 1 pF, and hence if $(\alpha_1 + \alpha_2)$ becomes significant at say 1.10^{-6} A, then the maximum rate of rise before V_S is affected is given by

$$\frac{dV}{dt} = \frac{I}{C(V)} = 1\ \text{V}/\mu\text{sec}.$$

It can be seen that Type (b) devices with high αs at low currents are more likely to show this effect.

Holding Current, I_H

This is the current density at which $(\alpha_1 + \alpha_2)$ is unity and is empirically controlled as mentioned in the previous section. As the temperature is increased

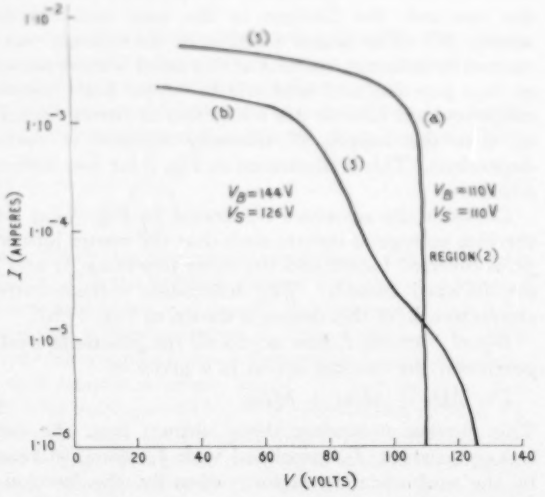

Fig. 5. *Negative resistance regions of two devices: (a) $(\alpha_1 + \alpha_2)$ low at small currents; (b) $(\alpha_1 + \alpha_2)$ high at small currents*

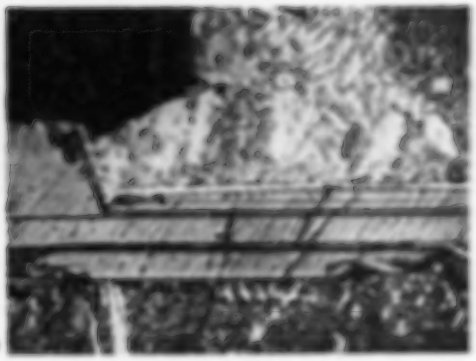

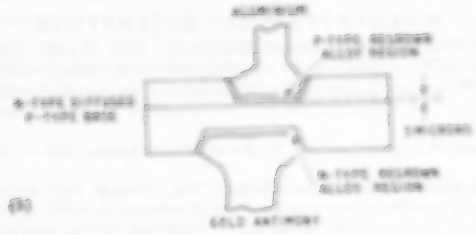

Fig. 6. (a) Section of alloy-diffused p-n-p-n switch; (b) Schematic diagram of the same switch.

α_1 and α_2 increase for a given current density and I_H is correspondingly lower, falling by about 60%, up to 100 °C in the devices to be considered.

Maximum Reverse Voltage, V_R

This is controlled by the same considerations as switching voltage, except that here one has two junctions, J_1 and J_3, reverse biased, leading to V_R being the sum of the respective avalanche voltages. Again two types of operation are possible, V_R initially increasing with temperature and then decreasing, or decreasing all the time. The reverse holding voltage also shows the same effect. The avalanche voltages of J_1 and J_3 are again under the control of the designer and the holding voltage to a limited extent, mainly because other parameters are more important.

When turning the device off rapidly by means of a negative voltage it is preferable to restrict the voltage below V_H, because the initial large current flow in the reverse direction, due to minority carrier stored charge, can carry the device into the low impedance region 6.

Off-Capacitance

The capacitance is the sum of the capacitances of J_1, J_2 and J_3 in series. The control of these by base resistivities and impurity gradients is well understood[5]. However, these factors are used to control V_S and I_H and it is more practical to adjust the capacitance by changes in area of the device.

The capacitance is at a maximum at zero bias and decreases with both forward and reverse bias as the space charge widths change. For a device capable of carrying 250 mA the capacitance can be less than 10 pF.

Off-Conductance, I_R

The current in the off state is given by Eqns. (3) and at low voltages and low currents it can be seen that $I = MI_R$ (at room temperature $\approx 1.10^{-8}$ A). As the temperature is increased one has the normal increase of I_R and in addition a further factor as $(\alpha_1 + \alpha_2)$ is increasing with temperature. This leads to a slightly higher current than in a normal diode at high temperatures, but the current is usually less than 10 μA at 100 °C for a 250 mA device.

On-Impedance

An expression for this is derived in Ref. (4) showing its relation to a single forward biased diode, and here it is important to ensure that $(\alpha_1 + \alpha_2) > 1$ at the desired holding current. In addition, low-resistance contacts must be made to the end regions to ensure a low series resistance in the device. As temperature is increased the forward on-voltage falls about 10%, up to 100 °C and is usually less than 1·5 V for currents within the dissipation of the device.

Switching Speeds

Switching speeds are determined by the fastest transition time of the minority carriers across the base regions for turn-on, and by the minority carrier charge stored in the base regions and its subsequent rate of decay for turn-off. The switching time is also critically dependent on the circuit in which the device is used. Times of the order of 5 mμsec have been achieved for turn-on and 1 μsec for turn-off.

Construction of Practical Devices

We will consider the construction of a p-n-p-n diode with a switching voltage of 100 V and holding current of 5 mA, capable of carrying about 100 mA in the on-condition with less than 1·5 V drop across the device.

Thus we require J_2 to have an avalanche breakdown of 100 V or slightly higher, and this can be achieved with a base material of resistivity 1 Ω cm at the junction. For high αs J_1 and J_3 must be good emitting junctions for holes and electrons respectively and this implies highly-doped p and n outer regions.

The first method used to achieve this was a mixed alloy-diffused structure which is illustrated in Fig. 6. Here J_2 was formed by diffusing phosphorus, n-type impurity, into a p-type base material to a depth of 45 microns, the surface concentration of the phosphorus being chosen to give a diffused gradient at J_2 for a 100 V avalanche breakdown. Both J_1 and J_3 were formed by alloying impurities, giving both high injection efficiencies and a good contact to the device. The junction depths were chosen by a combination of the minimum thickness of starting material available and the empirical values of base widths required to give the desired holding currents.

This device had a positive temperature coefficient for switching voltage at room temperature, indicating a Type (a) operation, and this was borne out by the very small spread on switching voltage from a diffusion batch, showing a dependence on the avalanche voltage

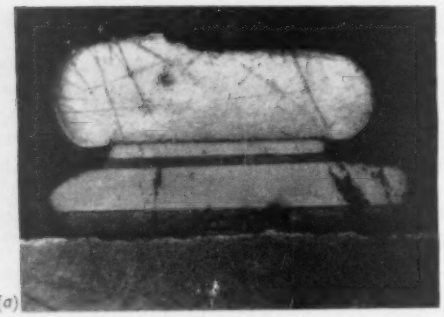

(a)

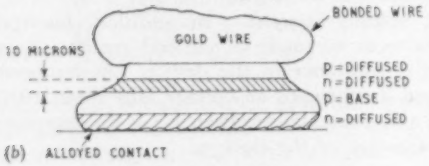

Fig. 7. *(a) Section of diffused p-n-p-n switch; (b) Schematic diagram of the same switch*

of J_2. The narrow, 3 micron, base width also gave a fast turn-on time, and a capacitance less than 5 pF, with a mean power dissipation of 100 mW.

The disadvantages of this construction were the poor reverse characteristics, the sum of the avalanche voltages of J_1 and J_3 being only slightly over 20 V. The most serious disadvantage was the poor control over the position of the aluminium junction, J_1. Firstly, it is necessary to alloy to within 1 micron in 50 microns. Secondly, due to regrowth of the aluminium, this junction (J_1) is formed parallel to the 1 1 1 plane of the silicon crystal lattice, whereas the diffused junction, J_2, follows the surface contours; hence, in order to give a uniform base width, the surface of the silicon must be prepared accurately parallel to the 1 1 1 plane.

The second structure, illustrated in Fig. 7, did not suffer from these disadvantages, all the junctions being formed by diffusion techniques. Here J_2, and J_3 which is diffused at the same time, are identical to J_2 in the previous device. J_1 is formed by a second diffusion using boron, a p-type impurity. The surface concentrations of the diffusants forming J_1 and J_3 are made as high as possible, in order to give a low contact resistance and a reasonable emitter efficiency at the junctions.

Here again the minimum thickness of the starting material is governed by lapping and polishing techniques, and the maximum base region width is governed by the holding current requirements. It will be noticed that the base widths of the two devices described are different, due mainly to differences in minority carrier lifetime, the areas of the devices being similar ($\simeq$ 0·25 mm diam.).

The main electrical advantage of the all diffused type is the high reverse voltage, due to the diffused junction J_3. These devices can be of Type (a) or (b), giving high or low switching currents at high voltages. In this particular structure, because of the wider base widths, the turn-on times will be higher. The advantages of this method of construction are those common to most diffused devices, notably the small spread in characteristics, as all devices are made on one slice of silicon before being cut into individual devices. There is also considerable flexibility for a family of devices with different switching voltages and holding currents.

The application of these devices is now widespread and includes switching in electronic telephone exchanges, ring counting and pulse generation. These and general application aspects will be discussed in a further article in the December issue.

REFERENCES

[1] S. L. Miller, "Avalanche Breakdown in Germanium", *Phys. Rev.*, 15th Aug., 1955, Vol. 99, pp. 1234–1241.
[2] W. Schockley, "Theories of High Values of Alpha for Collector Contacts on Germanium", *Phys. Rev.*, 15th April, 1950, Vol. 78, pp. 294–295.
[3] S. L. Miller and J. J. Ebers, "Alloyed Junction Avalanche Transistors", *Bell Syst. tech. J.*, Sept. 1955, Vol. 34, pp. 883–902.
[4] J. L. Moll et alia, "P-N-P-N Transistor Switches", Proc. I.R.E., Sept. 1956, Vol. 44, No. 9, pp. 1174–1182.
[5] W. Schockley, "The Theory of p-n Junctions in Semiconductors and p-n Junction Transistors", *Bell Syst. tech. J.*, July 1949, Vol. 28, pp. 435–489.

MANUFACTURERS' LITERATURE

Arcol Precision Wirewound Resistors. This 18-page catalogue deals with the current ranges of Arcol wirewound resistors which are either epoxy-resin coated or encapsulated in nylon; resistance tolerances from 0·025% to 1% are available for most resistance values.
Ashburton Resistance Co. Ltd., 72 Brewery Road, London, N.7.

Alma Resistor Selection Chart. This 16-page wall chart lists the range of Alma precision wirewound resistors in seven sections—selection by minimum inductance, resistance value, temperature coefficient, mounting, accuracy, physical size, type numbers.
Alma Components Ltd., 551 Holloway Road, London, N.19.

'Epophen' Epoxide Resins. This 4-page booklet and the accompanying 4-page data sheet describes the Epophen Epoxide systems for electrical uses. The booklet gives general details of the systems while the data sheet gives process details, mechanical and electrical properties, and lists suppliers of ancillary materials and equipment.
Leicester, Lovell & Co. Ltd., North Baddesley, Southampton, Hants.

High-Frequency Current Probe. This 2-page leaflet gives details of two Tektronix h.f. current probe systems for use in conjunction with oscilloscopes for the observation and measurement of current waveforms of a few milliamperes to several amperes at frequencies up to 20 Mc/s.
Tektronix Inc., P.O. Box 500, Beaverton, Oregon, U.S.A.

Siemens Screened Cubicles. A 4-page leaflet describing the Siemens & Halske range of screened cubicles and rooms. Details are given of the construction, sizes and electrical performances. Distributed in the U.K. by
R. H. Cole (Overseas) Ltd., 2 Caxton Street, London, S.W.1.

Ardente Miniature Electronic Components. This 42-page catalogue lists the 1961 ranges of miniature rotary switches, potentiometers, transformers and chokes which are produced by
Ardente Acoustic Laboratories Ltd., 8–12 Minerva Road, London, N.W.10.

Mullard Magnadur Permanent Magnets. This 8-page booklet contains information about the various types of Magnadur and their particular applications. Factors governing the length and cross-sectional area of any permanent magnet are discussed and some general rules are given for the guidance of designers.
Mullard Ltd., Component Division, Mullard House, Torrington Place, London, W.C.1.

Mazda Valves and Cathode Ray Tubes: Data Booklet 1961-62. This 154-page reference booklet contains information on the current range of Mazda valves and c.r.ts. It also lists obsolescent types, equivalents, and replacements for obsolete types.
Thorn-A.E.I. Radio Valves and Tubes Ltd., 155 Charing Cross Rd., London, W.C.2.

Feedback Analysis using the 'Root Locus' Method—3

The open-loop gain $A\beta$ of the three-stage RC amplifier considered in our last article was given by the equation

$$A\beta = \frac{A_0\beta_0}{(1+pT_1)(1+pT_2)(1+pT_3)} \quad .. \quad (1)$$

where T_1, T_2 and T_3 were the respective coupling time-constants, and $A_0\beta_0$ was the open-circuit loop gain. Particular attention was paid to the case in which T_1, T_2 and T_3 were 2, 5 and 10 μsec respectively, and the maximum value of $A_0\beta_0$ consistent with stability was then found to be 12·6. In this article we shall consider the effect of adding capacitance in the feedback network, so that this network is as in Fig. 2 instead of as in Fig. 1.

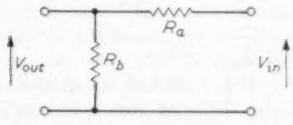

Fig. 1 (*Left*). *Feedback loop of original network*

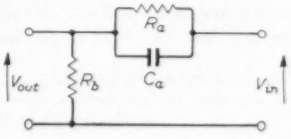

Fig. 2 (*Right*). *Feedback loop with added capacitance*

With the feedback network of Fig. 1, the gain β is the same at all frequencies, so that

$$\beta = \beta_0 = \frac{R_b}{R_a + R_b} \quad .. \quad .. \quad .. \quad .. \quad (2)$$

whereas in the case of Fig. 2, R_a must be replaced by the series impedance Z_a in Fig. 2, namely

$$Z_a = \frac{R_a}{1+pT_a} \quad (T_a = C_aR_a)$$

so that, although β_0 is unaltered, β is now given by

$$\beta = \beta_0 \frac{1+pT_a}{1+pT_a\beta_0} \quad .. \quad .. \quad .. \quad .. \quad (3)$$

In our last article we used the symbol K as an abbreviation for $A_0\beta_0/T_1T_2T_3$, and took 10^5 radians/sec as the unit for p; $A_0\beta_0$ was then numerically equal to $K/10$ for the particular values of the time constants considered. With the additional capacitance in the feedback loop as in Fig. 2, the equation whose roots determine the closed-loop behaviour of the whole system becomes

$$1+A\beta = 1+\frac{K}{\beta_0}\cdot\frac{p+(10/T_a)}{(p+1)(p+2)(p+5)(p+[10/T_a\beta_0])} = 0 \quad .. \quad .. \quad .. \quad .. \quad (4)$$

assuming that T_a is given in microseconds.

In practice β_0 is usually small compared to unity, and this suggests that an obvious possibility is to make T_a equal to 2 μsec, the smallest time-constant of the original amplifier. To fix our ideas, we shall take β_0 to be 0·1 henceforward; if we now cancel the term $(p+10/T_a)$ in the numerator and $(p+5)$ in the denominator and clear of fractions, Equ. (4) reduces to

$$(p+1)(p+2)(p+50) + 10K = 0 \quad .. \quad .. \quad (5)$$

As Equ. (5) is only a cubic, we can apply the rule mentioned in an earlier article that for critical stability, the product of the coefficient of p^3 and the constant term equals the product of the coefficient of p and the coefficient of p^2. This gives the critical value of K as 795·6 and the corresponding critical value of $A_0\beta_0$ is $K/10$ or 79·56, instead of 12·6 with the original system. Thus the effect of the additional capacitance in Fig. 2 is to multiply the open-circuit loop gain available by over 6. Nevertheless, we are not obliged to make T_a equal to 2 μsec, and it is of some interest to determine how the root-locus in general, and the critical value of $A_0\beta_0$ for stability in particular, varies with T_a when β_0 and the other time constants remain fixed (so that all the variations to be discussed can be achieved in practice by varying C_a). If $T_a = 0$, Equ. (4) reduces to the case considered in our last article, so Fig. 2 of that article is reproduced as Fig. 3 here for comparison. We shall also consider the cases $T_a = 1$, $T_a = 2$, $T_a = 4$ and $T_a = 5$; the corresponding rough diagrams of the root loci for $T_a = 1$, 2 and 4 are given in Figs. 4, 5 and 6 respectively.

If $T_a = 1$, Equ. (4) reduces to

$$1+\frac{K}{\beta_0}\frac{p+10}{(p+1)(p+2)(p+5)(p+100)} = 0 \quad .. \quad (6)$$

As there are 4 poles and one zero, the parts of the real axis that belong to the root locus are those where an odd number of poles and zeros lie to the right, that is to say $p<-100$, $-10<p<-5$ and $-2<p<-1$. For any value of K, there will be one real root less than -100 and one between -5 and -10; if K is sufficiently small, there will be two real roots between -1 and -2 but these will be replaced by a complex conjugate pair for larger values of K. As there are three more zeros than poles, the asymptotic directions of the locus remain 180° and $\pm 60°$ as in Fig. 3, but the major change is in the position of the centre of gravity, which is at $-32\frac{1}{2} + 0j$ instead of $-2\frac{1}{2} + 0j$ as in Fig. 3. (The rules for determining the parts of the real axis which belong to the root-locus, the asymptotic directions and the position of the centre of gravity through which all asymptotes pass were given in the October 'Tool'). Hence the locus is as in Fig. 4; it consists of the part of the real axis to the left of P_4 or $-100 + 0j$, the part joining Z_1 to P_3, the part joining P_2 to P_1 and the curve labelled C_1C_2.

We are obliged to use one-fifth of the scale of Fig. 3 in order to show all the poles and zeros. The breakaway point occurs at $p = -1{\cdot}478 + 0j$; it is easily obtained by trial and error from the equation

$$\frac{1}{p+1} + \frac{1}{p+2} + \frac{1}{p+5} + \frac{1}{p+100} - \frac{1}{p+10} = \frac{d}{dp}\log\left(\frac{K}{\beta_0}\right) = 0$$

which is the analogue for the case under discussion of *Equ. (19)* of the October 'Tool'. The first two terms are much more sensitive to variations of p in the neighbourhood of $-1{\cdot}5$ than any of the other terms. We now have sufficient information to draw the root locus as in Fig. 4 provided that we can find the position of one point on the complex part of this locus. Clearly the most useful point to determine is that on the imaginary axis (and above the real axis). Assuming that this part of the curve is not very different from the corresponding part of Fig. 3, we can start exploring near $p = 5j$, and the correct value of p is thus found to be $7{\cdot}2j$. The corresponding value of K/β_0 is found to be 3874 by substituting $7{\cdot}2j$ for p in Equ. (6) (or by drawing and measurement from a sufficiently accurate version of Fig. 4, since K/β_0 is the product of the distances from $7{\cdot}2j$ to the various poles, divided by the distance to the zero at $-10 + 0j$) and the maximum value of $A_0\beta_0$ consistent with stability has thus risen from 12·6 when $T_a = 0$ to 38·74 when $T_a = 1$ μsec.

If T_a is now increased to 2 μsec, Equ. (4) reduces to

$$1 + \frac{K}{\beta_0} \cdot \frac{1}{(p+1)\,(p+2)\,(p+50)} = 0 \qquad .. \quad (7)$$

instead of Equ. (6). It is surprising how little change this makes in the essential nature of the root locus. The pole that we called P_4 in Fig. 4 is now at $-50 + 0j$ instead of $-100 + 0j$, and the short segment $Z_1\,P_3$ disappears because Z_1 now coincides with P_3. The point G is now at $-17\frac{1}{2} + j0$, but the oblique asymptotes are still at $\pm 60°$ as before. The breakaway point occurs when

$$\frac{1}{p+1} + \frac{1}{p+2} + \frac{1}{p+50} = 0 \qquad .. \quad .. \quad .. \quad (8)$$

and in this case Equ. (8) can be solved as a quadratic in p to give the breakaway point as $-1{\cdot}497 + 0j$ and the point where the root-locus crosses the imaginary axis can be expected somewhere in the region of $8j$ (that is, somewhat above the corresponding point of Fig. 4) and it is in fact at about $12{\cdot}3j$. Substitution into Equ. (7) for K/β_0 gives the value of this quantity as 7945, so that the maximum value of $A_0\,\beta_0$ consistent with stability is now one-hundredth of this or 79·45; this is in remarkably good agreement with the more accurate value of 79·56 obtained by taking advantage of the fact that Equ. (5) is a cubic. A rough diagram of the complete root locus is therefore as given in Fig. 5 (which is drawn to the same scale as Fig. 4).

If we now increase T_a to 4 μsec, Equ. (4) reduces to

$$1 + \frac{K}{\beta_0} \cdot \frac{p+2{\cdot}5}{(p+1)\,(p+2)\,(p+5)\,(p+25)} = 0 \qquad .. \quad (9)$$

so the point G has moved to $-10\frac{1}{2} + j0$ and the zero Z_1 is now to the right of P_3. In drawing the root-locus (Fig. 6) we can therefore return to the scale of Fig. 3, as we are only obliged to omit the part of the real axis to the left of $-25 + j0$ as the price of having the

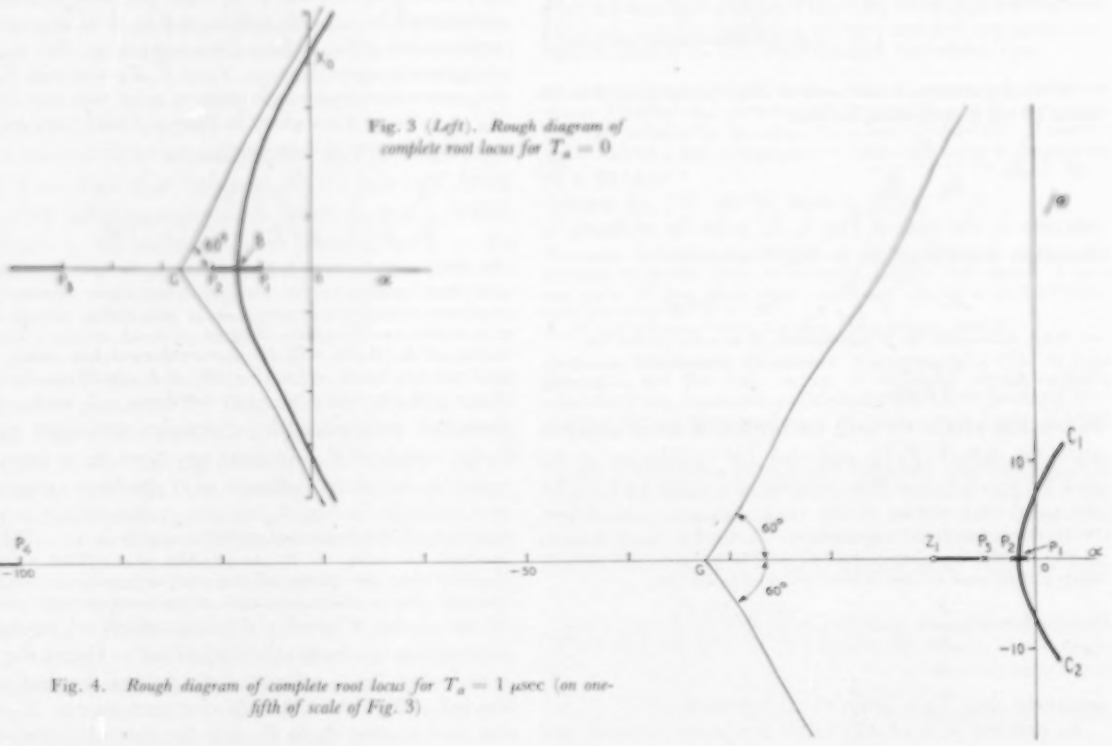

Fig. 3 (*Left*). *Rough diagram of complete root locus for* $T_a = 0$

Fig. 4. *Rough diagram of complete root locus for* $T_a = 1$ μsec *(on one-fifth of scale of Fig. 3)*

diagram near the original poles clearer. The breakaway point is given by

$$\frac{1}{p+1}+\frac{1}{p+2}+\frac{1}{p+5}+\frac{1}{p+25}-\frac{1}{p+2\cdot5}=0 \qquad (10)$$

and is therefore about $p=-1{\cdot}592+j0$. As before, the only other point worth reasonably accurate determination is the point on the imaginary axis; if we start looking for this in the region of $20j$, we find that it is in fact at $11{\cdot}87j$. The corresponding value of K/β_0 is 4772 (from Equ. 9) and the critical value of $A_0\beta_0$ is thus 47·72.

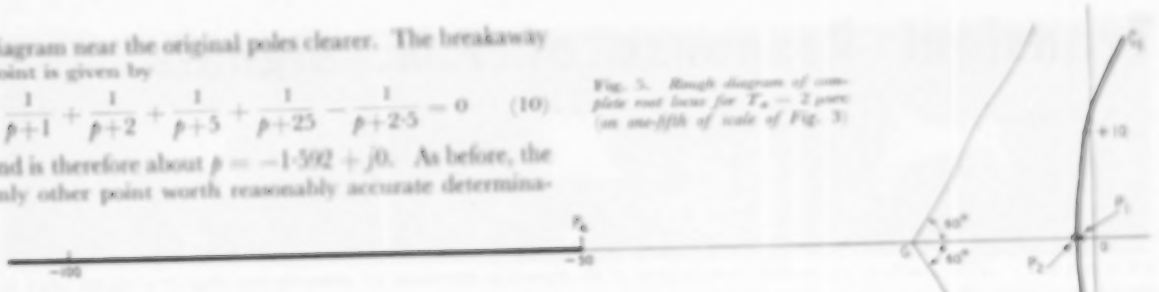

Fig. 5. *Rough diagram of complete root locus for $T_a=2$ μsec (on one-fifth of scale of Fig. 3)*

If T_a is now increased to 5 μsec, Equ. (4) again has cancelling factors, $(p+2)$ in this case, in numerator and denominator, and if we clear of fractions, the relevant cubic analogous to Equ. (5) becomes

$$(p+1)\,(p+5)\,(p+20)+10K=0 \qquad (11)$$

and the critical value of K will thus be found (as when we considered Equ. (5) to be 315·0 and the corresponding value of $A_0\beta_0$ is thus 31·5. The curved part of the root locus will have much the same general shape as in Fig. 6, so we have not determined it; the procedure is exactly the same as for Figs. 3, 4, 5 and 6. It thus appears that the greatest possible value of $A_0\beta_0$ consistent with stability is obtained when T_a is near but slightly above 2 μsec; the values of maximum permissible $A_0\beta_0$ we have obtained are plotted against T_a in Fig. 7.

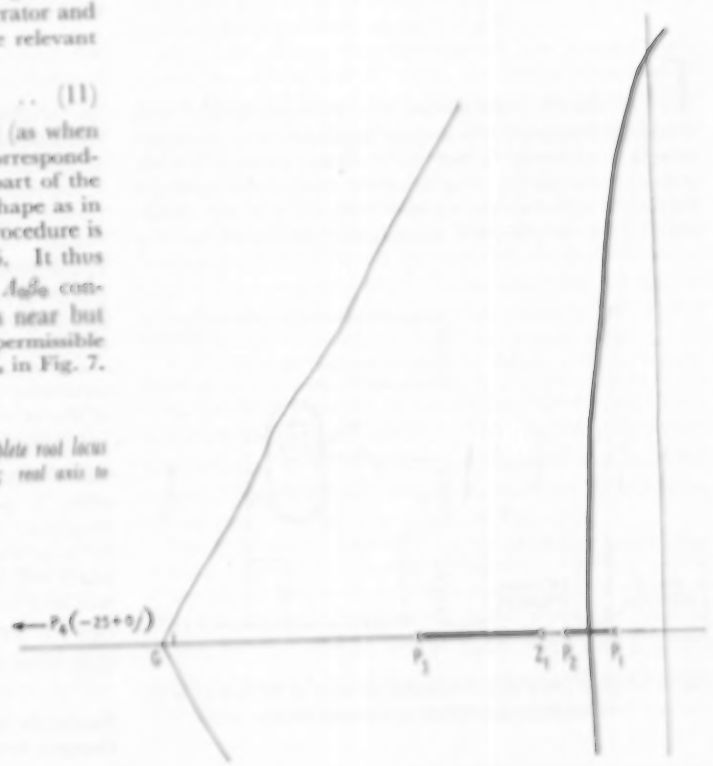

Fig. 6 (*Right*). *Rough diagram of complete root locus for $T_a=4$ μsec (same scale as Fig. 3; real axis to left of P_a also belongs)*

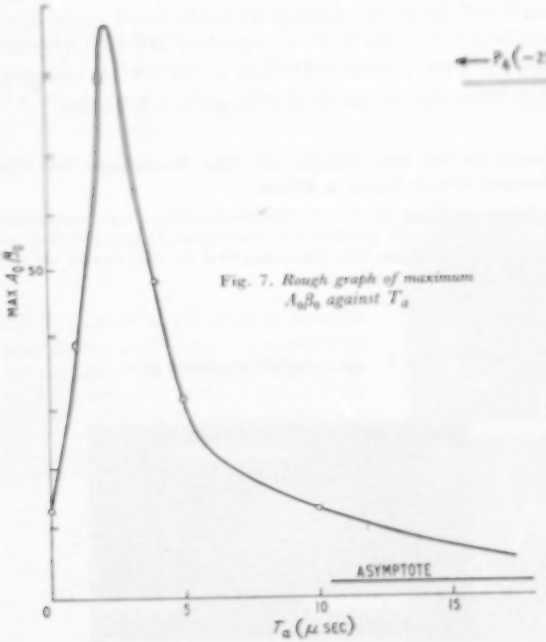

Fig. 7. *Rough graph of maximum $A_0\beta_0$ against T_a*

To complete Fig. 7 we have used the fact that when T_a is 10 μsec, Equ. (4) reduces to the cubic

$$(p+2)\,(p+5)\,(p+10)+K/\beta_0=0 \qquad (12)$$

so that the maximum value of K/β_0 consistent with stability is given by the rule for cubics mentioned after Equ. (5) and is 1260 (maximum $A_0\beta_0=12{\cdot}6$), and again, if $T_a\to\infty$, Equ. (4) reduces to the cubic discussed in our last article, except that K/β_0 takes the place of K, so that the maximum possible value of $A_0\beta_0$ is one-tenth of what it was in that article, namely 1·26.

Thus the common-sense idea of adjusting T_a so as to cancel out the factor $(p+5)$ in Equ. (4) appears to be very close to the best possibility available, but the root-locus technique shows us that a sufficiently small variation of T_a from the value of 2 μsec associated with exact cancellation is not significant.

Transient Response of F.M. Signals

By S. J. Cotton*, B.Sc.

SUMMARY. *This article is a practical investigation of the distortion introduced by networks and lines to a signal when its frequency suddenly changes. The problem of filters is first dealt with to see how the distortion is affected by the relative values of the resonant frequency of the filter and the signal frequency, the Q of the circuit, the value of the frequency jump, the bandwidth of subsequent circuits and a limiter stage immediately after the filter. The effects of reflection at the termination of a coaxial cable and also a resistive and resistive–capacitive network were also found.*

It has already been shown in a previous article[1] that when the frequency of a voltage applied to a single tuned circuit is suddenly varied the resultant current is composed of two parts—(i) a transient component having a frequency equal to the natural frequency of the circuit and (ii) a steady-state component produced by the applied signal. The amplitude of the transient component increases with the value of the frequency jump and also with the Q of the circuit. These two components can be added vectorially to give a resultant whose frequency can be found by obtaining the first time derivative of its phase angle. The resultant frequency of the current flowing is also composed of two parts: a mean frequency which varies exponentially, the rate of variation being governed by the decay factor of the circuit; and an alternating or 'flutter' component whose frequency of variation is equal to the difference between the final signal frequency and the natural frequency of the circuit. The combination of these two components gives an instantaneous frequency of current immediately after the change of frequency of the voltage equal to the original frequency. If, however, the effect of the second component could be removed a sudden frequency jump could occur and the response would be improved. If the final frequency of the applied signal is equal to the natural frequency of the circuit, there will not be any 'flutter' component, but there will still be a varying mean-frequency component due to the difference in phase between the applied signal and the transient signal so that in this case the response would not be improved by subsequent circuits.

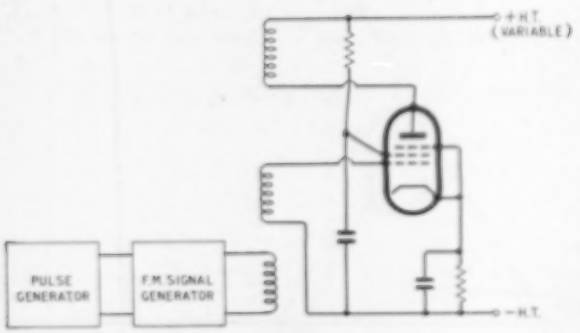

Fig. 1. *High Q circuit used in obtaining the shape of the envelope of the wave frequency modulated by a rectangular pulse*

No final conclusions were drawn from this analytical treatment as to the effect of the limiter stage; this part of the problem being left to the practical investigation.

When reflections occur in networks or lines at points where there is a sudden change of impedance, a similar effect is produced at the input terminals when the frequency of the applied voltage suddenly changes, since for a period of time the reflected wave arriving at the input will be of the original frequency and again there will be a combination of two signals of different frequencies. If there are no reflections in the line or network, then there should not be any frequency distortion.

Analysis of the Shape of the Envelope of the Output Wave from a Filter

Since a filter produces discrimination, any variation of frequency will produce a corresponding variation of amplitude and so can be observed in the shape of the envelope of the wave.

Fig. 2. *The rectangular modulating pulse*

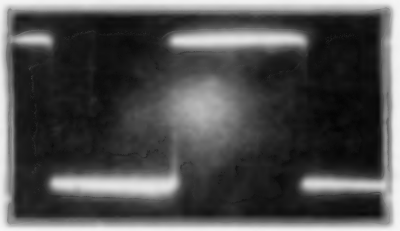

* *Senior Lecturer in Electrical Engineering at Nottingham and District Technical College.*

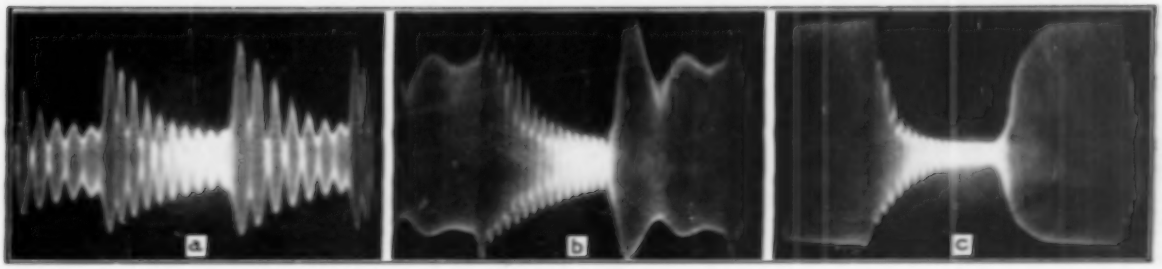

Fig. 3. Illustrates the effect of off-setting the centre frequency of the f.m. signal from the natural frequency of the tuned circuit. The centre frequency is off-set by 10 kc/s in (a), 40 kc/s in (b), and 50 kc/s in (c)

A normal f.m. signal generator was modulated with a square wave from a pulse generator and the output was applied to a tuned circuit of variable Q value as shown in Fig. 1.

The Q value was varied between 150 and about 300 by varying the value of the h.t. supply, and the value of the Q determined from the bandwidth as measured on the incremental frequency meter on the f.m. signal generator. Fig. 2 shows the 3·2 kc/s modulating signal which has a pulse width of 156 μsec.

Effect of Frequency 'Flutter' and Mean-Frequency Variation

With a circuit Q of about 200 the centre frequency of the frequency-modulated signal was set to be 10 kc/s different from the natural frequency of the tuned circuit and the height of the modulating signal was adjusted to give a frequency deviation of about 50 kc/s. This means that the frequency of the applied signal was jumping between two values, one about 40 kc/s and the other about 60 kc/s different from the natural frequency of the filter. Fig. 3(a) shows an oscillogram of the voltage across the tuned circuit. The effect of the 'flutter' component of the transient frequency can be seen clearly and it will be observed that the frequency of this 'flutter' is equal to the difference between the signal frequency and the natural frequency of the circuit. While there is no sudden variation of the instantaneous frequency, if a mean line is drawn through the variation of one edge of the envelope, it will be seen that this has a sudden jump and then decays exponentially. The decay in amplitude is due to the shape of the filter characteristic. The mean frequency must, therefore, experience a sudden jump and then vary exponentially towards the value of the frequency of the applied signal.

Fig. 3(b) shows the envelope of the voltage wave across the tuned circuit when the centre frequency is about 40 kc/s different from the natural frequency of the circuit. The frequencies of the 'flutter' corresponding to the negative and positive pulses of the modulating signal are now about 10 kc/s and 90 kc/s respectively. Fig. 3(c) shows the effect of off-setting the centre frequency from the natural frequency by 50 kc/s so that the flutter disappears from alternate sections and the gradual variation of the mean frequency can be observed. It will be seen that the effect for these sections without any flutter is very similar to that obtained in amplitude modulation.

The next step was to obtain the shape of the demodulated output pulses. The voltage across the tuned circuit was, therefore, applied to a cathode follower and then to a germanium diode detector. The frequency deviation was reduced to 20 kc/s and the shape of the detected output, when the centre frequency is off-set 20 kc/s from the natural frequency, is shown in Fig. 4(a).

Fig. 4(b) shows the same as (a) with the centre frequency equal to the natural frequency. The two values of the signal frequency are now equally spaced on either side of the natural frequency so that if there had been no distortion, the output would have been just a single curve—the curve being due to the response characteristic. The large positive pulse shows the instantaneous fre-

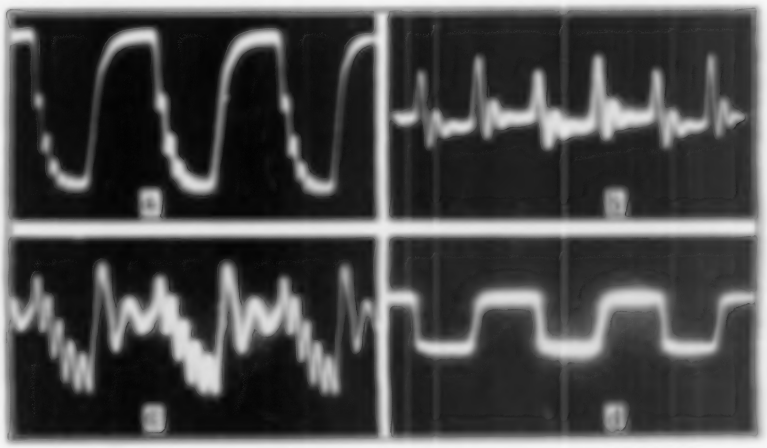

Fig. 4. Shows the shape of the output signal after demodulation; in these cases the frequency deviation was 20 kc/s. With the centre frequency off-set 20 kc/s output (a) results, output (b) occurs with zero off-set of the centre frequency and case (c) with 10 kc/s off-set. In case (d) the centre frequency was off-set 20 kc/s but with a considerably reduced value of Q for the tuned circuit

quency going through the resonant value of the tuned circuit and superimposed on this is the effect of the flutter component.

In Fig. 4(c) is seen the effect of off-setting the centre frequency 10 kc/s from the natural frequency, while (d) gives the detected output with a considerably reduced value of Q for the tuned circuit and the centre frequency f_c = the natural frequency $f_0 + 20$ kc/s.

The effect of the flutter components in the detected output was then removed by passing this output through a m-derived low-pass filter having a cut-off frequency of 80 kc/s. This allowed up to the 25th harmonic of the modulating signal to be passed.

Fig. 5(a), (b) and (c) show the output from this filter with large frequency deviations and with $f_c = f_0$, $f_c = f_0 + 20$ kc/s, and $f_c = f_0 + 30$ kc/s respectively. If Fig. 5(b) is compared with Fig. 4(a) the improvement in the wave shape is immediately apparent.

Effect of the Q of the Circuit and Value of the Sudden Frequency Jump on the Transient Component

The effect of varying the Q of the circuit and also the frequency jump was next investigated. A modulating pulse of equal mark-space ratio and 100 μsec pulse width was used. Fig. 6(a) shows the envelope for a Q of 150, the centre frequency equal to the resonant frequency and a maximum frequency deviation of 50 kc/s. About one cycle of the flutter effect can be observed. Fig. 6(b) is for the same condition except for a Q of about 300. It can be seen that the amplitude of the flutter effect has been greatly increased. This has been produced by the increased frequency variation of the transient and also by the increased slope of the response characteristic. Fig. 6(c) shows the result of reducing the frequency deviation to 40 kc/s and keeping the Q equal to 300.

In Fig. 6(d) the effect of off-setting the centre frequency by 20 kc/s from the resonant frequency is seen, while Fig. 6(e) shows the effect of subsequently reducing the Q to 150 again.

Instantaneous Frequency of Output Signal from a Single Tuned Circuit

For the frequency jumps that have been considered and for a centre frequency of about 12 Mc/s the frequency variation is only small compared with the centre frequency, so that nothing much will be gained from an inspection of the actual output waveform. If the modulated signal jumps from a frequency of $f_c - \Delta f$ to $f_c + \Delta f$ and this signal is mixed with one of frequency f_c the output signal from the mixer will have a frequency of Δf, if the higher frequency components are filtered out. If the modulated output from the tuned circuit is fed into the mixer circuit, together with a signal of frequency f_c, the transient variation of frequency could be observed. In order to obtain the centre frequency an Armstrong frequency modulator was built. The oscillator had a frequency of about 0·8 Mc/s and two outputs in quadrature were taken from two different parts of the oscillator circuit and fed into two cathode-follower circuits. One of these outputs was fed into a balanced modulator together with the integrated modulating signal, so that a pair of sidebands in quadrature with the other output were produced. These were then added to the other output to produce phase modulation. Since, however, the modulating signal had been integrated the result was frequency modulation. The modulated and unmodulated outputs were now each fed into separate frequency multipliers and their frequencies multiplied by 16 so that the new centre frequency was about 12·8 Mc/s. The Q of the circuits for the modulated-signal frequency multiplier was kept as low as possible to prevent distortion. Using a square-wave modulating signal the frequency was made to jump from $f_c - 4$ kc/s to $f_c + 4$ kc/s. It would have been better if the original frequency had been made 0·4 Mc/s or even 0·2 Mc/s and then the frequency multiplied by 32 or 64 so that the frequency variation would have been ± 8 kc/s or ± 16 kc/s respectively.

The effect of mixing the centre frequency signal with the output from the modulator is shown in Fig. 7(a). On this and all subsequent figures the modulating signal is also shown for reference.

Fig. 7(b) shows how the frequency varies in the output from a low-Q tuned circuit. The small flat occurs when the instantaneous frequency is equal to the centre frequency (equal to zero on this figure). It will be seen that the frequency rises fairly rapidly to this value and the rate of change gradually decreases.

Figs. 7(c) and (d) are for higher-Q circuits and the frequency takes longer to settle down.

Fig. 8(a) shows the resultant waveform for several cycles of modulating signal with the centre frequency equal to the resonant frequency, while (b) shows the effect of off-setting the centre frequency so that the frequency jumps from f_c to $f_c + 8$ kc/s.

The effect of removing the flutter by means of a low-pass series m-derived filter with a cut-off frequency of 8 kc/s is shown in Fig. 9(a). The conditions are the same as for Fig. 7(c) and it will be seen that the distortion has

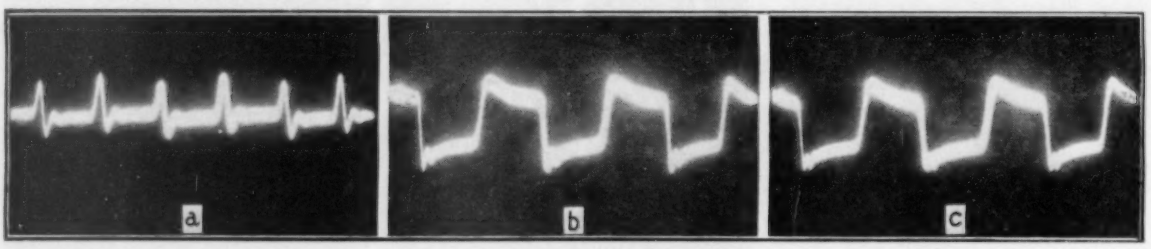

Fig. 5. *The demodulated signal with the flutter components removed by a low-pass filter (a) $f_c = f_0$, (b) $f_c = f_0 + 20$ kc/s and (c) $f_c = f_0 + 30$ kc/s*

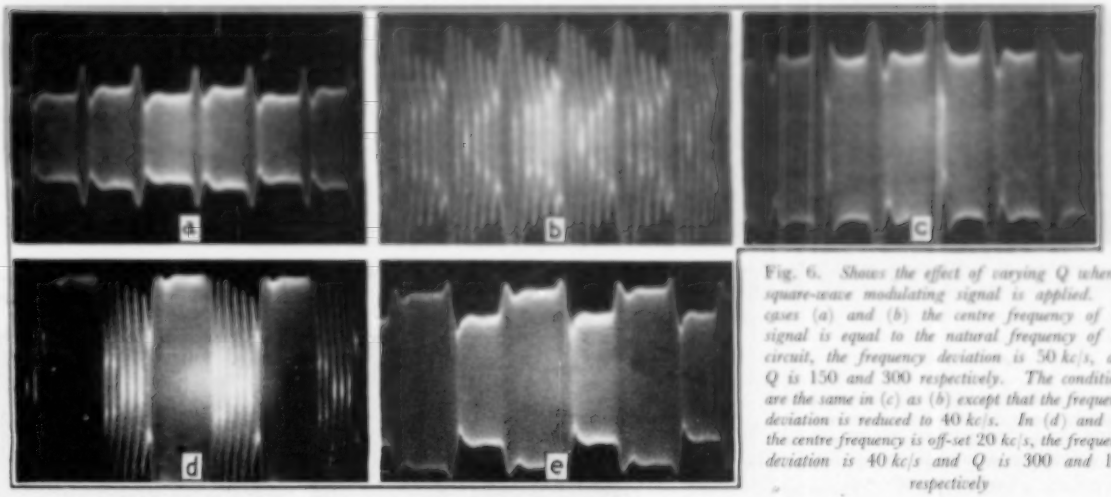

Fig. 6. *Shows the effect of varying Q when a square-wave modulating signal is applied. In cases (a) and (b) the centre frequency of the signal is equal to the natural frequency of the circuit, the frequency deviation is 50 kc/s, and Q is 150 and 300 respectively. The conditions are the same in (c) as (b) except that the frequency deviation is reduced to 40 kc/s. In (d) and (e) the centre frequency is off-set 20 kc/s, the frequency deviation is 40 kc/s and Q is 300 and 150 respectively*

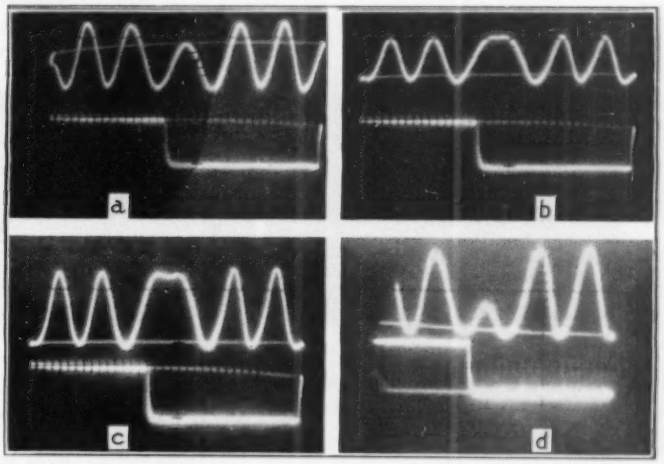

Fig. 7. *Shows the effect changing the Q of the tuned circuit when mixing the centre frequency signal with the output from the modulator. (a) illustrates the effect for medium Q, (b) low Q, (c) and (d) high Q. In this and all subsequent figures the modulating signal (bottom trace) is shown for reference*

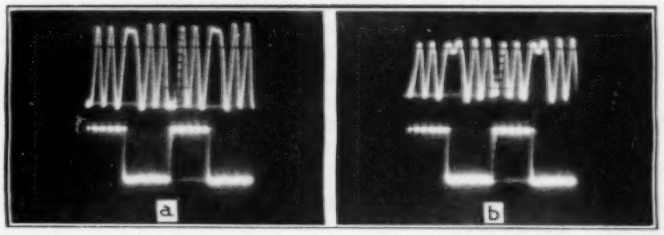

Fig. 8. *Illustrates several pulses of modulating signal with conditions similar to those in Fig. 7 (c) and (d). In (a) the centre frequency is equal to the natural frequency of the circuit. In (b) the centre frequency is off-set so that the frequency jumps from f_c to $f_c + 8$ kc/s*

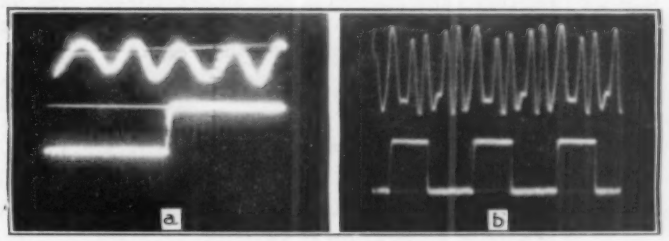

Fig. 9. *Shows the effect of removing flutter by means of a low-pass filter. The conditions are the same as for Fig. 7(c) in (a) and Fig. 8(b) in (b)*

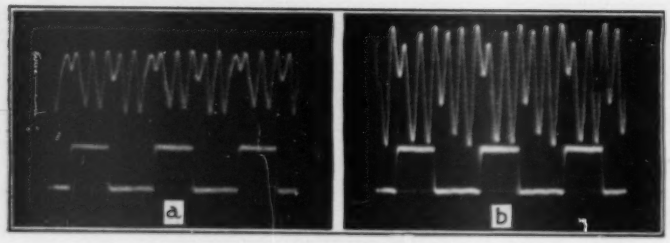

Fig. 10. *With the centre frequency off-set considerably output (a) results and (b) shows the effect of the low-pass filter with this condition*

Fig. 11. *Shows the effect on the instantaneous frequency due to reflections when a coaxial cable, with the far end o.c., is connected to the modulator. (a) without the cable connected. (b) with the cable connected*

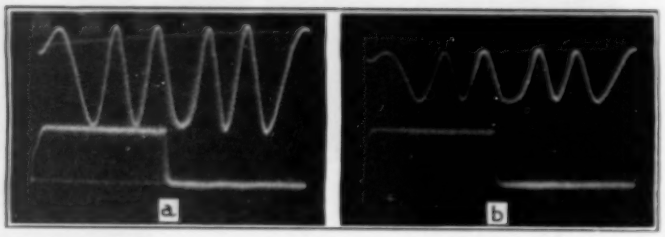

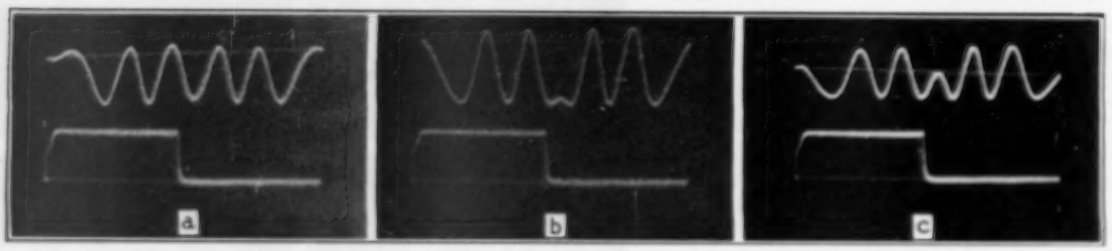

Fig. 12. *These oscillograms show the effect of different types of coupling circuit. (a) the coupling is by the coaxial line of Fig. 11(b). (b) the coupling is by means of a 2kΩ resistor. (c) the coupling is by means of the circuit of Fig. 13*

been largely removed. Fig. 9(b) shows the effect of the low-pass filter for conditions similar to Fig. 8(b).

Fig. 10(a) shows the output when the centre frequency is off-set well down the slope of the tuned circuit response characteristic, while (b) shows the effect of the low-pass filter with this condition.

Effect on the Instantaneous Frequency Due to Reflections in Lines and Networks

The output from the modulator was fed into about 100 yards of coaxial cable with the far end open circuit. The input of the line was also connected to the mixer.

The waveshape without the cable connected is shown in Fig. 11(a) and with the cable in (b). It will be seen that the frequency variation occurs over an appreciable time in the latter case.

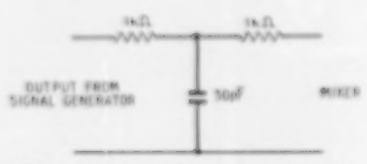

Fig. 13. *The coupling circuit for Fig. 12(c)*

Fig. 12(a) shows the effect of connecting the far end of the cable to the mixer with the input roughly matched, and hardly any distortion will be noticed

The modulator was connected to the mixer through a 2-kΩ resistor so that reflections could occur at the terminals and Fig. 12(b) shows the distortion produced.

The network shown in Fig. 13 was used to connect the modulator to the mixer and Fig. 12(c) shows that considerable distortion is produced.

Effect of a Limiter Circuit on the Instantaneous Frequency

A limiter circuit was connected directly across the tuned circuit and the output from the limiter fed into the mixer circuit. The frequency was caused to jump between $f_c - 4$ kc/s and $f_c + 4$ kc/s.

Fig. 14(a) shows the output from the mixer circuit with both the above frequencies well down the slope of one side of the response characteristic of the tuned circuit. It will be seen that the frequency takes a considerable time to vary from one value to the other, this period of time being longer when the new frequency is further removed from the natural frequency of the circuit.

Fig. 14(b) shows the effect of a frequency jump

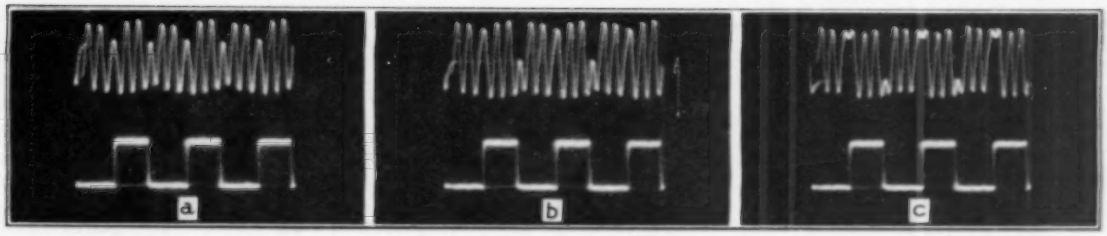

Fig. 14. *Shows the effect of a limiter connected directly across the tuned circuit (a) with the centre frequency off-set considerably. (b) with the centre frequency off-set from the circuit natural frequency by an amount equal to the frequency deviation. (c) with the centre frequency equal to the natural frequency of the circuit*

between $f_0 - 8$ kc/s and f_0. When the new frequency is f_0 there is hardly any distortion and for the reverse frequency jump the distortion is less than in (a).

In Fig. 14(c) the frequency jump is between $f_0 - 4$ kc/s and $f_0 + 4$ kc/s. The distortion is now equal for both jumps, but less than for the reverse jump of (b).

These results are identical with those obtained without any limiter, so that apart from some reduction, perhaps, in the Q of the circuit, the limiter has not affected the transient distortion produced by the filter.

Conclusions

These practical results have fully confirmed those obtained analytically, both for a single tuned circuit and also for lines and RC networks. The effect of a limiter on the distortion produced by a filter which, was in doubt, has been proved to be negligible.

REFERENCE

[1] S. J. Cotton, "A Comparison of the Transient Response of Amplitude-Modulated and Frequency-Modulated signals", Instn elect. Engrs Monograph No. 222R.

Correspondence

Letters to the Editor on technical subjects are always welcome. In publishing such communications the Editors do not necessarily endorse any technical or general statements which they may contain.

A Non-Boolean Algebra for Logical Circuitry

Sir,—It has been found possible to devise a symbolism capable of uniquely describing logical circuits. The symbolism is liable to an algebraic manipulation which gives functional equivalence as algebraic equivalence. That is to say, the algebra shows when circuits are equivalent, not as an assembly of logic-blocks, but in terms of components. This is best illustrated by examples of, first the symbolic form of a circuit, and then of reduction procedure.

A list of the symbols used is given below:

A, B, C	Signal input terminals
a, b, c	Signal output terminals
P	Positive supply terminals
N	Negative supply terminals
A	Resistance
$<$	Diode, proceeding to cathode
$>$	Diode, proceeding to anode
V	Inverting transistor
1	Short circuit
0	Open circuit

There are two operators, indicated thus:

$x + y$: x and y in parallel

$x \cdot y$: x and y in series

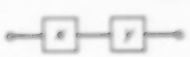

where x and y are components.

For convenience, the + operator is used with terminals and component lines beginning with terminals, to indicate a common point, thus:

$S + T$: S joining to T

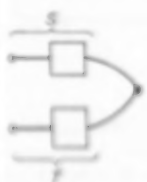

S and T being terminals or terminal-lines.

These symbols permit representation of all series-parallel circuits containing the components listed.

Starting with the inputs and listing all components and branches arrived at in order, gives the symbolic circuit.

For example, Fig. 1 becomes:

$(A.> + B.> + N.1).a$

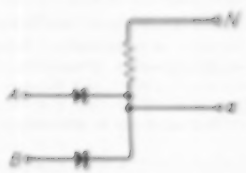

Fig. 1.

Some rules for the algebra are immediately evident, and are given below.

All components are commutative, except invertors with respect to diodes; all are associative and distributive.

$$>.>=>+>=>$$
$$<.<=<+<=<$$
$$A.\bar{A}=A+\bar{A}=A$$
$$>.<=0;\ >+<=1$$
$$N.<=N;\ N.>=0$$
$$P.<=0;\ P.>=P$$
$$>.0=A.0=0=<.0$$
$$>.1=>;\ A.1=A$$
$$>+1=A+1=1$$
$$>+0=>;\ A+0=A;\ <+0=<$$

An elementary theorem may now be proved.

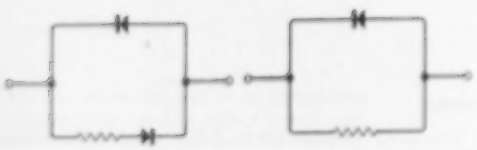

Fig. 2

To prove for Fig. 2: (a) = (b).
That is, to show: $A.>+<=A+<$
Inserting a diode in series: $(A.>+<).>;\ (A+<).>$
expanding $(\bar{A}.>.>+<.>);\ (\bar{A}.>+<.>.)$
$(A.>.>+0);\ (A.>+0)$
$A>\qquad ;\ A>$
When the identity is evident.

Another theorem, this one having some interest, is the well known Boolean equivalence:
$(A+B)+C=(A+B+C)$
Circuitally this becomes Fig. 3.

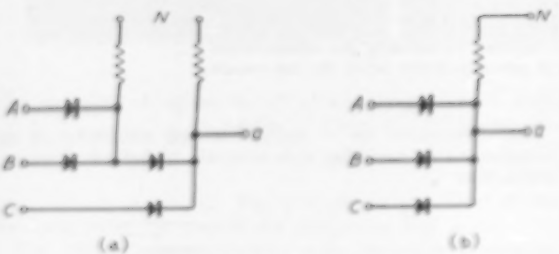

Fig. 3

To prove:
$([(N.A+A.>+B.>].>+C.>+N.A).a$
$=(A.>+B.>+C.>+N.A).a$
expanding: $(N.A.>+A.>+B.>+C.>+N.A).a$
but $N.A.>=N.>.A=0.A=0$
giving $(A.>+B.>+C.>+\bar{N}.A).a$

Q.E.D.

Terminals are not commutative with respect to components, but are associative and distributive. They are commutative, associative and distributive with respect to other terminals.

There are some additional rules for transistor invertors. The invertor is principally a series element which is commutative only with respect to resistances. For diodes, the following rules apply:

$$V.>=<.V$$
$$V.<=>.V$$

The invertor is associative and distributive, and obeys the rules:

$$V.V=1$$
$$V+V=V$$
$$P.V=N$$
$$N.V=P$$

It is now possible to prove a well known theorem in Boolean Algebra:
$\sim(A+B+C)=(\sim A).(\sim B).(\sim C)$

Circuitally this becomes Fig. 4.
To show (a) = (b)

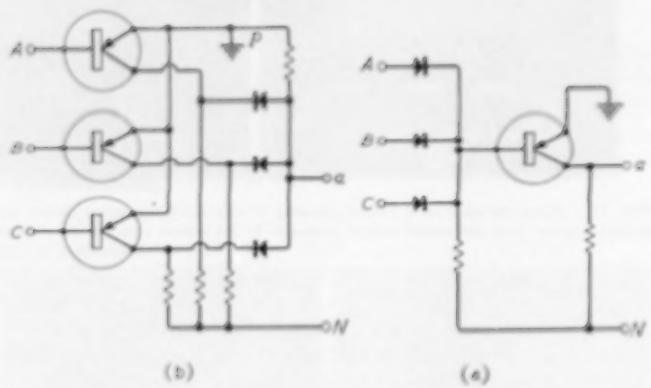

Fig. 4

To show:
$(A.>+B.>+C.>+N.A).V.a=(A.V.<+B.V.<+C.V.<+P.A).a$
expanding:
$(A.>.V+B.>.V+C.>.V+N.A.V).a$
giving $(A.V.<+B.V.<+C.V.<+P.A).a$

Q.E.D.

The Boolean proof is comparatively extensive. The objective of the algebra is to find a method of minimizing components, and its flexibility seems greater than Boolean algebra. It is hoped to extend the system to non-Boolean elements.

M. D. Evans.

Up Hatherley,
Cheltenham, Glos.
8th September 1961.

Historical Transistors

Sir,—At Monks Hall Museum, Wellington Road, Eccles, we have begun to collect obsolete diodes and transistors, in order that, when the time comes for the history of semiconductors to be written, examples may be available for examination and study. A number of leading manufacturers have generously supplied obsolete models, and have kindly agreed to supplement these with others as they become superseded by new developments.

I shall be glad to hear from anyone who may be in a position to add to our collection of early transistors from the initial stages of electronics development, so that they may be permanently preserved from loss, dispersal or destruction. Examples of early circuits, etc., would of course be equally welcome as a contribution to electronics history.

J. F. W. Bryon,
Borough Librarian and Curator.

Eccles Public Libraries,
Central Library,
Eccles, Manchester,
28th August 1961.

Transistor Mutual Conductance

Sir,—Mutual conductance cannot be used as a design parameter, in the strict sense of the word, since it is not capable of ready prediction. Certain elementary literature and manufacturers catalogues state and imply that $g_m \approx \alpha/r_e$. This is true, within my experimental experience, at $I_e = 1$ mA only and as I_e is increased the mutual conductance decreases until the curve of $I_e g_m$ becomes flat in some region dictated by the intrinsic parameters of the device.

The mutual conductance appears to behave according to the expression:

$$g_m \approx \frac{1}{r_e + R_{bb'}\beta}$$

from which it will be seen that as the emitter current increases $g_m \to \beta/R_{bb'}$. β, of course, varies with emitter current and $R_{bb'}$

tends to exhibit a saturation effect at high base currents. Hence, g_m is not a parameter in the usually understood sense of the term.

However, if the transistor is operating with emitter current feedback and is voltage driven on the base (i.e., from a low impedance source) then the gain may be stated as:

$$A_L = \frac{g_m R_L}{1 + g_m R_E} \approx \frac{R_L}{R_E}$$

This is a familiar valve equation and high-frequency compensation may be applied by means of a suitable capacitor shunting R_E.

From the foregoing it follows that a designable amplifier would be a common-emitter stage with adequate current feedback driven by a class A emitter-follower. In fact, such a configuration is extremely useful and enables the full gain-bandwidth of the device to be achieved.

T. G. Clark

Radar Development Laboratory,
Decca Radar Ltd.,
Chessington,
Surrey.
19th September 1961.

Transistor Symbols

Sir,—In your March issue a very interesting and brilliant comment on transistor symbols due to Dr. R. W. Jackson was published. Although Dr. Jackson himself is not very sanguine about his proposal, we think that sooner or later the different proposals on transistor symbols will have to be revised with the aim of stopping the anarchy existing in this field, such an anarchy Dr. Jackson has shown graphically in his Fig. 1.

Although we heartily agree with his ideas, there is one thing about which we don't see eye to eye with him; this is the rectangular shape he advocates for his symbols. This shape is generally reserved for passive elements—mostly impedances—the use of them also for transistors may produce confusion, and more than anything else it may be the cause of transistors not appearing clearly in a circuit. In Fig. 1, we have drawn a bistable multivibrator circuit for relay control, a circuit picked up by chance in a German technical magazine in which we only changed the original symbols referring to transistors T_1 and T_2 for the ones that Dr. Jackson proposed. If the drawing is looked at summarily the transistors tend to get lost amid the other elements of the circuit.

We believe that Dr. Jackson's proposal might be more effective if his symbols were given a circular shape, as we show in Fig. 2.

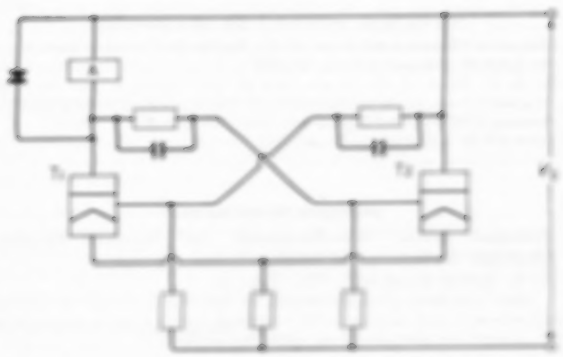

Fig. 1

Fig. 2

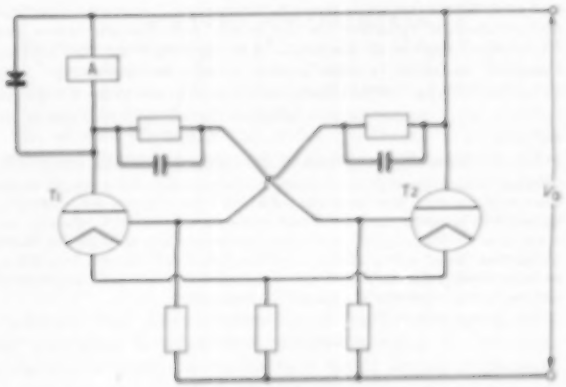

Fig. 3

If the circuit of Fig. 1 is repeated with the circular symbols (see Fig. 3) it will be seen how transistors stand out clearly from the other symbols.

It may be objected that these circular symbols for transistors look too much like those of vacuum tubes. But to us this is more an advantage than a disadvantage, as it gives a certain uniformity in the drawing of vacuum tube circuits and transistor circuits, a uniformity to which there is actually a decided tendency.

Luis Ruiz de Gordejuela

Instituto Nacional de Electrónica,
Madrid, Spain.
10th September 1961.

[While we have no objection to the use of a circular envelope for the transistor symbol, we would point out that the rectangular box is not a standard circuit symbol in British or American practice.

In British usage the rectangle is confined to the representation of generalized impedance when the nature of the impedance is either unknown at the time of drawing the diagram or may be of any kind. This generalized usage of the rectangle is convenient and widespread and we consider it a pity to adopt it also for a specific impedance element, such as a resistance, for which there is already a perfectly good and proper symbol. Ed.].

New Books

Linear Systems Analysis

By Paul E. Pfeiffer. Pp. 538 + xviii. McGraw-Hill Publishing Company Ltd., 95 Farringdon Street, London, E.C.4. Price £8 17s.

The author is attempting to provide in this book "a theoretical core of fundamentals requisite to understanding a variety of important and interesting systems and devices". This is a commendable objective, for it is now generally recognized in educational circles that both economy and broader understanding can be derived from teaching in a common course those principles of a subject that are extensively shared with others. In this country, *Electrical Theory* or its equivalent, for example, is now an established feature in many diploma and University courses. With proper integration of curricula, such a course may serve as a feeder of basic principles for a variety of special electrical subjects.

The fundamentals are here divided broadly between electric circuits, the dynamics of mechanical systems, and feedback systems. Throughout the book there is an obvious stress on the analogous forms of electrical and mechanical equations, which is consistent with the author's objective of generality.

A short introductory chapter is followed by "A Mathematical Miscellany", in which is briefly summarized essential mathematical principles, such as the complex-frequency plane, the Hurwitz criterion, determinants, integro-differential operators, etc. In the third chapter, the title "Linearized Dynamic Equations" is applied to electrical circuits, mechanical and electro-mechanical systems,

and even thermionic valve circuits. Chapters 4–7 deal with electrical and mechanical equations for the steady and transient states and for various degrees of freedom. The approach to the Laplace transform included in this section is mainly utilitarian. The technique of using it is lucidly explained, and at one point the author makes a practical comparison between the classical and transform methods.

The mathematical properties of the Laplace transform are greatly enlarged on in the eighth chapter, in preparation for transfer functions in the ninth. The final chapters, 10–12, are devoted to matrices, signal-flow graphs, and feedback theory. Signal-flow graphs are treated very thoroughly; but while the possibility of applying them to various basic valve circuits (as distinct from elaborate systems) is interesting, the merit of the method over the well-established simple use of equivalent circuits is debatable.

In general this book is well-written, lucid, and beautifully produced. It makes a valuable contribution to integrating the treatment of electric circuit and mechanical equations; but while the electrical theme is quite prominent in a fundamental sense, it is not elaborated sufficiently to interest the electrical specialist in many other respects. Nevertheless, the book may be recommended strongly to the student of control-system engineering, for whereas it does not deal in detail with particular systems, the fundamental concepts are covered more thoroughly than is usually possible in works specifically on control engineering. F.E.R.

Radio Valve Data (7th Edn)

Compiled by the staff of *Wireless World*. Pp. 156. Published for *Wireless World* by Iliffe Books Ltd., Dorset House, Stamford Street, London, S.E.1. Price 6s. (6s. 10d. by post).

The latest edition of this widely-used reference book has been still further enlarged. It now contains operating data on over 4,800 British and American radio valves, semiconductor devices including transistors and Zener diodes, rectifiers and cathode-ray tubes.

In this edition, the valve-base connection codes are included in the index, as well as being retained in the main table, which allows the user to find the base connections of a valve easily and quickly, without having to refer to the main tables. The book has been completely re-indexed and includes a list of equivalents.

The main tables first of all classify the valves by function (frequency changers, efficiency diodes, etc.) then by manufacturers' names and, finally, into current, replacement or obsolete types.

Cybernetics (2nd Edition)

By Norbert Wiener. Pp. 212 + xvi. Published by The M.I.T. Press and John Wiley & Sons, Inc., Gordon House, Greencoat Place, London, S.W.1. Price 52s.

"Cybernetics" should be read by every educated scientist because its author is one of the outstanding figures of the present generation of scientists. In the 1930s Norbert Wiener made valuable contributions to the generalization of Fourier analysis, so that the relationship between correlation function and power spectrum is generally known as the Wiener-Khintchine theorem; and during the 1939–45 war he established the theory of optimum filtering for the extraction of signals from noise and for the extrapolation of a statistically stationary series ("prediction"). Brought in contact at this time with work on closed-loop automatic-control systems and with Shannon's work on communication theory, he boldly suggested in "Cybernetics" that the combination of statistical mathematics with automatic control and communication theory holds the key also to the major biological and sociological problems.

In Chapter I he points out that the introduction of statistical mechanics, in contrast to Newtonian mechanics, provides an element of irreversibility which fixes the direction of time, and in Chapter II he discusses the theory of groups and the ergodic theorem. Chapter III on "Time Series, Information, and Communication" is heavily mathematical, but there are better books from which to learn the rigorous theory of communication in the presence of noise. The same applies to Chapter IV on "Feedback and Oscillation"; and the chapters on "Computing Machines and the Nervous System" and "Gestalt and Universals" now seem rather naïve after the lapse of 13 years. Chapter VII suggests physical mechanisms for some forms of psychopathology, but these can still be regarded as rather hypothetical; while Chapter VIII reviews the possible application of communication theory and of the theory of games to social organization and the social sciences.

In the second edition he adds two chapters, "On Learning and Self-Reproducing Machines" and "Brain Waves and Self-Organizing Systems". The three major points stressed in these chapters are (i) the essential non-linearity of self-adaptive machines, (ii) the superiority of autocorrelation techniques over spectrum analyses for the accurate delineation of low-frequency spectra (such as those of encephalograms) and (iii) a novel suggestion about the mechanism of self-reproduction of genetic material.

This book is for the *educated* scientist who can take for granted the basic mathematical analyses and concentrate on Wiener's application of them to wider problems. It is also an advantage if the reader has sufficient acquaintance with the biological sciences to realize the boldness of some of the analogies and suggestions. None the less, this is a stimulating book and worth reading.

D.A.B.

Transistors: Principles, Design and Applications

By Wolfgang W. Gartner, Ph.D. Pp. 675 + xii. D. Van Nostrand Co. Ltd., 358 Kensington High Street, London, W.14. Price 94s.

"No electrical engineer can afford to have no knowledge or only slight knowledge of transistor operation and circuitry. . . . This book has been written with the direct intention of providing this knowledge to the student as well as the practising engineer. Organized to provide a suitable textbook for a full year high-undergraduate or low-graduate course, it aims at conveying *all* the concepts and tools needed for original circuit and device design. No attempt has been made, however, to replace the several excellent handbooks available on the subject which are frequently quoted in the text. Rather, we hope that this book provides the introduction and background needed to use these handbooks in original design work."

High Stability Carbon-Film Fixed Resistors: D.C. Failure in Moist Atmospheres

By I. D. L. Bell and R. G. J. Butler. Pp. 10. Published as technical report Z/T124 (18th Jan. 1960) by the Electrical Research Association, Cleeve Rd., Leatherhead, Surrey. Price 7s. 6d. (postage 6d. extra).

CABMA Register 1961-62 of British Industrial Products for Canada

Pp. 620. Published jointly by Kelly's Directories Ltd. and Iliffe Books Ltd., Dorset House, Stamford St., London, S.E.1. Price 15s. post free.

NATIONAL BUREAU OF STANDARDS

Climatic Charts and Data of the Radio Refractive Index for the United States and the World

By B. R. Bean, J. D. Horn, and A. M. Ozanich, Jr. Pp. 178. Available from the Superintendent of Documents, U.S. Government Printing Office, Washington 25, D.C., U.S.A.
Price $2·00 (plus 50 cents postage).

BRITISH STANDARDS

Crimped Joints (Non-insulated) for General Purpose Electrical Cables for Aircraft

Pp. 8. British Standard G.178. Price 6s.

This Standard provides details of the requirements of aircraft constructors and operators for crimping non-insulated connections for general-purpose electrical cables for aircraft.

Schedule of Letter Symbols for Light-Current Semiconductor Devices (Mainly for use in catalogues and similar technical literature).

Pp. 16. B.S. 3363: 1961. Price 5s.

Beryllium Copper Crinkle Washers

B.S.3401: 1961. Pp. 6. Price 3s.

"This specification covers washers in sizes suitable for use with screwed fasteners from 10 B.A. (American No. 0) to ¾ in. nominal diameter."

These publications are available from British Standards Institution, 2 Park Street, London, W.1.

MEETINGS

I.E.E.

6th *November*. "The General Problems of P.M. Multi-Channel Communications", by R. G. Medhurst, B.Sc.

14th *November*. "Tracking in Irradiation", by N. Parkman.

15th *November*. "The Performance of Transistor Portable Receivers."

16th *November*. "The Design and Performance of High- and Low-Voltage Terminal Boxes", by K. K. Schwarz, M.A.

20th *November*. Discussion on "Electrical Accidents and their Causes, including the Legal Aspects", opened by S. J. Emerson, O.B.E., M.Eng.

21st *November*. Discussion on "The Precision Required in the Calibration of Industrial Instruments", opened by F. W. Clifford and A. Fellon, B.Sc.(Eng.).

22nd *November*. "Electronic Analogue Computer Simulation of Multi-Machine Power System Networks", by S. S. Akhtar, M.Sc., Ph.D. "Analysis of Overall Stability of Multi-Machine Power Systems", by J. G. Miles, B.Sc(Eng.).

23rd *November*. Discussion on "The 57 Effects of an Electrical Current", opened by G. S. Brown, Ph.D., B.Sc.(Eng.), at 6 o'clock.

29th *November*. "Recent Developments in Semiconductor Devices and their Applications", by E. Wolfendale, B.Sc.(Eng.).

4th *December*. Discussion on "Backward Waves in Waveguides", opened by P. J. B. Clarricoats, B.Sc.(Eng.), Ph.D., R. A. Waldron, M.A., and G. H. B. Thompson.

These meetings will be held at the Institution of Electrical Engineers, Savoy Place, Victoria Embankment, London, W.C.2, and will commence at 5.30 unless otherwise stated.

Brit. I.R.E.

8th *November*. "Electronics in Chromatography," by E. L. Gregory and E. A. Piper.

15th *November*. "Infra-Red Applications in Navigation," by C. M. Cade.

22nd *November*. Symposium on "Adaptive Optimizing Control".

29th *November*. "An Experimental Assessment of Loudspeaker Performance", by R. Yorke, B.Sc.(Eng.).

These meetings will be held at the London School of Hygiene and Tropical Medicine, Keppel Street, London, W.C.1, and will commence at 6 o'clock.

The Television Society

9th *November*. "The Colourimetric Requirements of Monochrome Television Phosphors: When Is Your White Screen White?", by C. G. A. Hill, B.Sc., A.R.C.S.

24th *November*. "Television Distribution by Wire: Factors Influencing the Choice of System," by A. Cormack, B.Sc., A.M.I.E.E., G. J. Hunt, M.I.E.E., R. P. Gabriel and R. E. Billham.

These meetings will be held at the Cinematograph Exhibitiors' Association, 164 Shaftesbury Avenue, London, W.C.2, and will commence at 7 o'clock.

The Radar and Electronics Association

9th *November*. "Space Communications," Part II: Orbits and their Economics," by W. F. Hilton, D.Sc., Ph.D., F.R.Ae.S., F.B.I.S., to be held at the Royal Society of Arts, John Adam Street, W.C.2, at 7 o'clock.

The Society of Instrument Technology

6th *November*. "Semiconductor Diodes and Rectifiers in Control Engineering," by P. R. Wyman, B.Sc.(Eng.). "The Transistor in Control Engineering," by G. D. Bergman, B.Sc., Ph.D., to be held at Manson House, 26 Portland Place, London, W.1, at 7 o'clock.

The Institute of Navigation

17th *November*. "The Navigation and Guidance of Supersonic Aircraft," by Captain William L. Polhemus, U.S.A.F., to be held at the Royal Institution of Naval Architects, 10 Upper Belgrave Street, London, S.W.1, at 5.30.

The Institution of Electronics

16th *November*. "Developments in Tunnel Diode Technology," by I Aleksander, B.Sc.(Eng.), Graduate I.E.E., and M. R. McCann, Grad.Brit.I.R.E., to be held at 7 o'clock in the Manson Theatre, the London School of Hygiene and Tropical Medicine, Keppel Street, Gower Street, London, W.C.1.

The Institute of Physics and The Physical Society

14th *November*. "Electron Beam Parametric Amplifiers," to be held at 5.30 at 47 Belgrave Square, London, S.W.1.

MARCONI APPOINTMENTS

The Hon. George Nelson, M.Inst.C.E., M.I.Mech.E., M.I.E.E., has been appointed Chairman of Marconi's Wireless Telegraph Company Limited. He succeeds **Lord Nelson of Stafford**, who remains a Director of the Company.

Sir Gordon Radley, K.C.B., C.B.E., Ph.D., M.I.E.E., has been appointed Deputy Chairman. Sir Gordon also becomes Chairman of three associate Companies, namely, the Marconi International Marine Communication Co. Ltd., Marconi Instruments Ltd., and the English Electric Valve Co. Ltd. He succeeds **Lord Nelson of Stafford** in these three posts.

Mr. F. N. Sutherland, C.B.E., M.A., M.I.E.E., Managing Director of Marconi's Wireless Telegraph Company Limited, has additionally been appointed Deputy Chairman of Marconi Instruments Ltd. In this post he succeeds the **Hon. George Nelson**, who has retired from the Board of Directors.

Dr. E. Eastwood, M.Sc., Ph.D., M.I.E.E., Director of Research at the Marconi Research and Development Laboratories, has additionally been elected a Director of Marconi Instruments Ltd.

I.C.T.—R.C.A. AGREEMENT

The International Computers and Tabulators Ltd. have announced an agreement with the Radio Corporation of America for the non-exclusive exchange of technical information and patents in the field of data processing.

This arrangement between these two companies will permit the reciprocal purchase of equipment, thus enabling I.C.T. to expand its range of computing machines.

RACAL CHANGE NAME

The broadening field of their activities in recent months has prompted Racal Engineering of Western Road, Bracknell, to change their name to Racal Electronics Ltd.

STANDARD-FREQUENCY TRANSMISSIONS

(Communication from the National Physical Laboratory)

Deviations from nominal frequency for September* 1961

Date 1961 September	MSF 60 kc/s 1500 U.T. Parts in 10^{9}	Droitwich 200 kc/s 1030 U.T. Parts in 10^{9}
1	— 15·1	— 8
2	NM	— 10
3	NM	— 11
4	— 14·8	— 9
5	— 15·0	— 10
6	— 14·9	— 10
7	— 15·1	— 9
8	— 15·3	— 11
9	— 15·1	— 10
10	— 15·0	— 12
11	— 14·8	— 13
12	— 15·0	— 14
13	— 14·7	— 14
14	— 14·9	— 14
15	— 14·9	— 15
16	— 14·9	— 16
17	— 14·7	— 18
18	— 14·8	— 17
19	— 15·0	— 17
20	— 15·4	— 18
21	— 15·0	— 20
22	— 14·9	— 20
23	— 14·7	— 21
24	— 14·6	— 20
25	— 14·5	— 20
26	— 15·1	— 20
27	— 15·0	— 21
28	— 14·9	— 21
29	— 15·2	— 24
30	— 15·2	— 24

* *Nominal frequency corresponds to a value of* 9 192 631 770 c/s *for the caesium F,m* (4,0) — *F,m* (3,0) transition at zero field. *NM = Not Measured.*

New Products

Rugged 30-Mc/s Oscilloscope

A rugged oscilloscope which has been designed by Hewlett-Packard to meet exacting U.S. military requirements with regard to shock, vibration, humidity and temperature effects is now available in the U.K.

This is the Model 170A which uses various plug-in amplifiers for both the X and Y

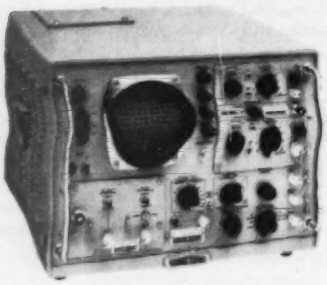

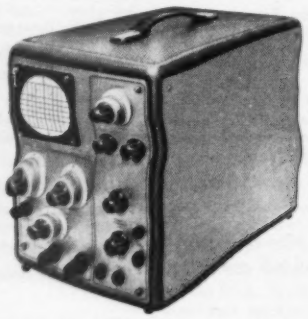

channels to modify the performance for specialized investigations. When fitted with the Model 162A Dual Trace Amplifier the Y-channel sensitivity is 20 mV/cm and the bandwidth is d.c. to 25 Mc/s; the general-purpose amplifier Model 170A provides a bandwidth of d.c. to 30 Mc/s at a lower sensitivity. Other plug-in units include Model 166C Display Scanner which enables permanent records of repetitive waveforms to be made on an X–Y Plotter and the Model 166D Sweep Delay Generator for delaying the sweep from 2 μsec to 10 sec as well as allowing observations of low- and high-speed phenomena on the same trace.

The oscilloscope has 24 calibrated sweep rates from 0·1 μsec/cm to 5 sec/cm, accurate to 3%, which together with a seven-range magnifier provide a maximum sweep speed of 0·02 μsec/cm. Other facilities incorporated in the instrument include the provision of an internal calibrator supplying accurate voltages from 0·2-mV to 100-V peak, an automatic beam finder, and versatile triggering arrangements.

Distributed in the U.K. by

Livingston Laboratories Ltd.,
31 Camden Rd., London, N.W.1.

General-Purpose Oscilloscope

A low-cost 3-in. oscilloscope with a constant bandwidth of d.c. to 10 Mc/s (−3 dB points), a maximum sensitivity of 100 mV r.m.s./cm and an input impedance of 1 MΩ shunted by 20 pF has been introduced recently by Dartronic Ltd., a newcomer to the oscilloscope market in the U.K.

This instrument is known as Model 381, it has nine switched ranges on the Y-input attenuator from 0·1 V r.m.s./cm to 50 V r.m.s./cm with an additional control to provide continuously variable adjustment between the steps. The time base is also controlled in nine switched steps augmented by a continuously variable control; the ranges covered are from 2·4–0·55 μsec/cm to 0·7–0·15 sec/cm, flyback is suppressed on all ranges. The X-amplifier has a sensitivity range of 0·3 V r.m.s./cm to 2 V r.m.s./cm and a bandwidth of 2 c/s to 400 kc/s (−3 dB).

Trace expansion is provided whereby the trace can be expanded to at least seven screen diameters with sufficient X shift being available to view a completely expanded trace throughout its whole length.

For synchronization a 4-position switch permits synchronization from positive- or negative-going portions of sine or square waves. The control is effective for both internal and external sync.

The instrument operates from a 200–250 V, 50–100 c/s mains supply.

Dartronic Ltd.,
3–7 Windmill Lane,
London, E.15.

P.T.F.E. Chassis Terminals

Two additional feedthrough p.t.f.e. chassis terminals have recently been announced by Sealectro; both terminals are designed for 'press-fit' fixing.

The first is type FT-500 T1, which is basically a p.t.f.e. mounting bush with a threaded stud projecting from one end and a plain stud projecting from the other end. A screwdriver slot is provided in the threaded stud to facilitate holding the mounted terminal while tightening the terminal nut. The overall length is 0·743 in. and the mounting bushing diameter is 0·171 in.

The second terminal is type RFT-SM-18-TUR-L2. This is a sub-miniature feedthrough chassis terminal, for 'press-fit' fixing, with one end of the stud projecting in the normal way along the axis of the bushing and the other end of the stud projecting, but bent through 90°. The overall height is 0·378 in. and the bushing diameter is 0·148 in.

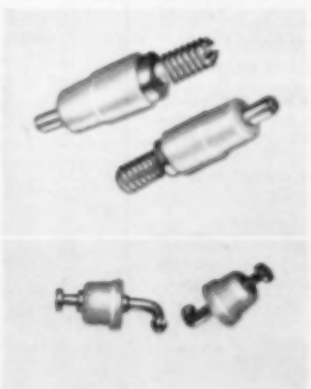

Sealectro Corporation,
Hersham Factory Estate,
Walton-on-Thames, Surrey.

Quadrupole Amplifier

English Electric have announced the introduction of a 400-Mc/s quadrupole amplifier ('Adler tube') for use in applications where a very low noise figure is a necessity.

Known as the type N1044, it has a gain of 20 dB with a bandwidth of 50 Mc/s (−3 dB points) and a noise figure of less than 2 dB over a bandwidth of at least 25 Mc/s. Operating at a centre frequency of 408 Mc/s the tube has a saturation output power of 50 μW.

The tube is fitted with a focusing solenoid and can be supplied complete with an associated stabilized power supply. Metering facilities are provided on the front panel to enable the tube beam current, cathode current, structure current and the electrode voltages to be measured. Controls enabling the pump level and pump frequency to be

adjusted over set limits are also brought out to the front panel.

English Electric Valve Co. Ltd.,
Chelmsford, Essex.

Voltage–Current Calibrator for C.R.Os.

A voltage–current calibrating unit that has been designed primarily for use in conjunction with oscilloscopes has been announced by Rese Engineering, Inc., U.S.A.

This is the Model 1082 which is basically a comparator-type signal-measuring instrument. When operating as a signal comparator it provides a calibrated positive or negative reference-voltage signal, which is fed to a built-in 400-c/s chopper. The unknown signal to be measured is also fed to the chopper, the output of which is displayed on a c.r.o. With the chopper alternately sampling the reference voltage and then the unknown, an effective superimposition of the reference voltage and unknown signal is presented on

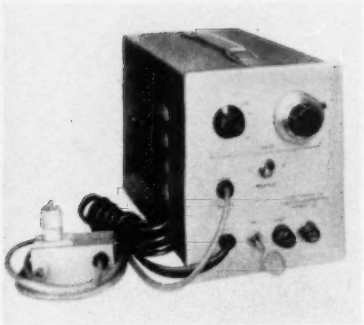

the c.r.t. To measure the unknown signal, the value of the reference voltage is changed until the trace which it generates on the c.r.t. coincides with the peak of the unknown. The peak value of the unknown signal is then read from a precision ten-turn potentiometer.

The sensitivity of the unit is 1 mV, the bandwidth is over 100 Mc/s, and the output accuracy is 0·1% full scale; power requirements are 105 to 125 V, 50/60 c/s, 15 W.

Distributed in the U.K. by

Scientific Furnishings Ltd.,
Poynton, Cheshire.

Portable Sound Level Indicator

The latest addition to the Dawe range of instruments is a pocket-sized sound-level indicator Type 1408D which uses transistors and is powered by a 9-V battery.

The indicator covers the sound-level range 64 to 110 dB (above the standard sound-

pressure level of 0·0002 dyne/cm²), employs a built-in crystal microphone, and utilizes circuits providing the three standard weighting curves A, B, and C to the I.E.C. specification. A four-step attenuator covers the range 70 to 100 dB in 10-dB increments.

Measuring 6 in. × 3 in. × 2¼ in., the unit weighs only 14 oz.

Dawe Instruments Ltd.,
Western Avenue, London, W.3.

1-kW H.F. Linear Amplifier

A 1-kW h.f. Linear Transmitting Amplifier has been added to the range of Plessey telecommunications equipment. The unit is suitable for operation within the frequency range 1·6 Mc/s to 27·5 Mc/s at temperatures from 55 °C to −15 °C and is capable of delivering a power output of 1 kW (p.e.p.)

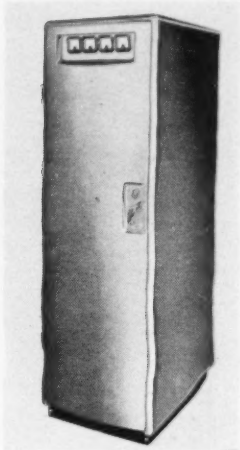

into a 50-Ω balanced line. The bandwidth is 12 kc/s.

The amplifier consists of an r.f. unit, a power unit and a control unit, with provision for incorporating a driver or converter unit.

Meeting the general requirement of I.C.A.O., DEF500 and I.S.T.C. specifications, the unit is designed to operate from power supplies of 100–120 V and 200–250 V, 40–60-c/s single phase. Power consumption is approximately 5 kVA for full-power single-tone operation.

The Plessey Co. Ltd.,
Ilford, Essex.

L.F. Signal Generator

The latest addition to the Airmec range of instruments, the l.f. signal generator type 252, has been designed for the generation of pure and stable sine-wave signals in the frequency range 30 c/s to 30 kc/s.

In conjunction with a step attenuator the output control enables the output level to be set to any value from less than 1 mV to 15 V open-circuit with an accuracy of ± 0·2 dB per step ± 0·3 dB overall. Output level variation over the whole frequency range of the instrument is approximately ± 0·5 dB, rising to ± 1 dB on the 0-dB attenuator setting with a 600-Ω resistive load. A screened and balanced output transformer provides either balanced or unbalanced outputs at an impedance of 600 Ω and the circuit design is such that the output impedance remains constant regardless of frequency and attenuator setting.

Long-term frequency stability is better than 0·1% ± 1 c/s over the frequency range, and stability with supply voltage variation is 0·02% (approximately) at 1 kc/s for a variation of 10%.

Airmec Limited,
High Wycombe, Bucks.

Form Error-Measuring Instrument

Elliott Brothers have announced the Elliott 'Rondell' Form Error Measuring Instrument which measures not only the roundness errors of an object but also errors in concentricity, in perpendicularity, in parallelism and in axial alignment, to within 3 micro-inches.

The instrument consists basically of an ultra-precision bearing which defines a reference axis and a reference plane for the measurement of the object under test, and enables the exact relationships between its various surfaces to be determined. Surfaces are examined by means of an electrical pick-off probe the output from which is amplified

and displayed on a meter or recorded on a polar chart; both the meter and polar chart are built into the instrument.

Elliott Brothers (London) Ltd.,
34 Portland Place, London, W.1.

Variable Phase Standard

A Gertsch variable phase standard which allows the phase between two internally-generated voltages to be shifted to any desired angle with an accuracy of ± 0·05° is now available in the U.K. through Wayne Kerr.

Known as VPS-1, it operates over three

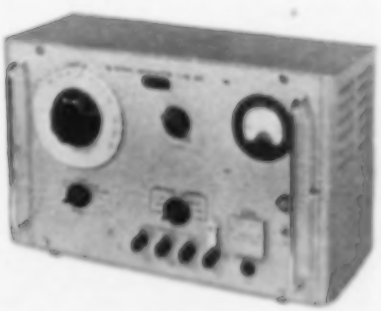

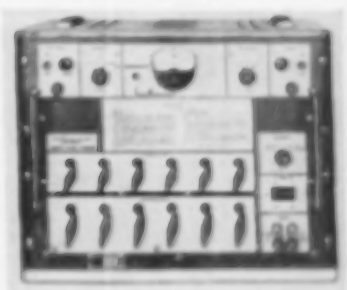

adjustable frequency ranges between 150 and 3,000 c/s and generates two voltages of equal amplitude differing in phase by any angle from 0° to 360°. The reference voltage has a fixed amplitude of 50 V r.m.s. while the vector output, which may be displaced in phase in increments of one minute of arc, has a maximum amplitude of 50 V r.m.s. and can be attenuated in 50-mV steps.

The instrument is entirely self-contained, requiring no external equipment for calibration or operation, and is available in a case or ready for rack mounting.

Wayne Kerr Laboratories Ltd.,
44 Coombe Road,
New Malden, Surrey.

High-Voltage Silicon Rectifiers

Two ranges of high-voltage medium-power silicon diodes are now available from Westinghouse. These are the series SXBR8 and SXBR25 which are rated at 18 and 30 A respectively; the SXBR8 may be used at

case temperatures up to 140 °C and the SXBR25 may be used at similar case temperatures. Both types are available in ten voltage ratings from 100 to 1,500 V peak.

The diodes are hermetically sealed using glass-to-metal seals and mounting in by means of a stud base which also serves as the anode connection; the cathode connection is made by means of an insulated flexible lead through the glass-to-metal seal.

Westinghouse Brake & Signal Co. Ltd.,
82 York Way, London, N.1.

Vernier-Dial Assemblies

A range of panel-mounted dial assemblies which have been designed for the accurate angular positioning of synchros, resolvers, potentiometers, etc., has been announced by Theta.

The basic unit is model DA which has a range of 0° to 360° continuous, a setting accuracy of 0·1°, a readability of 0·1° and a vernier control with two ratios of 10:1 and 1:1; the outside diameter of the dial is 5 in.

For the mounting of the servo devices to the dial, tapped holes are provided in the body of the dial and a spring-loaded split collet is used to grip the shaft.

Dial assemblies are available for servo devices of houses size 8, 10, 11, 15, 18 and 23, with nominal shaft diameters of 0·09, 0·12, 0·125, 0·1875, 0·2405 and 0·25 in.

Theta Instrument Corporation,
520 Victor Street,
Saddle Brook, N.J., U.S.A.

U.H.F. Dummy Load

The development of two precision high-power u.h.f. dummy loads has been announced by Weinschel Engineering, U.S.A.

These terminations, Models 569 and 624 are constructed with black anodized aluminium bodies and stainless steel Type 'N'

connectors. They are designed to dissipate heat efficiently and can handle an input power of 20 W c.w. with a 6-kW peak pulse power. The Model 624 covers a frequency range of 400 to 500 Mc/s and the Model 569 has a range of 1,200 to 1,400 Mc/s. The maximum v.s.w.r. over the frequency and power ranges is 1·05.

The units are 4¾ in. long × 1⅛ in. diameter.

Weinschel Engineering Co.,
Kensington,
Maryland, U.S.A.

Power Transformer Primary

The Farnell 'Primatran' is basically a power transformer primary winding which has been designed so that a secondary winding or a number of secondary windings can easily be added to provide any alternating voltage.

The transformer operates from an input

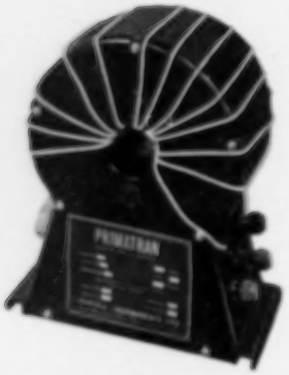

voltage of 220–250 V, 50–60 c/s and has an output rating of 250 VA (continuous) and 350 VA (intermittent). The secondary turns per volt ratio is 3:1.

When used as a current transformer the Primatran has an accuracy to Class C. BSS.81/1936 at 15 VA.

Farnell Instruments, Ltd.,
Light Industrial Estate,
York Rd., Wetherby, Yorks.

Automatic A.C. Stabilizer

A compact power unit which has been designed to provide rapid and accurate stabilization of a.c. supplies of 47–65 c/s has been announced by Claude Lyons. This is the Type TS-1 A.C. Automatic Voltage Stabilizer which gives an output of either approximately 1 kVA or 2 kVA depending upon the range of input-voltage variations over which the stabilizer is required to operate.

The output of the unit can be adjusted between 200 and 250 V a.c. in 10-V steps and it can be set to stabilize any one of six input-voltage variation ranges of −17½% to 7½%, ± 12½%, −7½% to 17½%, −8¾% to 3¾%, ± 6¼%, or −3¾% to 8¾% about the output voltage setting. When connected to handle any of the first three input-voltage variation ranges (a total variation of 25%) the possible output is approximately 1 kVA and when set to handle the last three input-

voltage variation ranges (a total variation of 12½%) the possible output is approximately 2 kVA.

From zero to full load the correction accuracy is better than ± 0·5% and the speed of correction is 40 V/sec.

Claude Lyons Ltd.,
Valley Works,
Ware Road, Hoddesdon, Herts

A BRILLIANT NEW

1 kVA VOLTAGE STABILISER

TYPE

TS-1

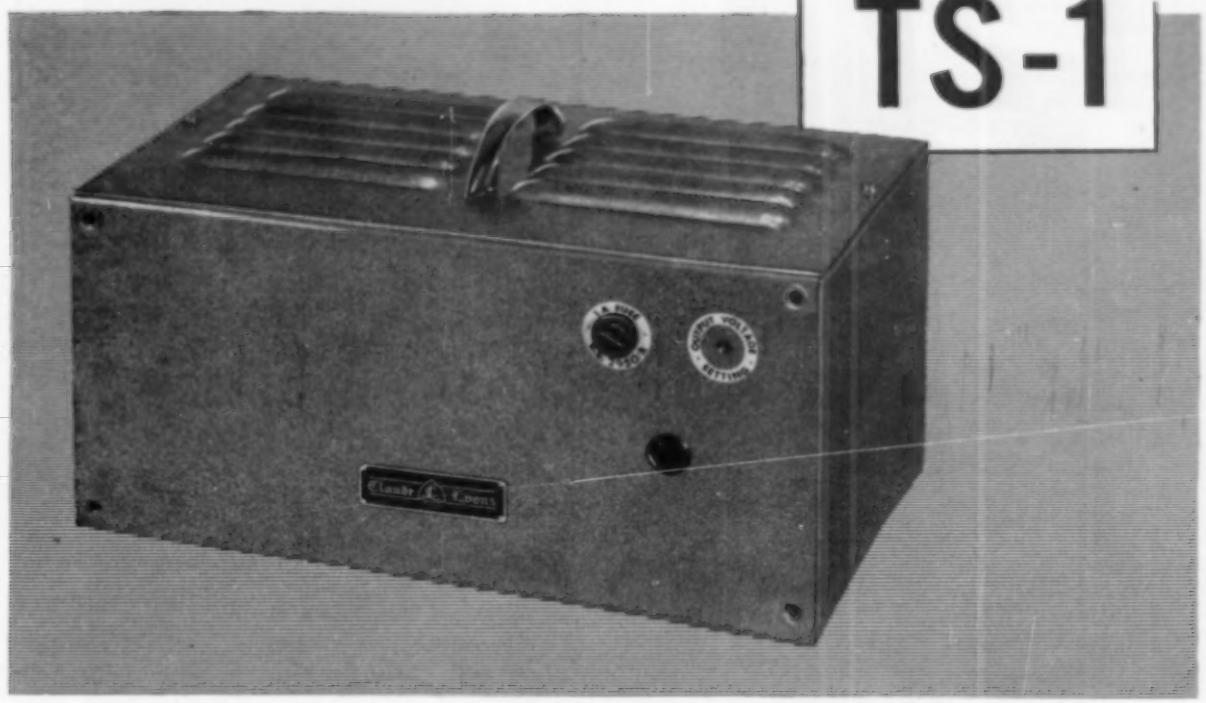

FAST 40 volts/sec correction speed

ACCURATE Better than ±0·5%

RELIABLE Transistorised control unit—no valves or relays

The TS-1 is something entirely new in the field of A.C. voltage stabilisation. This light and compact 1 kVA unit provides rapid, accurate and distortionless stabilisation over an input voltage range of 25%. Alternative connection gives 2 kVA output with 12½% input range.

Output is unaffected by variations in supply frequency, load current (zero to full load) or load power factor. Indoor tropical rating is standard. Cabinet model (readily adaptable for wall or chassis mounting) or rack model.

PRICE—ONLY **£69·10 net**

Rack Model **£72·5 net**

Claude Lyons Ltd.

VALLEY WORKS · HODDESDON · HERTS TEL: HODDESDON 4541 (6 lines)
76 OLDHALL STREET · LIVERPOOL 3 · LANCS · TEL: CENTRAL 4641/2

CL63/1A

ADCOLA
(Regd. Trade Mark)

Soldering Instruments and Equipment

Illustrated

INSTRUMENT L64 WITH COMBINED PROTECTIVE UNIT L700 SHOWING WIPER/ABRASION PAD AND SOLDER REEL

ALL VOLT RANGES 6/7 to 230/50 VOLTS

British & Foreign Pats. & Reg. designs.

Traditional British Quality and Workmanship

ADCOLA PRODUCTS LIMITED

Head Office, Sales and Service
ADCOLA HOUSE, GAUDEN ROAD, LONDON, S.W.4
Telephones MACAULAY 3101 & 4272
Telegrams SOLJOINT LONDON S.W.4
AUSTRALIAN OFFICE: 420 ST. KILDA ROAD, MELBOURNE, S.C.2

THE NATION'S REMEMBRANCE

POPPY DAY

Collectors urgently needed
British Legion · Haig's Fund
29-69 York Way · London · N.1
(Registered under the War Charities Act, 1940)

The first comprehensive survey
Transmission · reception · servicing

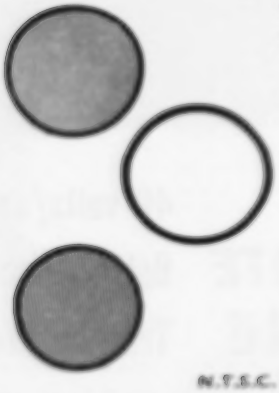

COLOUR TELEVISION

N.T.S.C. System, Principles and Practice

P. S. Carnt, B.Sc.(Eng.), A.C.G.I., A.M.I.E.E.,
and G. B. Townsend, B.Sc., F.Inst.P., M.I.E.E., A.K.C.

A comprehensive survey of the British adaptation of the American N.T.S.C. system. Introductory chapters enable the reader to understand the principles of colour measurement and the behaviour of the human eye in relation to colour reception. Most aspects of the transmission and reception of colour signals are discussed. For the service engineer, chapters on fault finding have been included. Block diagrams, which are given as well as full circuits, explain the connection between the various component units.

85s. net by post 87s. 3d. 487pp. illustrated

from leading booksellers

Published for "Wireless World" by **ILIFFE Books Ltd.**
DORSET HOUSE STAMFORD STREET LONDON S.E.1

Quartz Crystal Ovens

STABLE TEMPERATURE ENSURING MAXIMUM FREQUENCY STABILITY

Switching differential 0·0014°C.
No thermostat
No thermometer switch

Orthodox crystal ovens, using thermostats or thermometer switches, are available for applications where wider temperature variations are acceptable.

This symbol has been adopted by the Marconi Specialized Components Group. The Marconi Company undertakes the design and manufacture of specialized components only when no suitable alternative is available; and in almost every case, Marconi specialized components are designed to more exacting standards and built to closer tolerances than any similar components. A preliminary catalogue is available, listing ferrite isolators and circulators, coaxial connectors, attenuators, terminations and switches; waveguide filters, terminations, and bends; crystal filters and ovens.

MARCONI

SPECIALIZED RADIO COMPONENTS

Write for details of crystal ovens and other specialized components in the Marconi range, and address your enquiries to:

SPECIALIZED COMPONENTS GROUP

MARCONI'S WIRELESS TELEGRAPH COMPANY LTD.,
CHELMSFORD, ESSEX, ENGLAND

Samicanite AND Samicafolium

ELECTRICAL INSULATION MADE FROM

SAMICA

"SAMICA" is mica paper having a high degree of uniformity in both electrical and mechanical characteristics. Samicanite and Samicafolium are insulating materials prepared by impregnating "Samica" with high grade bonding agents, with or without the addition of backing material.

TAPE Samicanite tapes can be supplied impregnated with silicone, epoxide, polyurethane or alkyd resins and backed with glass fabrics either 0.001" or 0.002" in thickness.

FLEXIBLE MATERIAL Flexible Samicanite is available in various combinations with presspaper, "Melinex", "Terylene", glass fabrics and Empire varnished materials. They may be bonded with silicone, epoxide, polyurethane or alkyd resins.

FOLIUM Samicafolium is available with either shellac or epoxide bond.

MOULDING MATERIAL Various grades of moulding Samicanite are available with shellac, silicone or epoxide bond.

BOARD Hard Samicanite boards are manufactured with epoxide, silicone or alkyd bond.

TUBES AND MOULDINGS These are manufactured from Samicanite with various bonds including shellac, epoxide and silicone.

Insulating materials based on "SAMICA" are available in Great Britain, Northern Ireland, Eire and most of the British Commonwealth through The Micanite & Insulators Co., Ltd., the sole licensee for these territories. "Samica" is our registered trade mark. "Melinex" and "Terylene" are registered trade marks of I.C.I.

m and i

MIC

the electrical insulation people

THE MICANITE & INSULATORS CO., LTD.,

Empire Works, Blackhorse Lane, Walthamstow, London, E.17.

'GRAMS: MYTILITE, LONDON, TELEX. TELEX 25183

METEOR COIL WINDERS

(SWISS MADE)

No gears to cause backlash

Suitable for winding wires as small as 0·0004 in. diameter. Arranged for single or multiple winding; layer shortening device available. Traverse is obtained by magnetic clamping on to a non-reversing steel tape with extremely fine reversal settings by micro limit switches. Stops automatically if wire breaks.

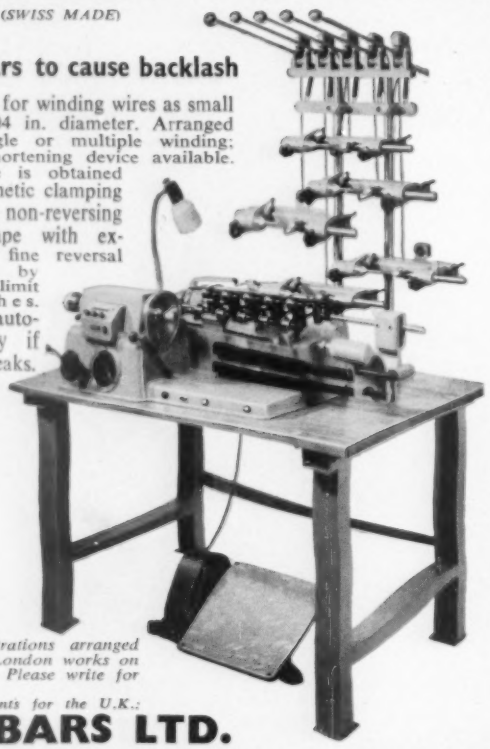

Demonstrations arranged at our London works on request. Please write for leaflet.

Sole Agents for the U.K.:

ACBARS LTD.

331-3 WALWORTH RD., LONDON S.E.17

RODney 7822 & 7191

STORED ENERGY CAPACITOR DISCHARGE WELD CONTROLLER

The Stored Energy Capacitor Discharge Controller delivers a precise amount of power to the welding electrodes regardless of mains fluctuation. Energy is stored in capacitors which are charged from a built-in stabilised DC supply. This DC supply is infinitely variable for weld power control and each setting can be reproduced within the limits of 1.5%.
Extremely short weld times are available—15 millisecond max. and 3 millisecond min.

HED

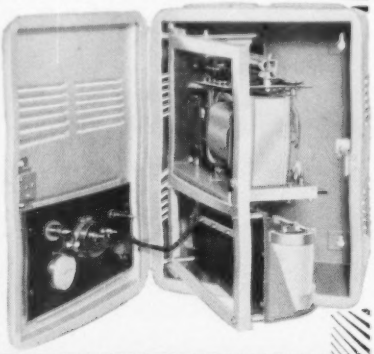

'Hinged book' construction for easy servicing.

Write for leaflet.

HIRST ELECTRONIC LTD.

GATWICK ROAD, CRAWLEY, SUSSEX

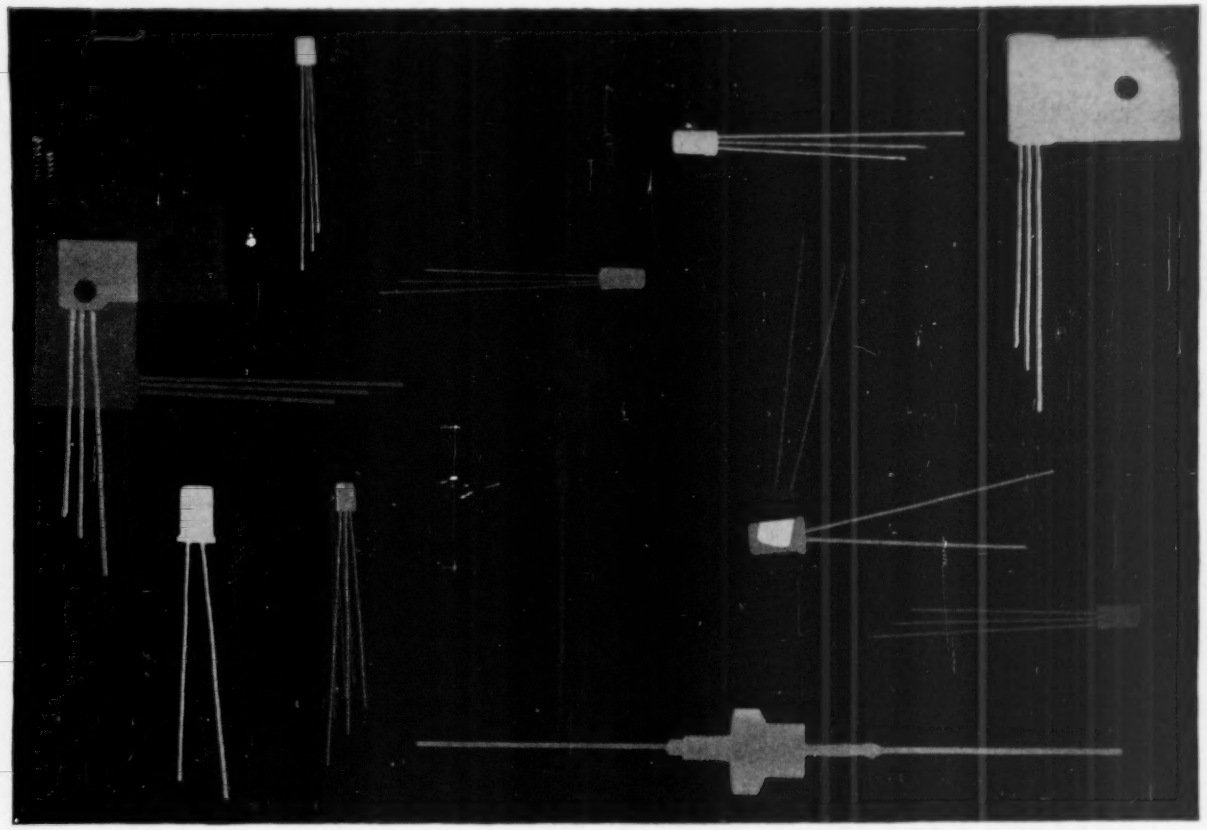

A maze of high quality semiconductors, clearly defined in the Brush literature now available, which shows the tremendous range of Brush semiconductor devices. Supported by Clevite, Shockley and Intermetall research, Brush offers the widest range of semiconductors in this country. Brush quality semiconductors are now in quantity production providing deliveries to fit your production schedules.

Write or 'phone to Semiconductor Division, Brush Crystal Co. Ltd.

BRUSH
CRYSTAL CO. LTD.

SEMICONDUCTORS

Outstanding in the Brush diode range are the following:

Silicon
* Zener and power zener
* Rectifiers
* Sub-miniature

Germanium
* Co-axial glass
* Single end metal
* Fast switching

HYTHE · SOUTHAMPTON · HANTS · Phone: HYTHE 3031

ANNOUNCING A NEW INTERNATIONAL JOURNAL FROM THE ILIFFE GROUP

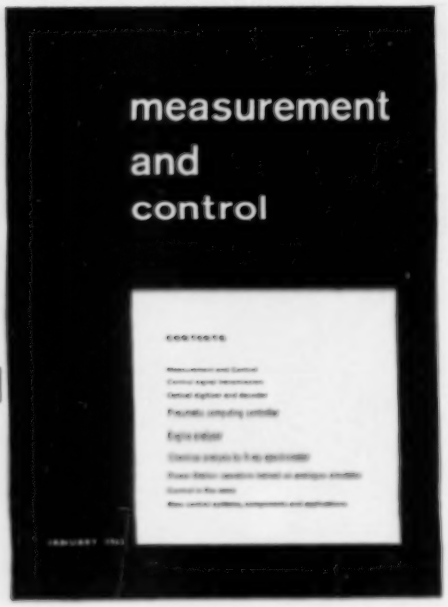

measurement and control

To be published monthly beginning in January 1962

Instruments, systems, methods . . . of industrial control

MEASUREMENT AND CONTROL—first issue January 1962—is designed for those responsible for the choice, installation, operation and maintenance of automatic control equipment in all branches of industry.

Each month, MEASUREMENT AND CONTROL will report, analyse, and interpret in a practical down-to-earth manner the world's latest installations, instruments, equipment, systems—every facet of this new major science.

Produced by highly qualified engineers, writers and Iliffe's unique team of illustrators, MEASUREMENT AND CONTROL is a progressive journal for progressive people. In a world of fiercely growing competition it will be a major influence in the progress of large and small organizations to higher peaks of more efficient production.

a new journal from ILIFFE—world leaders in technical and specialist publishing

SECURE THIS NEW SERVICE FROM THE BEGINNING—POST TODAY

To ILIFFE Production Publications Ltd
Dorset House, Stamford Street, London, S E 1

Please enter my subscription as indicated (tick appropriate box on right).

I enclose remittance for _____

Name _____

Company _____

Address _____ Date _____

Post today

One year

- ☐ 12 issues including postage .. £3. 0. 0
- ☐ U.S. and Canada $9.50
- ☐ Special student rate (for registered students and apprentices only) £1.10.0

Three years (overseas only)
saving cost of 12 issues

- ☐ 36 issues including postage .. £6. 0. 0
- ☐ U.S. and Canada $19.0

Multiple orders from the same company enjoy a bulk discount rate: i.e. 3-10 subscriptions, 10%; over 10 subscriptions, 20%.

Electronic technology

Press date for the December 1961 issue is first post 22nd November 1961

CLASSIFIED ADVERTISEMENTS

Advertisement Rates. *6d. per word, minimum charge 6/- each paragraph charged separately. Remittances payable to "Electronic Technology," Dorset House, Stamford St., S.E.*1. *Series discount 15% is allowed for 12 consecutive insertions.*

Box Numbers *are available at an additional charge of 2/- to defray cost of registration and postage. Replies should be addressed Box No. 0000, c/o "Electronic Technology," Dorset House, Stamford Street, London, S.E.*1.

Semi-Display *advertisements with centralized lines £1/15/- per single column inch—no additional charge for Box Numbers. The Publishers are not responsible for clerical or printers' errors although every care is taken to avoid mistakes.*

TENDERS

GENERAL POST OFFICE

THE Postmaster-General offers for sale a quantity of E.D.T. Crystals lying at the Post Office Supplies Department Depot, Kidbrooke Park Road, London, S.E.3.

APPLICATIONS for forms of tender should be made to:

DIRECTOR OF CONTRACTS,
POST OFFICE CONTRACTS DEPARTMENT
(DISPOSALS),
TELEPHONE HOUSE,
TEMPLE AVENUE,
LONDON, E.C.4. [1496

SITUATIONS VACANT

ROYAL NAVAL SCIENTIFIC SERVICE
GOVERNMENT COMMUNICATIONS
HEADQUARTERS
Oakley, Priors Road, Cheltenham

Vacancies for Senior Scientific Officers and Scientific Officers.

APPLICATIONS are invited from graduates and postgraduate research workers as follows:

PHYSICISTS (with an interest in telecommunications, electronics or computing).

MATHEMATICIANS.

ELECTRICAL ENGINEERS (Radio and Electronics).

CANDIDATES must normally be natural born British subjects of natural born British parents with 1st or 2nd class hons. degrees or equivalents. S.S.O.s must have min. 3 years' post-graduate experience and be not less than 26 years of age.

SALARIES: S.S.O. £1,342/£1,654 (National); S.O. £738/£1,222 (National).

APPOINTMENTS unestablished (with F.S.S.U. benefits) but opportunities exist for those between the ages of 21 and 32 to compete for established posts.

THERE are also vacancies for supporting staff in the Experimental Class. Candidates should possess G.C.E. Advanced Level in 2 Science or Maths. subjects plus 3 subjects at "O" Level; a Pass Degree, H.N.C. or equiv. quals.

SALARIES: Exp. Officer £1,087/£1,336 (National). Asst. Exp. Officer £458 (age 18) (National); £801 (age 20)–£981 (National).

FORMS from Ministry of Labour Technical and Scientific Register (K), 26 King Street, London, S.W.1, quoting A.405/18. Closing date November 16, 1961. [1408

THE UNIVERSITY OF SHEFFIELD
DEPARTMENT OF PHYSICS

A Research Assistant is required to take part in a Space Research Project under Dr. T. R. Kaiser. The work will involve the development of instruments for installation in rockets and satellites. A candidate with graduate or equivalent qualifications and appropriate experience in electronic instrument design and construction is required. Salary according to qualifications and experience. Applications, together with the names and addresses of two referees, should reach the Registrar as soon as possible. [1500

LONG-RANGE INDUSTRIAL RESEARCH

THERE are openings for Scientists able to make original contributions to fields such as physical properties of materials, automatic control systems, applications of digital techniques. Publication of results will be encouraged. Contributory superannuation scheme, removal expenses and assistance with rehousing provided.

SEND details of interests, research achievements, and qualifications to:

THE DIRECTOR OF RESEARCH,
RESEARCH CENTRE,
BLOUNTS COURT,
SONNING COMMON, READING. [1495

ASSISTANT TO PLANT MANAGER required. Excellent opportunity for young Physicist interested in production of permanent magnets, development of their application and control of magnetic testing, etc. Write giving full details to Staff Dept., Mures Ltd., Rainham, Essex.

SITUATIONS VACANT

MIDLANDS ELECTRICITY BOARD

THIRD Assistant Engineer (Communications) required in the Chief Engineer's Department at Headquarters.

DUTIES will cover work associated with the design, development, operation and maintenance of wired and radio telephone communications and control systems, together with similar work on other associated electronic and light current equipment. Technical qualifications desirable.

SALARY within the range £1,285–£1,610 per annum, according to qualifications and experience (N.J.B. Schedule "B," Grade 6 BX). Superannuable.

APPLY, by letter, within 14 days, stating age, experience, present position and salary, to The Secretary, Midlands Electricity Board, P.O. Box No. 8, Mucklow Hill, Halesowen, nr. Birmingham.

F. W. CATER,
SECRETARY. [1497

THE ROYAL COLLEGE
OF
SCIENCE AND TECHNOLOGY,
GLASGOW
DEPARTMENT
OF
ELECTRICAL ENGINEERING

APPLICATIONS are invited for the post of Lecturer from those having some experience in design, teaching, or technical sales, in the fields of Telecommunications or in the Application of Electronics in Industry.

THE salary for the post is on the scale £1,050 to £1,850 with F.S.S.U. and family allowances. The Department has excellent facilities for both undergraduate and postgraduate work. [1499

BOOKS, ETC.

"ADVANCED Theory of Waveguides." By L. Lewin. Sets out various methods of treating problems arising in work on this complex subject. The author has selected for discussion a number of topics as representative of the field in which the centimetre-wave engineer is engaged, many of the examples being concerned with the rectangular waveguide. 30s net from all booksellers. By post 31s from Iliffe Books Ltd., Dorset House, Stamford Street, London, S.E.1.

BOOKS, ETC.

"RADIO Circuits: A step-by-step survey." By W. E. Miller, M.A.(Cantab), M.Brit.I.R.E. Revised by E. A. W. Spreadbury, M.Brit.I.R.E., associate editor of WIRELESS & ELECTRICAL TRADER. This established introduction to superheterodyne receiver circuits has been greatly enlarged and brought completely up to date with the inclusion of transistor and f.m. receivers; there are new chapters covering battery receivers and car radio sets, while the modern a.m./f.m. receiver is fully described. Mathematics and obscure theoretical considerations are entirely omitted, and over 90 easy-to-follow circuit diagrams are explained in a simple but practical manner, splitting up the circuit into sections and working from the aerial terminal through to the loudspeakers. 15s net from all booksellers. By post 15s 10d from Iliffe Books Ltd., Dorset House, Stamford Street, London, S.E.1.

"WIRELESS Servicing Manual" (9th Edition). By W. T. Cocking, M.I.E.E. A carefully revised edition of the handbook known since 1936 as an invaluable, comprehensive guide for radio servicemen and others. Completely up to date, it deals in a lucid, practical way with the problems that arise in the repair, maintenance and adjustment of modern wireless receivers. All recent developments in receiving equipment have been incorporated and the servicing of frequency-modulated v.h.f. receivers—a development of great importance to all servicemen—is thoroughly covered in a completely new chapter. Here is a work of proven value to professional and amateur, written by a widely known authority on modern radio engineering. 17s 6d net from all booksellers. By post 18s 8d from Iliffe Books Ltd., Dorset House, Stamford Street, London, S.E.1.

"SECOND Thoughts on Radio Theory." By *Cathode Ray* of WIRELESS WORLD. Forty-four articles reprinted from popular WIRELESS WORLD series, in which the author examines various aspects of elementary radio science, explains them clearly, and shows that there may be more behind them than is apparent from the usual text-book. This volume deals with basic ideas; circuit elements and techniques; circuit calculations; and some matters in lighter mood. An entertaining and helpful text-book for the student, refresher course for the engineer, and reference book for all, combined. 25s net from all booksellers. By post 26s 6d from Iliffe Books Ltd., Dorset House, Stamford Street, London, S.E.1.

COMMONWEALTH OF AUSTRALIA

WEAPONS RESEARCH ESTABLISHMENT

MISSILE ELECTRONICS

The Department of Supply invite applications for the following vacancy at the Weapons Research Establishment, Salisbury, near Adelaide:—

POSITION: HIGHER SCIENTIFIC OFFICER.

SALARY: £2,036/£2,296 (Australian Currency).

DUTIES: To lead a small team undertaking research and development in the field of telemetry required in testing guided missiles.
The duties of the team include:
(a) Development of UHF Diversity receiving and low-noise amplifier techniques;
(b) Coherent methods of detection;
(c) Special magnetic tape recording systems;
(b) Coherent methods of detection.

QUALIFICATIONS: An honours degree in electrical engineering or physics is desirable and experience in at least one of the above fields, and in leading a small research or development team, would be an advantage.

TRAVEL: Under certain conditions, first class air/sea transport for the successful candidate and dependants (wife and dependent children) will be provided by the Commonwealth.

CONTRACT EMPLOYMENT: Consideration may be given to entering into an agreement for a three (3) or five (5) year contract of employment in Australia. In this case the Commonwealth will bear the cost of return fares together with the cost of removing the successful applicant's furniture and effects up to a maximum cost of £500 (Australian): £250 each way.

NOTE: Assistance will be given in obtaining married accommodation.

APPLICATIONS: Forms obtainable from Senior Representative (Av128/6), Department of Supply, Australia House, Strand, London, W.C.2, with whom completed applications should be lodged as soon as possible.

just out

a new comprehensive and scientific treatment of the problem of choosing a career

A study of British industries and the opportunities they offer

INDUSTRY and CAREERS

Compiled with the official support of leading industrial and educational organisations

Foreword by H.R.H. The Duke of Edinburgh. General Editor: D. E. Wheatly, M.A., B.Sc.

Here for the first time is a completely up-to-date and scientific approach to the problem of choice of career. INDUSTRY AND CAREERS will be of the greatest help to young people themselves and to headmasters, careers officers and others who advise them. Every effort has been made to make it as nearly as possible the complete answer to their requirements. Not only does it provide a treatment based on new ideas, but it is unquestionably the most up-to-date and comprehensive book of its kind. The product of five years' research and study, supervised by a distinguished Editorial Advisory Committee, it fills what has long been recognized as a serious gap.

55s. net by post 57s. 9d. over 872pp. inc. 96pp. of charts & illustrations

From leading booksellers

Published by **ILIFFE Books Ltd**

DORSET HOUSE · STAMFORD STREET · LONDON · SE1

Locate Hard to Get Tubes at Big Savings

DIRECTORY and BUYERS' GUIDE

for American Electron Tubes

GET YOUR COPY ABSOLUTELY FREE!

This brand new "Directory" covers almost every tube made by American manufacturers. Top name brands as well as specialized brands are included. Receiving, Television, and Special Purpose tubes are listed by type numbers and low, low prices.

Send for your copy now, it's **FREE** *and will*

Save You Money On Tubes

METROPOLITAN OVERSEAS SUPPLY CORPORATION

1133 Broadway, New York 10, N.Y., U.S.A.

Cable address: LECIMEX, New York.

SHORT-WAVE RADIO & THE IONOSPHERE

By T. W. BENNINGTON, *Engineering Division, BBC*

Long-distance communication by means of short waves is dependent on the state of ionosphere, which changes during the day and at different seasons of the year. This book explains simply the reasons for these changes and shows how they influence the choice of wavelength for signalling between different points of the earth's surface. *Published for the "Wireless World".*

8½" × 5½" 138 pp. 2nd Edition 10s 6d net. By post 11s 4d

Obtainable at all booksellers. Published by

ILIFFE Books Ltd.,

Dorset House, Stamford Street, London, S.E.1

A.I.D. Approval

TRANSFORMERS of all types up to 25 KVA for Single or Three phase operation. Phase conversion, etc.

MAINS Output and Special Purpose Transformers for Radio Equipment, Chokes, etc.

COILS for Connectors, E.M. Brakes, Air Valves, etc. and COIL WINDINGS for all purposes.

SOLENOIDS for A.C. and D.C. Operations.

W. F. PARSONAGE & CO. LTD.
INDUCTA WORKS
Fryers Road, Bloxwich, Walsall
Telephone: Bloxwich 76777-8

For Laboratory, Production Line, Test Departments and Colleges.

LOW COST DECADE RESISTANCE BOXES

ALSO, 4 DECADE STEPPED POTENTIAL DIVIDERS with 10 or 100 ohms input resistance

Write for further information to:

LIONMOUNT & CO. LTD. 40 Hatton Garden, London, E.C.1

Index to Advertisers

	PAGE
Achars Ltd.	14
Adcola Products Ltd.	12
Appointments Vacant	17
Associated Electrical Industries Ltd.	8, Cover iii
British Insulated Callender's Cables Ltd.	Cover ii
Brush Crystal Co. Ltd.	15
Commonwealth of Australia	17
Cossor Instruments Ltd.	2, 3
Ferranti Ltd.	5
Gardners Radio Ltd.	4
Hirst Electronics Ltd.	16
Iliffe Books Ltd.	13
Lionmount & Co. Ltd.	18
Lyons, Claude, Ltd.	11
Mallory Batteries (Commercial) Ltd.	1
Marconi Wireless Telegraph Co. Ltd.	13
"Measurement & Control"	16
Mervk & Co. Inc.	Cover iv
Metropolitan Overseas Supply Corps.	18
Micanite & Insulators Co. Ltd., The	14
Mullard Ltd.	10
Parsonage, W. F., & Co. Ltd.	18
Servomex Controls Ltd.	7
Stratite & Porcelain Products Ltd.	6

Printed in Great Britain for the Publishers, Iliffe Electrical Publications Ltd., Dorset House, Stamford Street, London, S.E.1, by Gibbs & Bamforth, Ltd., St. Albans. Distributed in U.S.A. by Eastern News Company, 500 West 11th Street, New York, 14.

TRIODE TETRODE FOR VIDEO OUTPUT APPLICATIONS

MAZDA 30FL12

The 30FL12 consists of a high slope tetrode with frame grid construction for use in a video output stage, and a general purpose triode.

Higher peak current with an appreciably higher slope is available from the tetrode, as compared with the 30FL1, so enabling adequate video drive to be provided for the cathode ray tube, with anode loads down to 4,700 ohms. This low value of load eases the problems of HF video compensation.

The triode has identical characteristics to the 6/30L2.

Heater current (amps)	I_h	0.3
Heater voltage (volts)	V_h	9.8

TENTATIVE RATINGS AND DATA

Maximum Design Centre Ratings

		Triode	Tetrode
Anode Dissipation (watts)	$P_{a(max)}$	1.5	2.5
Screen Dissipation (watts)	$P_{g2(max)}$	—	0.8
Anode Voltage (volts)	$V_{a(max)}$	250	250
Screen Grid Voltage (volts)	$V_{g2(max)}$	—	250
Heater to Cathode Voltage (volts rms)	$V_{h-k(max)}$	—	150*

*Measured with respect to the higher potential heater pin.

Inter-Electrode Capacitances†(pF)

		Triode	Tetrode
Input	C_{in}	2.3	8
Output	C_{out}	2.0	2.6
Control Grid to Anode	C_{g1a}	2.4	0.04
Grid Triode to Grid 1 Tetrode	C_{g1-g1}	0.003	
Anode Triode to Anode Tetrode	$C_{a(t)a}$	0.012	
Grid Triode to Anode Tetrode	C_{g1a}	0.004	
Anode Triode to Grid 1 Tetrode	C_{a-g1}	0.009	

†Measured in fully shielded socket without can.

Characteristics

		Triode	Tetrode
Anode Voltage (volts)	V_a	200	100
Screen Grid Voltage (volts)	V_{g2}	—	100
Anode Current (mA)	I_a	10	10
Mutual Conductance (mA/V)	g_m	5.6	12.5
Amplification Factor	μ	19	—

Tetrode Operation as Video Amplifier

Allowance must be made in circuit design, not only for component variations, but also for valve spread and deterioration during life. Values of tetrode peak anode current, for an average valve when new and at the assumed end-of-life point for any valve, are as follows:—

	V_a (V)	V_{g2} (V)	V_{g1} (V)	I_a (mA)
Average New Valve	70	100	−1	40
Assumed End of Life Condition	60	100	−1	25

Mounting position: Unrestricted.

Base: B9A (Noval).

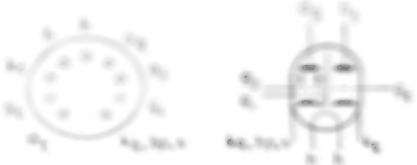

Maximum Dimensions (mm)

Overall Length	56
Seated Height	49
Diameter	22.2

Tentative Characteristic Curves of Mazda Valve Type 30FL12

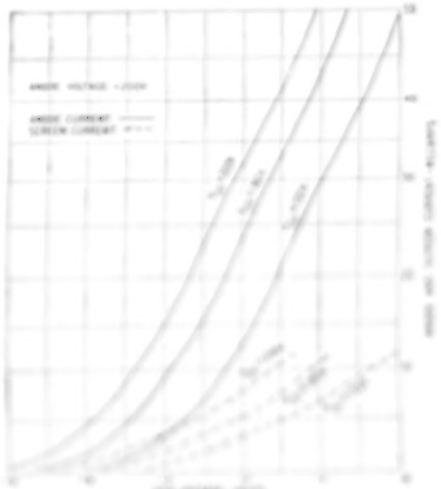

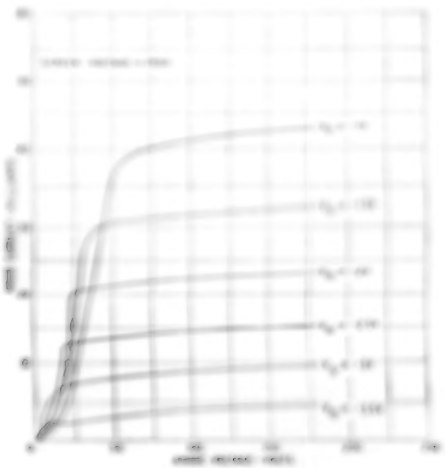

Thorn-AEI Radio Valves & Tubes Ltd.

105 Charing Cross Road, London WC2.

Telephone: GERrard 8787 Telegrams: Exvacuo Westcent London

MAZDA

TH 1611P

Important to all users of solid-state materials

MERCK & CO., INC.
ULTRA-PURE SILICON

SINGLE CRYSTAL SILICON · EPITAXIAL SILICON
POLYCRYSTALLINE SILICON · EPITAXIAL GERMANIUM
GALLIUM ARSENIDE · INDIUM ARSENIDE
Z-MET* THERMOELECTRIC MATERIAL

Your profits in the next decade will to a great extent depend on your choice of supplier of solid-state materials — but how to choose? The simplest, most reliable criterion will be PAST PERFORMANCE. Judged on this basis, The Electronic Chemicals Division of Merck & Co., Inc., deserves your attention. In just four short years, it has achieved these exclusive major breakthroughs:

1958 **Float zone, vacuum refined, doped single crystal silicon**
1959 **Z-Met* thermoelectric materials**
1960 **Epitaxial silicon N + N wafers and III-V compounds**
1961 **Epitaxial germanium P + P wafers**

When you link your product development to Merck materials research, you are enlisting a proved producer. To be the first to exploit new developments in this field, join the ranks of Merck customers.

United Kingdom and European enquiries should be addressed to:

Electronic Chemicals Division
MERCK & CO., INC.
c/o THOMAS MORSON & SON LTD.
Summerfield Chemical Works, Enfield, Middlesex
(Subsidiary of Merck & Co., Inc.)

**Trademark*